Interaction of Th2Al and related getters with hydrogen

INTERACTION OF Th_2Al AND RELATED GETTERS WITH HYDROGEN

J. H. N. VAN VUCHT

INTERACTION OF Th_2Al AND RELATED GETTERS WITH HYDROGEN

PROEFSCHRIFT

TER VERKRIJGING VAN DE GRAAD VAN DOCTOR IN DE TECHNISCHE WETENSCHAP AAN DE TECHNISCHE HOGESCHOOL TE EINDHOVEN OP GEZAG VAN DE RECTOR MAGNIFICUS DR. K. POSTHUMUS, HOOGLERAAR IN DE AFDELING DER SCHEIKUNDIGE TECHNOLOGIE, VOOR EEN COMMISSIE UIT DE SENAAT TE VERDEDIGEN OP DINSDAG 26 MAART 1963 DES NAMIDDAGS TE 16 UUR

DOOR

Johannes Hendrikus Nicolaas van Vucht

GEBOREN TE ARNHEM

DIT PROEFSCHRIFT WERD GOEDGEKEURD DOOR
DE PROMOTOR PROF. J. D. FAST

Aan mijn ouders

VOORWOORD

Dit proefschrift beschrijft werk, verricht in de jaren 1953 t/m 1959 op het Natuurkundig Laboratorium van de N.V. Philips' Gloeilampenfabrieken te Eindhoven. Gedeelten van dit werk zijn reeds eerder gepubliceerd in de vorm van artikelen in Philips Research Reports. Naar mijn oordeel behoren deze gedeelten zo wezenlijk tot het onderwerp van het proefschrift, dat besloten werd deze hieraan toe te voegen. Het proefschrift is daarom gegoten in de vorm van een bundeling van losse artikelen — hier hoofdstukken genoemd — waarvan de twee reeds verschenen artikelen deel uitmaken. In verband hiermee moest het verwijzen tussen de artikelen (hoofdstukken) onderling op enigszins ongebruikelijke wijze geschieden, nl. via de bij ieder hoofdstuk apart gegeven literatuurlijst. Elk hoofdstuk is afzonderlijk voorzien van een drietalige samenvatting en heeft zijn eigen nummering van figuren, tabellen, formules en paragrafen. Ter vergemakkelijking bij het naslaan is aan de kop van elk paar pagina's het hoofdstuk met nummer en titel aangegeven.

Het onderzoek is verricht in de prettigste samenwerking met assistenten, collega's en superieuren van het Natuurkundig Laboratorium en met enkele collega's van het Joint Establishment of Nuclear Energy Research, die ik allen mijn dank betuig. Het zou te ver voeren al hun namen hier te vermelden. Slechts enkelen die wezenlijke bijdragen hebben geleverd tot het werk en die gewoonlijk op de achtergrond blijven, wil ik noemen: De Heren A. I. Luteyn, J. P. Boogaard, J. Pegels en P. Colijn.

De directie van het Natuurkundig Laboratorium, in het bijzonder Dr. E. J. W. Verwey, ben ik veel dank verschuldigd voor de gelegenheid die zij mij gegeven heeft dit proefschrift te bewerken. Mijn promotor Prof. J. D. Fast dank ik voor zijn daadwerkelijke aanmoediging. De altijd zeer vruchtbare en verhelderende discussies met hem en ook met Prof. Dr. J. L. Meijering hebben zeer veel bijgedragen tot de totstandkoming van dit werk.

CONTENTS

CHAPTER 1

GENERAL INTRODUCTION

Summary.

This introduction gives an outline of the importance of getters, their task and their physical and chemical properties. It also explains why the investigation of the getter Ceto was undertaken and how this investigation was carried out.

Zusammenfassung

Die Bedeutung von Gettern, ihre Aufgabe sowie ihre physikalischen und chemischen Eigenschaften werden beschrieben. Ferner wird dargelegt, warum und in welcher Form die Untersuchung des Getters Ceto durchgeführt wurde.

Résumé

Cette introduction donne un extrait de l'importance de getters, leur tâche et leurs propriétés physiques et chimiques. Elle traite également de la motivation de la recherche du getter Ceto et de la méthode dont on a effectué cette recherche.

1. Task of a getter

In the vacuum technique, more in particular in the technique of electronics, where small enclosed and evacuated spaces e.g. bulbs are concerned, gas binders are used which are commonly named getters. At the end of the pumping process, which is usually carried out by means of diffusion pumps or sometimes by two-stage mechanical pumps, the pressure in the bulbs is not as sufficiently low as is required for the application. The task of the getter is to bind the remaining gas in the envelope and to take up all those gases which are produced during subsequent operation of the device.

For example fig. 1 demonstrates the action of a getter on the "vacuum" in three valves of a certain type, which was manufactured very thoroughly and only on a small scale. Without activating the getter (i.e. putting it into action) the pressure in the valves increases rapidly after sealing off and reaches in short times fatal values in spite of the pumping and degassing process applied. This is caused by desorption of gases, a rather slow liberation, from the valve parts. The barium getter used in this case cleaned them up in a short time and maintained the pressure at a very low value. This action can be looked upon as the task of a getter.

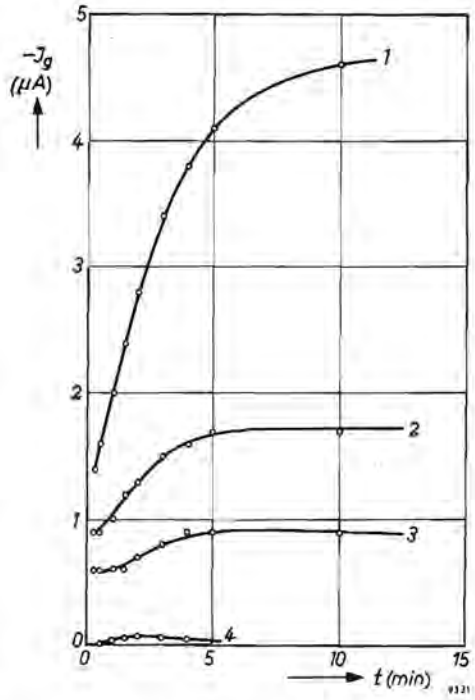

Fig. 1. Positive-ion current (indicating gas density) plotted against time, for three valves of a certain type (E80L) chosen at random from a large batch. Curves 1,2 and 3 represent the ionic currents in the different tubes. Curve 4 (relating to all three valves) gives the ionic current after a Barium getter has been evaporated. The valves were degassed at pumps with a low residual pressure and sealed after a low pressure was obtained.

2. Nature and origin of the gases to be bound

The composition of the gas that has to be sorbed differs widely from that of the air [1]). Nitrogen, oxygen and inert atmospheric gases are never evolved in appreciable quantities after the valve has been sealed off. The presence of these gases in significant amounts nearly always means leakage, or is due to special pretreatments of valve constituents.

The gases that normally have to be cleaned up by the getters are released from solids forming phase boundaries with the vacuum, mainly glass, ceramics and metals. They are the origin — or play a role in the formation — of the gases that are generally found in evacuated spaces i.e. hydrogen, water vapour, carbon dioxide, carbon monoxide and hydrocarbons. The quantities of these gases vary, depending on the nature of the solids, their pretreatment and their temperature.

Hydrogen is found dissolved in metals like iron and nickel. A very important source of hydrogen is the glass on which it is potentially present in the form of adsorbed water. Depending on the chemical affinity of a metal and on the tem-

perature the equilibrium of the reaction

$$H_2O + \text{metal} \lesseqgtr \text{metaloxide} + H_2$$

will lie more to the left or the right of the equation. For example, let us take the reaction between a tungsten filament and water vapour:

$$3H_2O + W \lesseqgtr WO_3 + 3H_2.$$

At low temperatures the equilibrium lies at the left-hand side of the equation since $\Delta G = \Delta H - T\Delta S > 0$. When the temperature is increased the entropy difference ΔS between right and left becomes important, and since WO_3 is much more volatile than tungsten, ΔS is large and positive. This causes ΔG to become negative and the equilibrium to shift from left to right, especially at low pressures. The result is the premature blackening of the glass envelope of a lamp if it contains water vapour: H_2O reacts with the hot filament and forms WO_3; this evaporates and forms a deposit on the glass wall. Here the reverse process occurs and WO_3 is reduced by the hydrogen formed at the filament. The net result is a transport of tungsten from filament to glass envelope (water cycle).

Not only glass but also metals and ceramics can produce hydrogen from adsorbed layers, mostly, however, in much smaller amounts. The glass surface can be looked upon, it appears, as resembling silica gel, a surface with very fine pores on a nearly atomic scale, in which very much water can be imbibed. It is likely that a large amount of this water is also chemically bound. If the glass is "baked out", i.e. is heated, while pumping, to as high a temperature as possible (below the softening point) the larger part of this water disappears, accompanied by some CO_2 and CO. However, even after this treatment some gas slowly desorbs. The mass-spectrograph shows that this also consists of water vapour and some CO_2 and CO.

Carbon monoxide is chiefly formed at the metals (e.g. nickel). These always contain carbon, homogeneously dissolved or present as carbides, and beside this also some oxygen is present as oxide at the surface or homogeneously dissolved in the bulk. Upon annealing in vacuum, CO is slowly produced because of the increased diffusion rate of carbon towards the oxide present on the surface, or both of carbon and oxygen to the surface, where they combine:

$$C + NiO \rightarrow Ni + CO.$$

Also a reaction of CO_2 (from the glass) with metals or with carbon can produce CO:

$$CO_2 + NiO \rightarrow NiO + CO,$$

$$CO_2 + C \rightarrow 2CO.$$

The *hydrocarbons* like CH_4 and C_2H_2 can be looked upon principally as the reaction products of water vapour with metalcarbides:

$$\text{metalcarbide} + H_2O \rightarrow \text{metaloxide} + CH_4.$$

The metal carbide in this reaction may possibly originate in a reaction of the metal with CO, as is found in some cases with barium getters [2]). Other possible sources of hydrocarbons are, for example, traces of grease (from the fingers), oil (from the diffusion pump) or dust particles (cellulose, keratine etc.). At the increased temperatures in the valve these are rapidly cracked or decomposed.

Meanwhile it will have become clear that a pumping process can only be really effective if it is accompanied by a baking out i.e. an annealing process of all parts at as high as possible a temperature and during as long a period as possible, possibly in conjunction with an electron bombardment. Preferably it is preceded by a thorough degreasing and cleaning process and by a pretreatment in a reducing atmosphere. During this high-temperature treatment virtually all the gas adsorbed on the surface is removed. Only those gases whose components have long diffusion paths will be given off subsequently (H_2O, CO, CH_4). The amounts liberated, however, are amply sufficient to shorten the life of a valve or to spoil its characteristic properties.

3. Generalities about getters and their functioning

Any material placed in an electronic valve in order to maintain or to correct its vacuum after sealing off from the pump can be called a getter (or gas binder). Often the getter is a metal though sometimes metalloids like phosphorus are still used (in incandescent lamps). At present mostly barium is used which is precipitated as a deposit on the glass envelope by evaporation from solid barium or from a barium alloy. These getters are called evaporating or "flashed" as contrasted with the non-evaporating or "non-flashed" getters.

Examples of non-evaporating getters are zirconium and titanium. Both are capable of being evaporated, but normally they are used unevaporated in the form of sheet or wire or more often as a powder. If they are used as a powder, either pure, or mixed or possibly alloyed with other metals, they are fixed at appropriate parts of the valve by means of electrophoresis or with the help of a binder. Afterwards they are sintered to their metallic carriers.

Not every material that is sufficiently reactive with respect to the gases to be cleaned up is usable as a getter. An essential thing is that we must be able to choose arbitrarily the point of time at which the getter starts its work. If this is not possible it "corrodes" in such a way during the manufacturing process (before sealing off) that, at the time when it is required to perform its proper work, the getter is unfit. This putting into action is called *activating*. Before

activation the getter is prevented from doing its work either by technical or chemical means. Barium, for example, is placed into the glass envelope while still packed in a small piece of nickel tube with both ends squeezed, or it is incorporated in the form of a non-reactive alloy with aluminium: $BaAl_4$ (placed in a tiny iron "boat"). In both cases activation occurs by heating. Barium either evaporates through the slits in the ends of the nickel tube or is liberated by the reaction of $BaAl_4$ with iron, and is deposited on the glass wall as an active mirror.

Non-evaporating getters are prevented from doing their work by protecting surface layers. Zirconium and titanium in their normal state are coated with oxide. By heating these metals to 1000 °C the protecting oxide (or possibly nitride) is dissolved in the metal. After cooling down, the purified surface is able to work as a getter.

This property — the formation of a protecting skin — is obviously a mixed blessing. Often it means that the getter in the valve is rapidly de-activated by some gases, particularly at such temperatures as are normal during storing (shelf life).

All metals used as (or in) getters have the common property of their oxides, nitrides, carbides, and last but not least their hydrides — or the homogeneous solutions of these compounds in the metal itself — being extremely stable. This property must even be stipulated for a getter metal. A high stability of these compounds — or their solutions — means a low equilibrium pressure of the gaseous component, i.e. a favourable position of the equilibrium in cases where more complicated reactions are involved e.g.

$$MH_2 \rightleftarrows M + H_2 \uparrow \tag{1}$$

or

$$MO + MC \rightleftarrows 2M + CO \uparrow . \tag{2}$$

In the case of reaction (1), neglecting the vapour pressures of M and MH_2, the equilibrium condition reads

$$\Delta G^0_F = RT \ln p_{H_2}$$

or

$$p_{H_2} = \exp (\Delta G^0_F / RT),$$

where ΔG^0_F is the standard free enthalpy (Gibbs free energy) of formation of MH_2. With increasing stability of MH_2 (i.e. with its free enthalpy of formation more negative) the equilibrium pressure decreases. In the equilibrium of reaction (2), neglecting the vapour pressures of M, MO and MC it follows that

$$\Delta G^0 = - RT \ln p_{CO} ,$$

where ΔG^0 is the algebraic sum of the tabulated G values of the four participants in this reaction.

$$p_{CO} = \exp(-\Delta G^0/RT).$$

Here again it is shown that the gas pressure becomes low when the reacting compounds are more stable with respect to the reaction products i.e. when ΔG^0 is large and positive.

However, the above requirement of stability can be a serious difficulty in the preparation of the getters and certainly in the fundamental study of the getter properties. It means that during their preparation the air has to be locked out. A getter material that has once been contaminated with oxygen, nitrogen or carbon stays impure i.e. purification is very complicated. It means that any contact at high temperature with oxides, nitrides or carbides that are equally or less stable than those of the getter metal causes an attack of the first-mentioned materials and the contamination of the getter.

4. Some details about non-evaporating getters

Non-evaporating getters have some special advantages, which is why technicians prefer them sometimes to evaporating getters. These advantages are, for instance, the wider choice concerning the place where the getter can be built in (in small valves this is sometimes a serious problem), the absence of annoying effects caused by metal deposits like capacities, and the smaller chance of an electrical short-circuit such as is caused by the sublimation of the getter-metal on insulating parts.

As non-evaporating getters are used the metals titanium, zirconium, and thorium, pure or alloyed with each other or with other metals. Sometimes mixtures are used that change wholly or partially into alloys during the activation process. These metals are to be found in the above sequence in group IV*a* of the Periodic System (The zirconium used is always mixed with 1% hafnium, which has nearly identical getter properties). The stability of their oxides, nitrides and carbides increases in this order. This is illustrated by table I which gives the heats of formation of these compounds.

In many cases titanium and zirconium are used in the form of a powder. Then they are sintered on a metal carrier or pressed into a pellet. Sometimes they are applied in the form of sheet or wire. In that case they must have a high grade of purity since comparatively small amounts of oxygen, nitrogen, carbon or hydrogen already make them brittle and unworkable.

The metal thorium in its pure form is not widely used in practice. Yet it finds application as the principal component of a getter that is known under the name of *Ceto* [3]). This brittle alloy is obtained by sintering together thorium powder *) with 25% by weight of *Ceral*. *Ceral* is the industrial name of the

*) The thorium powder used in the preparation of *Ceto*, contains in its commercial form some 2-8% by weight of oxide, depending on the grain size, and not seldom some sodium or calcium left over from the reduction process.

TABLE I

Heats of formation per gramatom oxygen, nitrogen and carbon of their compounds with the group IV*a* metals.

titanium		zirconium		thorium	
ΔH (kcal)	compound	ΔH(kcal)	compound	ΔH (kcal)	compound
$-124 \ldots -113$	$TiO \ldots TiO_2$	-130	ZrO_2	-147	ThO_2
-80	$TiN_{0.4-1.0}$	-82	ZrN	-78	Th_3N_4 *)
-44	$TiC_{0.6-6.0}$	-48	ZrC	-22	ThC_2 **)

*)**) Like titanium and zirconium, thorium has compounds ThN and ThC, both with a NaCl structure. Their ΔH is probably greater than that of ZrN and ZrC.

intermetallic compound of "mixed metal" Mi (ca 80% Ce, 19% La) with aluminium: $MiAl_2$. *Ceto* is crushed under a protecting liquid and subsequently, mixed with a binder to a paste, it is painted on the proper parts of the valve. The binder has, during part of the manufacturing process, a protecting function: *Ceto* is less stable in air then thorium, it is often inflammable.

5. Aspects of a fundamental investigation into the working of non-evaporating getters

From the preceding sections it will have become clear that the working of a getter is in no case chemically simple. The sorption of each of the gases alone is a separate process, and that of a mixture of gases will certainly be more intricate. Therefore one must make a choice, already at the start, which gas reaction to study. Both reaction partners have to be defined in the chemical and physical sense: their chemical composition must be known and it must be possible to obtain them in a reproducible way. The same applies to the surface of the getter, its area and quality. Exactly at these points, however, we meet the difficulties already mentioned in the preceding sections: (1) the attack on the crucibles, (2) the impossibility of a direct removal of oxygen, nitrogen and carbon, in the bulk or on the surface and (3) the impossibility of working the getter alloys, which means an extra difficulty if a reproducible surface area is wanted.

In practice it is important to know how low is the residual pressure above the getter. Therefore two properties will have to be measured: (a) the equilibrium pressure in the thermodynamical sense, in case true equilibrium can be reached, and (b) the sorption rate at low pressures if the residual pressure in

the valve is a question of a dynamic equilibrium between desorption from its parts and ab- or adsorption by the getter. In practice the latter case always appears to occur. Both properties, the equilibrium pressure and the sorption rates are temperature-dependent, and they are, at least over certain regions, depending on how far the reaction has proceeded. The sorption rate can be pressure dependent and very sensitive to surface conditions (poisoning). These reactions are best studied in those regions of temperature and pressure that are realized in valves or at least in regions from where an extrapolation to the conditions obtaining in the valves seems to be justified. This involves extra difficulties. For example, the choice of a manometer is very limited if one demands that the latter is required to give rapid and continuous indication, if it has to cover a range down to 10^{-6} torr and last but not least if its action should neither influence the course of the reaction nor the pressure by its own sorbing properties. Because of the last points, ionisation gauges must be rejected. It is known that the ionization current activates the gas molecules, partly by forming ions, partly radicals (atomic hydrogen and oxygen, methyl) and partly by forming activated molecules (N_2*). These activated gases are more rapidly taken up by the getter but they are also "gettered" by the filament of the manometer itself (electrical clean up).

In measurements at low pressure another difficulty, viz. the incessant desorption (or possible adsorption) of gases by the enclosing walls. Desorption of "poisoning" gases directly influences the reactions, while exchange of each kind of gas between the vacuum and the walls affects the measurement.

6. Investigation of Ceto leading to the present work

The following chapters report a part of the work which for some years has been carried out on the subject of a particular getter, namely Ceto, and its reaction with one particular gas, namely hydrogen. At the beginning it was not even known whether Ceto was a mixture of thorium and ceral, or whether it consisted of a homogeneous phase. It is indeed possible, that in an inhomogeneous getter the diverse phases show different reactivities with respect to the various gases which thus may supplement each other in such a way that the mixture is technically perfect. If the getter consisted of a single phase the question would arise what the atomic structure was of this phase, and whether it was possible to explain its properties with it. Therefore a fundamental investigation was undertaken with the help of metallographical, thermoanalytical and X-ray analytical methods in order to obtain some more data about the ternary phase diagram of Th-Ce-Al, of which elements Ceto is composed. The results of this preliminary work are compiled in the second chapter of this thesis. They enabled us to determine the atomic structure of the getter. The thermodynamics of its reaction with hydrogen were studied by measuring equilibrium pressures at various temperatures. This work is reported in chapter 3.

Chapter 4 describes X-ray diffraction experiments with the getter loaded with hydrogen. Together with the neutron diffraction and the nuclear magnetic resonance work, to be found in chapter 5, they served to build up a picture of the behaviour of hydrogen in the getter lattice. Mainly these properties were studied with the ceto-like structure Th_2Al. At some points, however, the effect of replacing some of the thorium atoms by cerium, which is the way how Ceto is built, was checked. Chapter 6 enters into the problem of order or disorder of the hydrogen atoms occluded in Th_2Al. Chapter 7, at last, contains the kinetic experiments. Here the influence of cerium is more directly felt because of its effect on the inhibiting oxide layer covering the getter metal.

Some of the measurements were carried out in cooperation with colleagues, partly at the Natuurkundig Laboratorium of N.V. Philips' Gloeilampenfabrieken, partly at other institutes, and therefore have already been reported elsewhere. In order to obtain a full picture they are nevertheless reported here again be it in somewhat greater detail.

REFERENCES

[1]) A. Klopfer, S. Garbe and W. Schmidt, Vacuum **10**, 7-12, 1960.
[2]) J. J. B. Franssen and H. J. R. Perdijk, Philips tech. Rev. **19**, 290-301, 1957.
[3]) W. Espe, M. Knoll and M. P. Wilder, Electronics **23**, 80, 1950.

CHAPTER-2

TERNARY SYSTEM Th-Ce-Al

Summary

A report is given of investigations into the ternary system Th-Ce-Al and the results obtained. Included is a review of data, in part published previously, about the binary systems Th-Al, Ce-Al and Th-Ce. Furthermore some data about the behaviour of the element cerium are communicated. No ternary compounds were found. The structure of a non-evaporating getter named Ceto, because of which the investigations were started, was determined.

Résumé

On rapporte des recherches dans le système ternaire Th-Ce-Al et les résultats obtenus. Des données des systèmes binaires Th-Al, Ce-Al et Th-Ce, déjà publiées partiellement, sont inclues. Quelques résultats concernant la conduite de l'élément cérium sont aussi communiqués. La structure d'un getter non-évaporisant appelé Ceto, cause des recherches, était déterminée.

Zusammenfassung

Es wird über Untersuchungen und ihre Ergebnisse im ternären System Th-Ce-Al berichtet. Zugleich wird auch ein Überblick über teilweise schon früher veröffentliche Daten der binären Systeme Th-Al, Ce-Al und Th-Ce gegeben. Daneben werden einige Ergebnisse hinsichtlich des Verhaltens des Elementes Cer mitgeteilt. Ternäre Verbindungen wurden nicht aufgefunden. Die Struktur eines nicht-verdampfenden Getters namens Ceto, der Anlaß der vorliegenden Arbeit, wurde aufgeklärt.

1. Introduction

The investigation of the system Th-Ce-Al was originally part of a more elaborate programme of research concerning the nature and behaviour of a non-evaporating getter known as Ceto. This getter Ceto is composed of thorium, aluminium and "mixed metal" and it therefore belongs to a more-than-three-components system, because "mixed metal" itself is already a mixture of about 80% cerium, 19% lanthanum and 1% other rare-earth metals. Preliminary experiments showed that a replacement of "mixed metal" by pure cerium yielded a product that was essentially identical. Now it became possible to restrict the investigation of the structure of Ceto to the ternary system, in which the composition of "pure Ceto" lies on the line $Th\text{-}CeAl_2$ (fig. 1). The composition (in atoms) is about $Th_{10}Ce_3Al_6$. Later on the conclusions drawn from the work on "pure Ceto" were checked on the factory product.

It proved impossible to draw direct conclusions about the structure of Ceto either from microscopic examination (because of the brittleness of the specimen and its chemical reactivity) or from X-ray diffraction diagrams of the getter powder. Consequently a systematic investigation of all the phases occurring in the ternary system was started, beginning with the binary boundary systems.

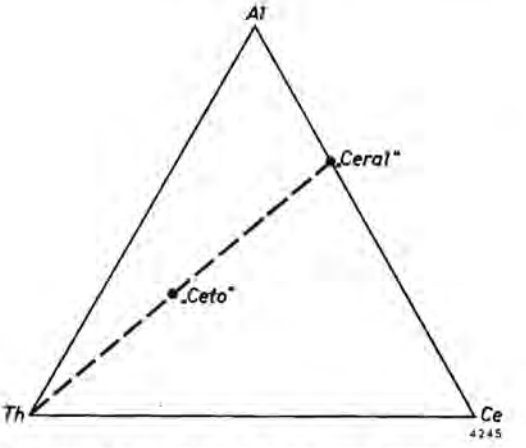

Fig. 1. Ceto as a composition of the ternary system Th-Ce-Al.

2. Literature

Very little information was found in the literature at the start of the investigation. The ternary system and the binary Th-Ce were not even mentioned. The boundary system Th-Al had already been studied to some extent by Leber [1]), Grube and Botzenhardt [2]), and by Bückle [3]), but only on the side of the system with a high Al concentration. Here a compound $ThAl_3$ was found, of which Brauer [4]) established that it was hexagonal with $a = 6{\cdot}480$ Å and $c = 4{\cdot}601$ Å. The compound was reported [1])[2]) to melt at 860 °C with decomposition, and formed a eutectic with aluminium at 620 °C (see fig. 2). The third boundary system Ce-Al was known more completely. Vogel [5]) described it already in 1912 but in 1943 he published in co-operation with Rolla, Iandelli and Canneri [6]) a correcting paper (see fig. 3). The structure of two of the intermetallic compounds actually occurring, $CeAl_4$ and $CeAl_2$, was elucidated in 1942 by Nowotny [7]). Of the other compounds (according to Vogel's first view three, viz. CeAl, Ce_2Al and Ce_3Al; according to his later paper two: CeAl and Ce_3Al_2) no X-ray diffraction data were given.

For the sake of completeness, the facts known about the pure components should be mentioned. Aluminium [8]) has a f.c.c. structure with $a_0 = 4{\cdot}049$ Å, and this structure is retained up to the melting point at 660 °C. Thorium at room temperature is also cubic close-packed (f.c.c.), with a unit cell of 5·084 Å[9]).

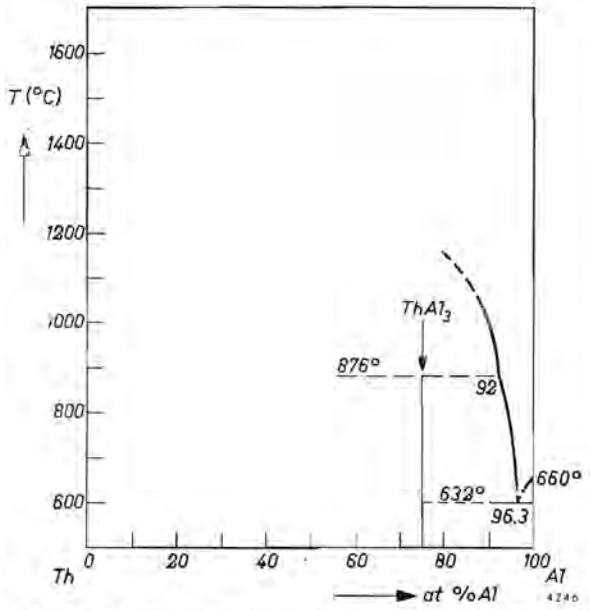

Fig. 2. The Al-Th phase diagram as given by Grube and Botzenhardt [2]).

In 1954 Chiotti [10]) found that above 1400 °C thorium had a cubic body-centred structure with a cell dimension of $a_0 = 4{\cdot}11$ Å. The melting point given at the moment is 1700 °C [11]).

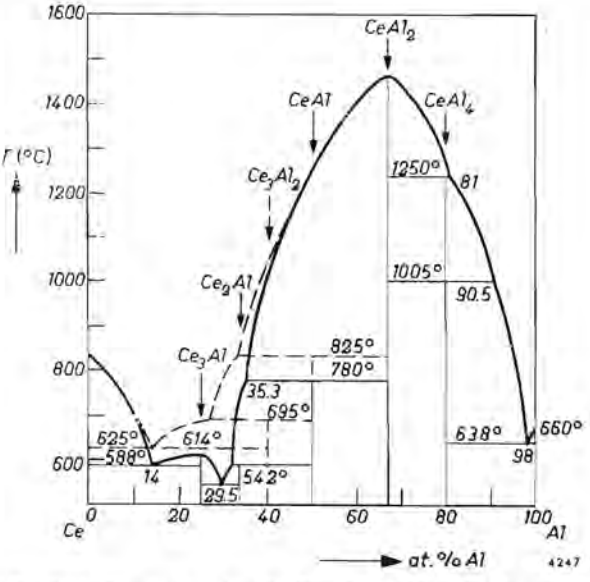

Fig. 3. The Al-Ce phase diagram as given by Vogel in 1912 (fully drawn lines) and by Rolla, Iandelli, Canneri and Vogel in 1943 (broken lines).

Of cerium [12]) three modifications were known with certainty. At room temperature a — possibly metastable — cubic close-packed structure is mostly found, with $a = 5{\cdot}149$ Å. It also seems possible that below 300 °C the hexagonal close-packed structure is found, with $a = 3{\cdot}65$ Å and $c = 5{\cdot}96$ Å. The first mentioned close-packed phase, the f.c.c. phase with $a = 5{\cdot}149$ Å, can transform into another f.c.c. phase again, with $a = 4{\cdot}82$ Å, if it is cooled down to 120 °K at normal pressure. The same transformation could be brought about [13][14]) at temperatures up to 94·5 °C if simultaneously the pressure was increased to 11 100 kg/cm². According to Pauling the conversion to the contracted phase is caused by the shift of a $4f$ electron of the cerium ion to a $5d$ level, where it participates in the conduction band. At normal pressures another transformation is found at 14 °K, which becomes more pronounced the more of the h.c.p. phase was present in the room-temperature cerium. Just below the melting point of 804 °C [15]) another transformation is observed clearly at 754 °C (other investigators find 700 °C [16])). It is not known up to now what structural change accompanies this last transformation.

3. Experimental

It is understandable that so little was known about the systems discussed in this paper. What was known with certainty lay to the side of the less reactive and lower-melting component aluminium. The other side was much more difficultly accessible because during the preparation of the alloys strong reactions occurred with the crucibles and gases or with protective masses. An example is found in Vogel's second paper on Ce-Al [6]; see also [23]).

To start with we also melted our specimens in crucibles, but in the meantime an argon-arc furnace was built, at first powered by a Philips welding rectifier, and afterwards by a D.C. generator. In this furnace (fig. 4) about 1 cm³ of a metal or mixture of metals could be melted to a button. The metal lay on a water-cooled copper plate and was thus joined to the positive pole of the generator. The negative pole was a thoriated tungsten rod fixed in a water-cooled copper tube which was mounted movably. The furnace was pumped out until a good vacuum was obtained and was subsequently filled, at a pressure of 10-20 cm Hg, with argon (freed from oxygen and nitrogen). Then the apparatus was closed and an electric arc was struck between the tungsten rod and the metal specimen lying on the copper plate. The specimen fused completely, except for a very thin layer between the melt and the copper. This cold metal layer prevented alloying with the underlying copper, but it also necessitated repeated fusions — turning the solidified button on its back each time — in order to reach sufficient homogeneity.

All alloys described in this paper were produced in this way. During melting there was never a loss of material — due to evaporation or sputtering — of such an extent that a significant deviation from the composition weighed-in was

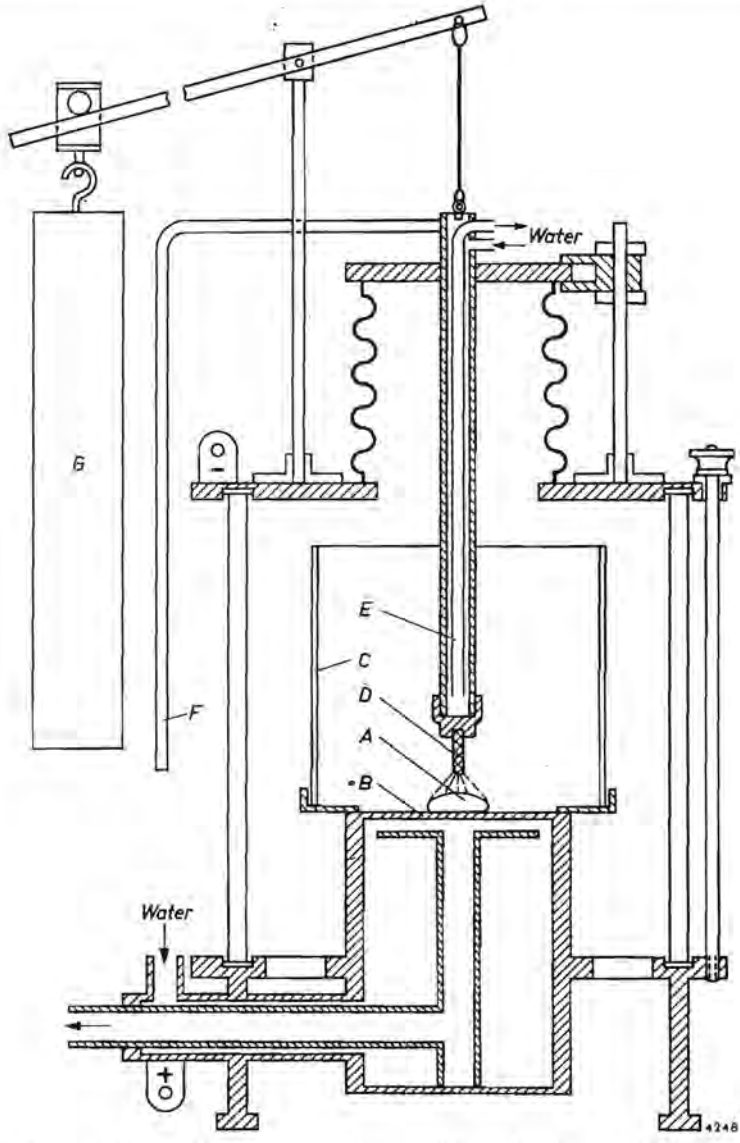

Fig. 4. Schematic picture of the argon-arc furnace. *A* is the fused sample, lying on the water-cooled copper anode *B*. *D* is the tungsten cathode, attached to a water-cooled copper tube *E*, which can be moved about by means of the handle *F* and the counterweight *G*. *C* is a glass shield to prevent sputtering against the outer glass wall. The system can be pumped out at the bottom.

caused. Contamination with copper or tungsten was not chemically demonstrable. In order to exclude contamination by gaseous components a piece of thorium — especially brought into the apparatus for this purpose — was always melted first for some 5 minutes, in which time it served as a getter.

One half of each metal specimen made in the way described was ground, polished, and finally etched for metallographic examination. The other half was powdered, sieved until all grains passed the meshes of a 35-μ sieve and was then degassed in vacuo (10^{-7} mm Hg) and annealed for 1 hr at 500-600 °C. Nearly all the intermetallic compounds and their mixtures were brittle, to such an extent that the specimens could be crushed very easily "by hand", first in a steel mortar and afterwards in an agate mortar. The ductile specimens were ground

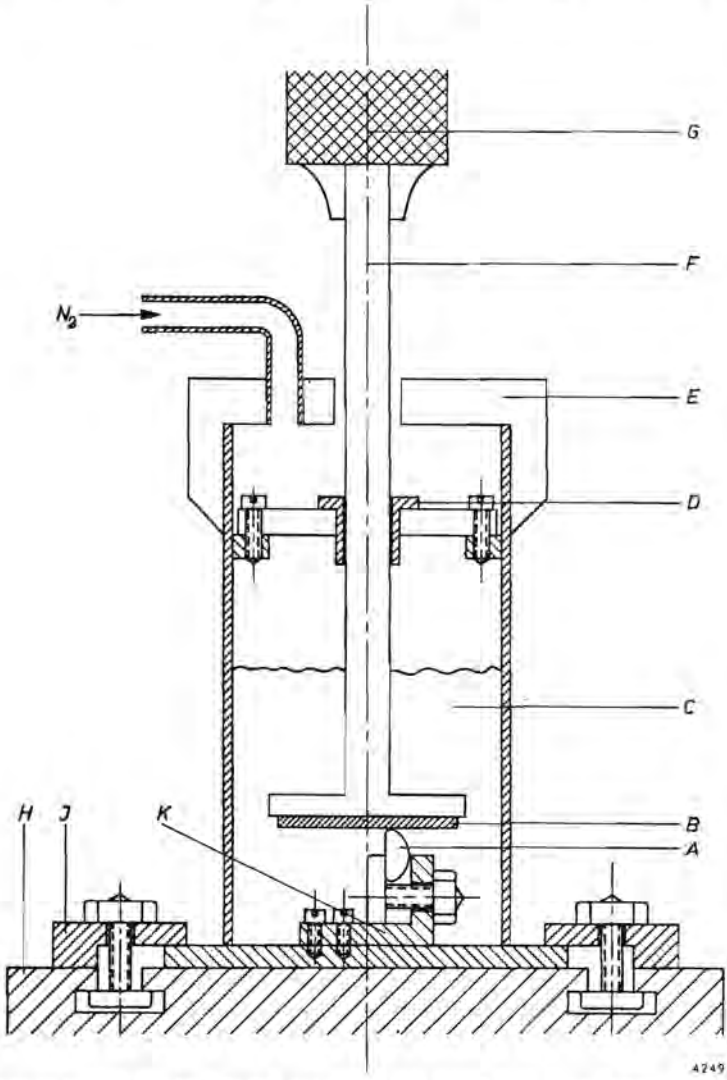

Fig. 5. Apparatus for grinding ductile specimens into powder. *A* = specimen; *B* = diamond grinding disk; *C* = toluene; *D* = teflon bearing; *E* = cover; *F* = shaft of grinding disk; *G* = chuck of drilling machine; *H* = table of drilling machine; *I* = clamp; *K* = sample holder.

to powder — with the help of a diamond polishing disk — under toluene over which nitrogen was blown. Figure 5 gives a schematic drawing of the apparatus used. In fact it had to be used only for specimens of the system Ce-Th and for Ce_3Al, as well as for compositions lying in their neighbourhood.

In order to obtain X-ray diffraction diagrams of the powder specimens a "Norelco" high-angle diffractometer was used. For the examination of the systems Th-Al and Th-Ce, Cu$K\alpha$-radiation was available, while during the investigation of the Ce-Al system only Mo$K\alpha$-radiation could be used because of trivial reasons.

In the Th-Al system several pure compounds were obtained. On behalf of the determination of their structure their density was measured. The compounds available as powder were freed from enclosed air by boiling them out under toluene in vacuo in the picnometer. Then the density was measured in the usual way.

Raw materials used were:

(a) Thorium powder with an oxide content of 2·5% (by weight) and a content determined spectrochemically (in per cent by weight) of $\leqslant$ 0·02 Fe, $\leqslant$ 0·07 Cu, $\leqslant$ 0·005 Si, $\leqslant$ 0·005 Ti, $<$ 0·003 Mg, $\leqslant$ 0·0008 Mn, and with traces of Al and Ca. In order to be sure that the oxide content did not influence the results, some control experiments were performed with oxide-free thorium. This thorium had been made in the Philips laboratories around 1935 by thermic decomposition of ThI_4, in a way analogous to that described for pure titanium and zirconium [17]). The results showed no essential differences from those obtained when using oxide-containing thorium.

(b) Compact cerium metal of New Metals Co., London, which contained in % by weight determined spectrochemically 0·23 Fe, 0·7 La, $\leqslant$ 0·03 Si, 0·006 Mn, $\leqslant$ 0·004 Mg and 0·009 Ni.

(c) Raffinal (99·998% Al) which was sometimes used as a powder (obtained by filing) but more generally in the form of sheet.

4. Binary system Th-Al

4.1. *Introduction*

This system was investigated in 1954 in co-operation with Dr Braun of this laboratory. The results were published in 1955 in the form of short notes [18])[19]), while tables with observed and calculated spacings and intensities were sent to the A.S.T.M. Card Index.

Already within a year the detected structures were confirmed by Miss Murray [20]), except for the structure of the orthorhombic ThAl; this she did not find or at least did not publish. Andresen and Goedkoop [21]) corroborated the structure of $ThAl_2$ by means of neutron diffraction. In 1958 Miss Murray published a more elaborate study of the Th-Al system. All the results reported by her appeared to be in close agreement with our earlier observations.

TABLE I

Data obtained with Th-Al intermetallic compounds

compound	structure					lattice constants (Å)	"moles" per unit cell	atomic sites			density (g/cm³)	
	system	space group (Intern. Tables)			type			thorium	aluminium	value of parameters	calc.	obs.
		H.M. symbol	Schoenflies symbol	no.								
$ThAl_3$	hex.	$P6_3/mmc$	D^4_{6h}	194	Ni_3Sn DO_{19}	$a=6{\cdot}499$ $c=4{\cdot}626$	2	$2d$: $\pm(\frac{2}{3},\frac{1}{3},\frac{1}{4})$	$6h$: $\pm(x,2x,\frac{1}{4})$ $\pm(2\bar{x},\bar{x},\frac{1}{4})$ $\pm(x,\bar{x},\frac{1}{4})$	$x=0{\cdot}143$	6·14	6·14
$ThAl_2$	hex.	$P6/mmc$	D^1_{6h}	191	AlB_2 $C32$	$a=4{\cdot}393$ $c=4{\cdot}164$	1	$1a$: (0,0,0)	$2d$: $\pm(\frac{2}{3},\frac{1}{3},\frac{1}{2})$		6·85	6·84
$ThAl_x$ (Th_2Al_3?)	tetr.					$a=9{\cdot}86$ $c=7{\cdot}81$	(4)					
ThAl	orthorhomb.	$Cmcm$	D^{17}_{2h}	63	CaSi B_c or: CrB Bf	$a=4{\cdot}42$ $b=11{\cdot}45$ $c=4{\cdot}19$	4	$4c$: $(0,y,\frac{1}{4})$ $(0,\bar{y},\frac{3}{4})$ $(\frac{1}{2},\frac{1}{2}+y,\frac{1}{4})$ $(\frac{1}{2},\frac{1}{2}-y,\frac{3}{4})$	$4c$: $(0,y,\frac{1}{4})$ $(0,\bar{y},\frac{3}{4})$ $(\frac{1}{2},\frac{1}{2}+y,\frac{1}{4})$ $(\frac{1}{2},\frac{1}{2}-y,\frac{3}{4})$	$y_{Th}=0{\cdot}147$ $y_{Al}=0{\cdot}443$	8·11	8·10
Th_3Al_2	tetr.	$P4/mbm$	D^5_{4h}	127	U_3Si_2 D_{5a}	$a=8{\cdot}127$ $c=4{\cdot}222$	2	$2a$: (0,0,0) $(\frac{1}{2},\frac{1}{2},0)$ $4h$: $\pm(x,\frac{1}{2}+x,\frac{1}{2})$ $\pm(\frac{1}{2}+x,\bar{x},\frac{1}{2})$	$4g$: $\pm(x,\frac{1}{2}+x,0)$ $\pm(\frac{1}{2}+x,\bar{x},0)$	$x_{Th}=0{\cdot}674$ $x_{Al}=0{\cdot}116$	9·02	8·98
Th_2Al	tetr.	$I4/mcm$	D^{18}_{4h}	140	$CuAl_2$ $C16$	$a=7{\cdot}616$ $c=5{\cdot}861$	4	$8h$: $\pm(x,\frac{1}{2}+x,0)$ $\pm(\frac{1}{2}+x,\bar{x},0)$ $\pm(\frac{1}{2}+x,x,\frac{1}{2})$ $\pm(x,\frac{1}{2}-x,\frac{1}{2})$	$4a$: $\pm(0,0,\frac{1}{4})$ $\pm(\frac{1}{2},\frac{1}{2},\frac{1}{4})$	$x=0{\cdot}162$	9·63	9·61

4.2. *Results*

A compilation of the results is given in table I. They will be discussed in detail in the treatment of the various compounds below.

$ThAl_3$

This phase was already known. Leber [1]) isolated it and Brauer [4]) determined its crystal system and the lattice dimensions. Qualitatively their results were confirmed by us. The dimensions found by various investigators up till now for the unit cell are:

Brauer [4])	Braun and Van Vucht [18])	Murray [20])
$a = 6{\cdot}493$ Å	$a = 6{\cdot}499$ Å	$a = 6{\cdot}500$ Å
$c = 4{\cdot}610$ Å	$c = 4{\cdot}626$ Å	$c = 4{\cdot}626$ Å
$c/a = 0{\cdot}710$	$c/a = 0{\cdot}712$	$c/a = 0{\cdot}712$

On the basis of the 54 observed reflexions — indexed in table II — we concluded that the compound possessed a Ni_3Sn structure, as described in table I. The value of x there mentioned was obtained by finding the minimum value of R_F in the formula $R_F \equiv (\sum_{25} |F_o - F_c|)/(\sum_{25} F_o)$ for the first 25 reflexions. Figure 6 shows the behaviour of R_F when x is varied. The value of the reliability index

TABLE II

X-ray data, observed and calculated, of the intermetallic compound $ThAl_3$

hkl	*d*(Å)		I_{obs}	I_{calc}	*hkl*	*d*(Å)		I_{obs}	I_{calc}
	obs.	calc.	(arb. units)			obs.	calc.	(arb. units)	
101	3·57	3·57	144	138·3	411	—	1·187	0	
110	3·24	3·24	67·3	69·5	004	1·157	1·157	3·5	
200	2·81	2·81	28	28·1	104	—	1·133	0	
201	2·40	2·40	94	102·5	322	—	1·128	0	
002	2·31	2·31	27·5	21·1	500*)	1·125	1·126	2·5	
102	2·139	2·139	9	7·7	313	1·097	1·097	14	
210	2·126	2·127	17	16·2	501	1·094	1·094	4·5	
211	1·932	1·933	37	42·1	114	1·090	1·089	7·5	
112	1·886	1·885	29	31·9	412 }	1·085	1·085	16·5	
300	1·875	1·876	16	14·0	330 }		1·083	11·5	
202	1·787	1·787	16	14·0	204	1·070	1·070	4·3	
301	1·738	1·738	2	1·2	420	1·063	1·063	3	
220	1·623	1·624	19	18·6	403	1·039	1·039	9	
212	1·565	1·565	12·5	13·0	421	1·037	1·036	17	
310	1·560	1·561	5	3·9	214	1·016	1·016	4·8	
103	1·487	1·488	11·4	12·1	502	1·0122	1·0121	4·7	
311	1·478	1·479	23·0	26·0	510	1·0105	1·0107	4·2	
302	1·457	1·457	11·6	12·3	323	0·9900	0·9901	10·5	
400	1·406	1·407	3·5	3·1	511	0·9877	0·9875	16	
203	1·353	1·353	15·5	16·7	304	0·9848	0·9846	10	
401	1·346	1·347	13·5	14·1	332	0·9810	0·9809	9	
222	1·329	1·330	16·5	18·5	422	0·9659	0·9662	4	
312	1·294	1·294	5·0	4·3	224	0·9424	0·9422	10·7	
320	1·290	1·291	0·5	0·7	600	0·9380	0·9380	4·6	
213	1·248	1·249	9·5	10·1	314	0·9295	0·9293	3·5	
321	1·243	1·244	14		512	0·9261	0·9263	6·5	
410	1·228	1·228	8·5		430	—	0·9253	0	
402	1·202	1·202	3·5		105	0·9129	0·9129	5·5	
303	1·192	1·191	2		431	0·9070	0·9072	7	

*) The reflexions 500 and beyond were measured with a four-degrees slit.

$R_I \equiv (\sum_{25} |I_o - I_c|)/(\sum_{25} I_o)$, calculated with the value of x corresponding to the minimum value of R_F was 7·9%. Due to the favorable atom ratio it was thus possible to establish fairly easily the position of the light aluminium atoms between the heavy thorium atoms.

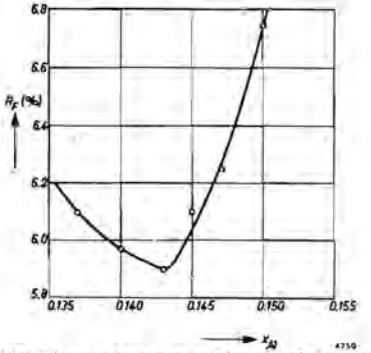

Fig. 6. $R_F \equiv (\sum_{25} |F_o - F_c|)/(\sum_{25} F_o)$ as a function of the aluminium parameter x_{Al} in the structure of $ThAl_3$.

A basal-plane projection of the structure, shown in fig. 7, clarifies the stacking of the atoms. Strings of triangular groups of Al atoms run along the c-axis. Each thorium atom is in "contact" with 4 Al atoms in each of 3 strings. The atom distances thus are

Th — 2×3 Th	4·408 Å	
Th — 2×1 Th	4·626 Å	
Al — Al	2·79 Å	(in a "string")
Al — Al	2·82 Å	
Al — Al	3·71 Å	(closest between different strings)
Th — 3×2 Al	3·26 Å	
Th — 2×3 Al	3·15 Å	

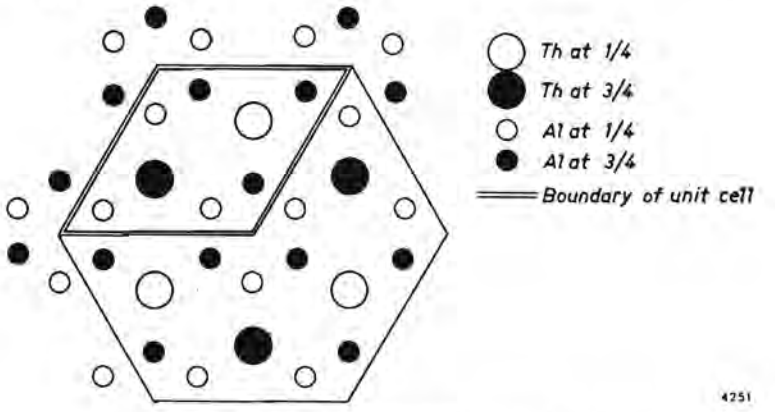

Fig. 7. Basal-plane projection of the structure of $ThAl_3$.

$ThAl_3$ was obtained without difficulty by cooling the molten specimen in the normal way on the copper anode of the arc furnace. The compound melted, with decomposition into a liquid and $ThAl_2$, at a peritectic temperature which Grube and Botzenhardt determined to be 876 °C. Murray [22]) found 1120 °C. The difference was possibly due to difficulties in observation.

$ThAl_2$

This compound gave an X-ray diffraction diagram with 41 lines, which were indexed on the basis of a hexagonal unit cell with dimensions:

$a = 4{\cdot}393$ Å	Murray [20]) found $a = 4{\cdot}388$ Å
$c = 4{\cdot}164$ Å	$c = 4{\cdot}162$ Å
$c/a = 0{\cdot}948$	$c/a = 0{\cdot}948$

The measured intensities pointed to an AlB_2 structure. The thorium atoms here are placed at the corners of the unit cell, while the aluminium atoms are found in the centres of each cell half, thus forming layers consisting of a network of regular hexagons. The intensities calculated for this structure yield a value for R of $R \equiv (\sum_{39} |I_o - I_c|)/(\sum_{39} I_o) = 13{\cdot}8\,\%$ (see table III and fig. 8).

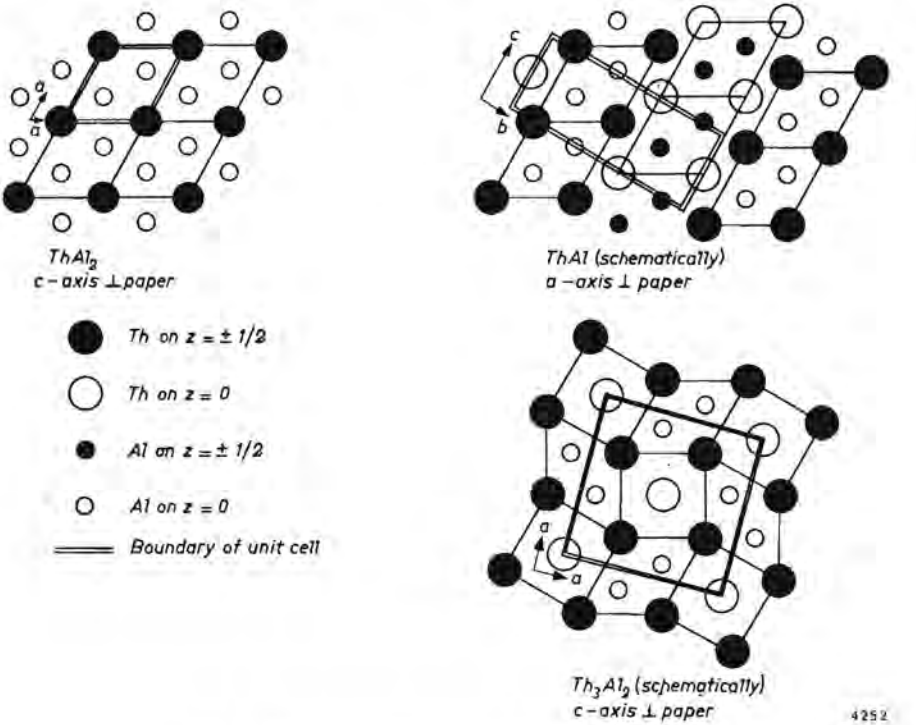

Fig. 8. Three related structures in the system Th-Al.

TABLE III

X-ray data of the compound $ThAl_2$

hkl	d(Å) obs.	d(Å) calc.	I_{obs} (arb. units)	I_{calc} (arb. units)	hkl	d(Å) obs.	d(Å) calc.	I_{obs} (arb. units)	I_{calc} (arb. units)
001	4·16	4·16	68	72·5	302	1·0832	1·0831	28	24·6
100	3·80	3·80	≈244	239·8	221	1·0618	1·0620	17	9·6
101	2·80	2·81	≫244	370·2	310	1·0551	1·0553	9	12·3
110	2·196	2·196	117	112·3	004	1·0414	1·0411	3	3·9
002	2·083	2·083	26	32·6	311*)	1·0228	1·0228	52	37·5
111	1·942	1·943	70	59·9	104	1·0040	1·0041	9	11·9
200	1·901	1·902	44	37·6	213	0·9988	0·9987	35	36·3
102	1·825	1·826	66	67·7	222	0·9714	0·9714	22	21·3
201	1·731	1·731	111	91.0	400	0·9511	0·9511	6	5·8
112	1·510	1·511	59	69·2	312 }	0·9412	0·9412	39	45.0
210	1·438	1·438	30	30·5	114 }		0·9407		
202	1·404	1·404	29	28·4	303	0·9362	0·9362	10	9·2
003	1·387	1·388	4	3·4	401	0·9274	0·9273	20	18·0
211	1·359	1·359	83	80·2	204	0·9133	0·9133	16	12·2
103	1·304	1·304	26	35·4	320	0·8730	0·8729	15	13·9
300	1·268	1·268	22	19·7	402	0·8652	0·8652	17	14·3
301	1·213	1·213	11	13·7	223	0·8612	0·8612	13	11·4
212	1·183	1·183	30	32·7	321	0·8542	0·8543	39	44·3
113	1·173	1·173	8	12·1	214	0·8432	0·8433	28	31·6
203	1·121	1·121	13	21·9	313	0·8401	0·8401	40	47·3
220	1·098	1·098	9	12·7					

*) The reflexions 311 and beyond were measured with a four-degrees slit, the others with a one-degree slit.

The distances in this lattice are

Th — Th	4·393 Å
Th — Th	4·164 Å
Al — Al	2·54 Å
Al — Al	4·164 Å
Th — Al	3·28 Å

The remarkably short Al-Al distance aroused some doubt about the correctness of the Al parameter in the z-direction. The almost three times more favourable ratio of the scattering amplitude of Al and Th for neutrons than for X-rays led us to beg Andresen and Goedkoop to apply neutron diffraction as a means for studying this structure. They confirmed completely our X-ray diffraction results [21].

$ThAl_2$ proved to be readily obtainable by normal cooling of a molten specimen in the arc furnace. The compound was very brittle and melted at a high temperature. Murray [22] found a congruent melting point at a temperature somewhere above 1520 °C.

$ThAl_x$

We never succeeded in obtaining this compound in a pure condition. Its composition lay in the neighbourhood of $x \approx 1{\cdot}6$. Annealing experiments gave the impression that only in a very narrow temperature region (about 1300 °C) was the phase stable. At 1200 °C we found it decomposing into $ThAl_2$ and ThAl. The same was the case at 1400 °C, but at this temperature melting phenomena

could not be observed either. At 1500 °C melting did occur clearly. Murray [22]), who attributes to this phase the composition Th_2Al_3, found that it splits up eutectoidically into ThAl and $ThAl_2$ below 1100 °C and peritectically in liquid and $ThAl_2$ at 1394 ± 14 °C.

The dimensions of the tetragonal unit cell calculated from the reflexions given in table IV are:

$a = 9{\cdot}86$ Å Murray [22]) found $a = 9{\cdot}870$ Å
$c = 7{\cdot}81$ Å $c = 7{\cdot}837$ Å
$c/a = 0{\cdot}79$ $c/a = 0{\cdot}795$

Just like us, Miss Murray did not succeed in obtaining the pure phase; therefore there remains some doubt about its real composition.

TABLE IV

X-ray data of a compound $ThAl_x$ ($x \approx 1{\cdot}6$)

hkl	d(Å) obs.	d(Å) calc.	I_{obs} (arb. units)	hkl	d(Å) obs.	d(Å) calc.	I_{obs} (arb. units)
111	5·22	5·20	17	331	2·229	2·228	10
200	4·93	4·93	11	422	1·921	1·921	15
002	3·91	3·91	13	431 }	1·914	1·912	18
211	3·84	3·84	29	501 }			
102	3·64	3·64	6	323	1·887	1·887	23
220	3·49	3·49	56	204	1·819	1·818	23
202	3·08	3·06	55	521	1·782	1·783	14
301	3·03	3·03	28	413	1·761	1·762	11
222	2·602	2·602	29	440	1·74	1·743	8
321	2·580	2·582	14	433 }	1·572	1·573	8
103	2·521	2·520	16	503 }			
400	2·465	2·465	29	424	1·464	1·463	10
213	2·244	2·244	12				

It is possible, using the X-ray analytical data now available, to try and make a reasoned estimate of the composition. We therefore plotted in fig. 9, for each compound, the percentage difference between the measured cell volume

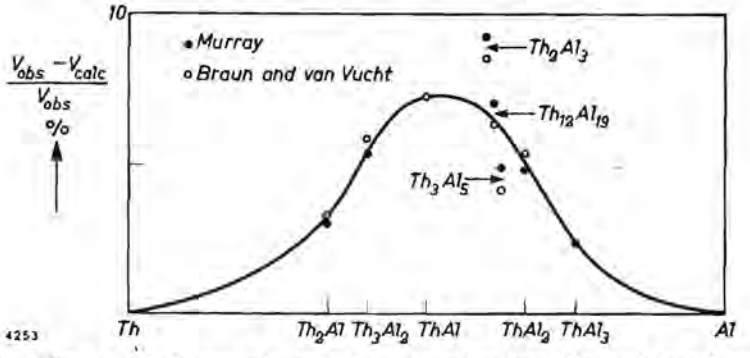

Fig. 9. The relative difference between the measured volumes V_{obs} and the volumes calculated by addition of the atomic volumes of the composing elements V_{calc}, for the various phases in the system Th-Al.

and the volume calculated from the close-packed pure metals thorium and aluminium. The values for Th_2Al_3 (6 "molecules" per unit cell) appear to lie rather unfavorable. Some slight preference might be felt for a composition of corresponding simplicity Th_3Al_5 (4 "molecules" per unit cell). However, if one accepts unorthodox atom ratios then the composition $Th_{12}Al_{19}$ is perhaps more interesting. Besides, fig. 9 also shows the volume effects accompanying the formation of the compounds from their elements.

ThAl

A Weissenberg diagram around the long axis of a small needlelike splinter of this compound made it possible to index the powder diagram. Table V gives the 54 observed reflexions. On the basis of these we concluded that it had an

TABLE V

Observed and calculated X-ray data of the compound ThAl

hkl	*d*(Å) obs.	*d*(Å) calc.	I_{obs} (arb. units)	I_{calc} (arb. units)	*hkl*	*d*(Å) obs.	*d*(Å) calc.	I_{obs} (arb. units)	I_{calc} (arb. units)
110	4·13	4·12	45	48	080	1·432	1·432	2	1
021	3·39	3·38	91	99	062	1·413	1·412	3	5
111	2·95	2·94	134	126	311	1·382	1·380	8	13
130	2·891	2·891	91	83	330	1·376	1·375	≈ 6	9
040	2·864	2·866	45	41	261	1·366	1·366	10	10
131	2·382	2·380	30	22	023	1·361	1·359	≈ 4	7
041	2·367	2·366	≈20	20	081	1·355	1·355	12	6
200	2·212	2·211	23	25	242	1·346	1·344	10	11
002	2·101	2·099	19	22	113	1·326	1·325	7	11
220	2·064	2·063	1	1	331	1·307	1·307	2	3
150	2·035	2·034	1	0	133	1·262	1·259	3	3
022	1·972	1·971	≈ 2	1	043	1·259	1·257	3	3
060	1·909	1·909	8	6	350 / 172	1·239	1·239 / 1·239	10	15
112	1·872	1·870	12	12					
221	1·852	1·851	30	37	190	—	1·223	0	1
151	1·831	1·830	38	36	280	1·203	1·202	2	1
240	1·751	1·750	15	14	312	—	1·200	0	3
061	1·738	1·738	20	12	262 / 351	1·188	1·190 / 1·189	8	14
132	1·700	1·698	32	35					
042	1·694	1·693	≈14	12	082	—	1·183	0	1
241	1·616	1·615	11	13	191	1·174	1·174	9	9
170	1·535	1·535	25	15	223	—	1·158	≈ 6	8
202	1·523	1·522	16	16	281	1·155	1·155	≈10	8
222	1·472	1·471	4	1	153	—	1·153	≈ 4	8
310 / 152	1·462	1·462 / 1·461	4	3	332	1·151	1·150	≈12	10
					0100	1·145	1·145	6	3
260	1·445	1·445	5	5	063	1·129	1·128	2	3
171	1·442	1·441	≈ 2	1					

orthorhombic unit cell with $a = 4{\cdot}42$ Å, $b = 11{\cdot}45$ Å and $c = 4{\cdot}19$ Å. The specific extinction of the reflexions (hkl) with $h + k = 2n + 1$ and $(00l)$ with $l = 2n + 1$ indicates the space group *Cmcm* (no. 63) *). The missing $(h0l)$ reflexions with $l = 2n + 1$ led us to propose for thorium the position (*c*).

*) In a former paper [19] we described this structure as belonging to the space group $C\,222_1$ with the special position (4*a*) common to both the thorium and aluminium. This leads to an identical structure (the *a* and *b* axes being interchanged) with the one given in the present paper for the higher-symmetry space group. Because of our then different description we overlooked the isomorphism with CaSi [37][38].

Geometrical considerations led to the same position for aluminium. Application of the trial - and - error method helped to determine the parameters given in table I. Figure 10 shows the variation of R with y_{Th}, where $R \equiv (\sum_{54} |(I_o - I_c|)/(\sum_{54} I_o)$, while y_{Al} — having only a small effect because of the small scattering amplitude of aluminium compared with thorium — was kept constant at 0·477. The minimum of R lies at 17·7%. This finally became 17·2% when y_{Al} was changed to 0·443. The value of the Al parameter was chosen in such a way that the distances of the aluminium atoms to their six surrounding thorium atoms were equal. Thus y_{Th} and y_{Al} are connected by the formula $\frac{1}{2} - y_{Al} = (c/2b)^2/4y_{Th}$. Here c and b are the lattice parameters of the orthorhombic cell. Table V shows that the reflexion intensities calculated with these values agree well with the observed intensities.

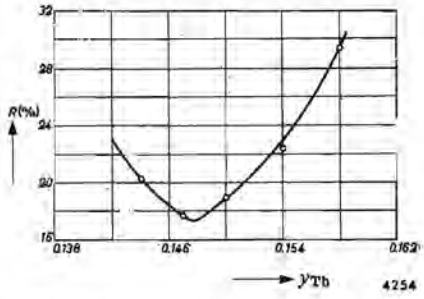

Fig. 10. $R \equiv (\sum_{54} |I_o - I_c|)/(\sum_{54} I_o)$ plotted against y_{Th} in the structure of ThAl. The parameter of Al was kept constant at 0·447.

The structure of ThAl, schematically given in fig. 8, is related to $ThAl_2$. This relation will be discussed in a separate section. The "$ThAl_2$ parts" of ThAl, however, are not exactly hexagonal: the cell angles are 58°4′ and 63°52′.
The calculated distances are

Th — 4 Th	3·85 Å
Th — 2 Th	3·96 Å
Th — 2 Th	4·19 Å
Th — 2 Th	4·42 Å
Al — Al	2·46 Å
Th — 3 Al	3·22 Å
Th — Al	3·39 Å

The Al-Al distance here is even shorter than in $ThAl_2$.

The preparation of ThAl did not cause any difficulties. The alloy was brittle and quite stable in air. Miss Murray established a melting point of 1318 ± 19 °C, at which temperature it was decomposing into a liquid and $ThAl_x$.

Th_3Al_2

Like $ThAl_2$ this compound appeared to be stable only at higher temperatures (above 1100 °C). Murray [22]) mentioned a eutectoid temperature of 1075 ± 2 °C and a congruent melting point of 1301 ± 2 °C. From this stability region it proved very easy to quench the compound without causing it to decompose into its constituent alloys. Without annealing the powdered, brittle specimen we obtained a good diffraction diagram. We measured 36 lines. From these data we had to conclude that the compound possessed a tetragonal unit cell with dimensions of

$a = 8{\cdot}127 \pm 0{\cdot}004$ Å
$c = 4{\cdot}222 \pm 0{\cdot}006$ Å
$c/a = 0{\cdot}519$

Murray [20]) found $a = 8{\cdot}125 \pm 0{\cdot}009$ Å
$c = 4{\cdot}217 \pm 0{\cdot}003$ Å
$c/a = 0{\cdot}519$

TABLE VI

X-ray data of the intermetallic compound Th_3Al_2

hkl	d(Å)		I_{obs}	I_{calc}	hkl	d(Å)		I_{obs}	I_{calc}
	obs.	calc.	(arb. units)			obs.	calc.	(arb. units)	
001	4·21	4·22	4·0	2·9	401 }	1·827	1·831 }	13·3	12·1
200	—	4·06	0	0·1	212 }		1·825 }		
210	3·64	3·64	33·0	24·3	420	1·817	1·817	5·5	4·1
111	3·40	3·40	18·4	20·3	411	1·786	1·786	8·9	11·3
201	2·928	2·928	44·2	40·9	331	1·744	1·745	12·1	16·2
220	2·875	2·875	14·3	11·3	222	1·701	1·702	4·9	5·0
211	2·756	2·755	36·3	37·9	421	1·670	1·669	0·5	1·2
310	2·570	2·570	29·4	24·7	312	1·631	1·631	7·8	12·7
221	—	2·376	0	0·5	510	1·594	1·594	0·3	0·4
320	2·252	2·255	1·6	0·7	322	—	1·541	0·0	0·4
311	2·194	2·195	0·8	0·3	520	1·507	1·509	0·2	1·4
002	2·111	2·110	7·2	9·0	511	1·491	1·491	5·0	7·3
400	2·030	2·032	0·9	0·0	402	—	1·464	0·0	0·0
321 }		1·989 }			412	1·441	1·441	4·2	6·0
112 }	1·968	1·981 }	9·3	8·8	440	1·438	1·438	1·4	1·1
410 }		1·971 }			521	1·421	1·422	2·5	3·4
330	1·91	1·916	1·2	3·5	332	1·418	1·419	1·5	1·1
202	1·87	1·873	0·7	0·0	003	—	1·407	0·0	0·1

The intensities of the lines (cf. table VI) fitted the calculated values best if the atoms were placed at the positions given in table I with $x_{Th} = 0{\cdot}674$, $x_{Al} = 0{\cdot}116$. Murray found $x_{Th} = 0{\cdot}679$ and $x_{Al} = 0{\cdot}110$. The value of the Al parameter given here has been calculated on the assumption that in the "$ThAl_2$ parts" of the lattice (cf. sec. 4.3) the distances of an Al atom to its six thorium neighbours are equal. Thus x_{Th} and x_{Al} are mutually dependent in such a way that $x_{Al} = (3/4 - x_{Th})/2(1 - x_{Th})$.
The interatomic distances then become

$Th_{z=0}$ — 8 Th	3·67 Å
$Th_{z=0}$ — 2 Th	4·22 Å
$Th_{z=0}$ — 4 Al	3·26 Å
Al — Al	2·68 Å

$Th_{z=\frac{1}{2}}$ — Th	4·00 Å
$Th_{z=\frac{1}{2}}$ — 2 Th	4·22 Å
$Th_{z=\frac{1}{2}}$ — 4 Th	4·25 Å
$Th_{z=\frac{1}{2}}$ — 6 Al	3·20 Å

The reliability factor calculated for this structure from the first 36 lines became 20·3 % after a minimum of $R = 19{\cdot}0\,\%$ had been found for a value of $x_{Al} = 0{\cdot}1$ (see fig. 11).

A description of the structure — isomorphous with U_3Si_2 — can best be given in connection with the structures of $ThAl_2$ and ThAl. This will be done in sec. 4.3.

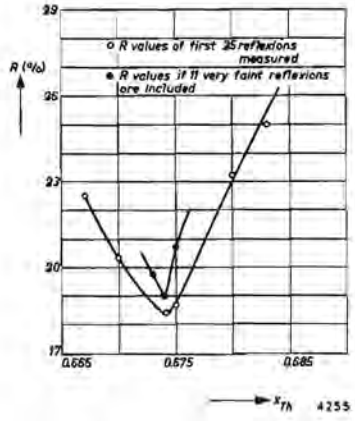

Fig. 11. $R \equiv (\Sigma\,|I_o - I_c|)/(\Sigma\,I_o)$ as a function of the thorium parameter x_{Th} in Th_3Al_2. The aluminium parameter was kept at $x_{Al} = 0{\cdot}1$.

Th_2Al

This compound, which according to Murray [22]) melted congruently at 1307 °C, showed a diffraction pattern of 47 lines. It was possible to index these on the basis of a tetragonal unit cell with

$a = 7{\cdot}616 \pm 0{\cdot}001$ Å	Murray found	$a = 7{\cdot}614 \pm 0{\cdot}003$ Å
$c = 5{\cdot}861 \pm 0{\cdot}001$ Å		$c = 5{\cdot}857 \pm 0{\cdot}003$ Å
$c/a = 0{\cdot}77$		$c/a = 0{\cdot}77$

The intensities of the reflexions indicated that the structure of Th_2Al might be of the $CuAl_2$ type. The thorium and aluminium atoms had to be placed in this structure as tabulated in table I. The value of x_{Th} was determined, using the trial - and - error method, by seeking the minimum of $R \equiv (\sum_{47}|I_o - I_c|)/(\sum_{47} I_o)$. The variation of R with x_{Th} is shown in fig. 12. The calculated intensities, given in table VII are based on the value of $x_{Th} = 0{\cdot}161$, corresponding to the minimum of $R = 12{\cdot}8$ %. Murray found 0·158, while earlier the authors [19]) had given the value of 0·162.

TABLE VII

X-ray data, observed and calculated, of the compound Th_2Al

hkl	d(Å) obs.	d(Å) calc.	I_{obs} (arb. units)	I_{calc} (arb. units)	hkl	d(Å) obs.	d(Å) calc.	I_{obs} (arb. units)	I_{calc} (arb. units)
110	5·39	5·39	17	17	521	1·375	1·375	27	27
200	3·81	3·81	26	24	204	1·368	1·368	4	3
211 }	2·95	2·95 }	250	{ 210	440	1·347	1·346	4	2
002 }		2·93 }		{ 40	413	1·343	1·342	12	15
220	2·70	2·69	8	6	512	1·331	1·331	3	2
112	2·576	2·575	20	15	530	1·304	1·307	3	2
310	2·410	2·409	44	36	224	—	1·288	0	1
202	2·325	2·322	19	23	600	1·269	1·270	6	7
321 }	1·985	1·987 }	6	{ 1	314	1·252	1·251	9	9
222 }		1·983 }		{ 1	611	—	1·224	≈1	1
400	1·906	1·904	9	8	442	1·223	1·223	4	1
312	1·862	1·861	22	22	620	1·204	1·204	2	2
330	1·798	1·796	19	19	433	1·201	1·201	2	0
411	1·764	1·762	30	37	532	1·193	1·193	2	2
420	1·704	1·703	≈5	4	541 }	1·165	1·165 }	16	{ 12
213	1·696	1·695	35	43	602 }		1·164 }		{ 9
402	1·597	1·597	13	14	404	1·162	1·161	4	3
332	1·531	1·531	25	29	523	1·146	1·146	11	15
510	1·496	1·494	≈1	0	334	1·135	1·135	9	9
431 }	1·474	1·474 }	3	{ 0	631	—	1·115	1	0
422 }		1·473 }		{ 2	622	1·114	1·114	5	4
004	1·466	1·465	4	6	424	1·110	1·111	3	2
323	1·436	1·434	4	0	215	1·109	1·109	9	11
114	1·415	1·414	≈1	1					

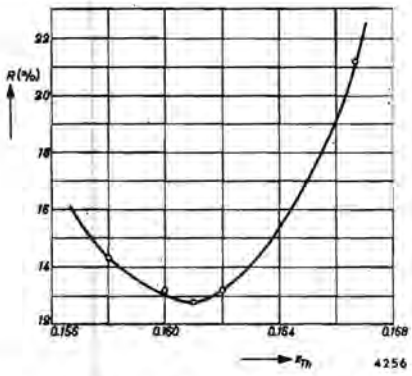

Fig. 12. $R \equiv (\sum_{47} |I_o - I_c|)/(\sum_{47} I_o)$ as a function of x_{Th} in the structure of Th_2Al.

The structure thus obtained is shown in projection in fig. 13. The principal distances are

Th — 1 Th	3·468 Å
Th — 2 Th	3·502 Å
Th — 4 Th	3·821 Å
Al — Al	2·931 Å
Th — 4 Al	3·212 Å

The preparation of the compound caused no particular difficulties. It was brittle and easily crushed.

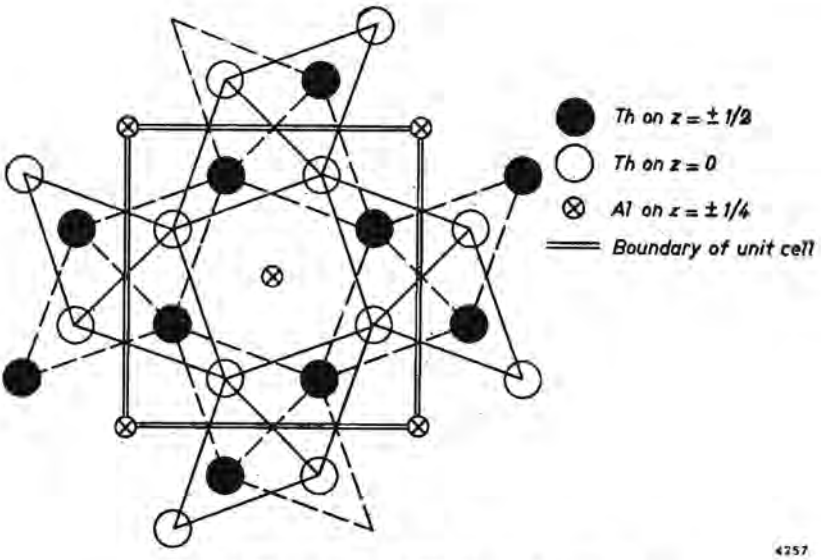

Fig. 13. The structure of Th_2Al; c-axis $\perp$ paper.

4.3. *A relation of three of the structures in the* Th-Al *system*

In sec. 4.2 we purposely postponed a detailed description of the structures of $ThAl_2$, ThAl and Th_3Al_2. By means of fig. 8, where all three structures are assembled, albeit somewhat schematically, we shall try to demonstrate an interesting structural relation. The basic structure is that of $ThAl_2$ with a hexagonal unit cell, which is drawn in projection. In this cell on each corner a thorium atom is to be found and an aluminium atom on $\frac{1}{3},\frac{2}{3},\frac{1}{2}$ and $\frac{2}{3},\frac{1}{3},\frac{1}{2}$.

This cell, only slightly deformed, can be recognized as a part of the compound ThAl. The c-axis of the original $ThAl_2$ has here become the a-axis of ThAl. Looking along the c-axis of ThAl one sees the normal sequence of these "hexagonal" $ThAl_2$ cells. So here we have "plates of $ThAl_2$", cut out of the hexagonal lattice parallel to the original c-axis. In $ThAl_2$ each thorium atom belongs to two of these "plates". If the number of thorium atoms is doubled — the composition then becomes Th_2Al_2 — the plates can be imagined to be separate. Now we have only to shift the separate plates with respect to one another in such a manner that the thorium atoms of the shifted plate become situated in the sites where, in the original $ThAl_2$ lattice, the neighbouring aluminium atoms were placed (from 0,0,0 to $\frac{1}{3},\frac{2}{3},\frac{1}{2}$). The ThAl lattice is then completed. The unit cell may be chosen as indicated in the figure. The length of the b-axis is determined by the fact that after placing a third "plate of $ThAl_2$" against the second one its atoms have landed on the a and c-coordinates of those of the first plate. The dimensions of the new cell are thus coupled with those of the $ThAl_2$ cell. In the ideal case the a-axis of ThAl (experimentally 4·42 Å) had

to be equal to the c-axis of $ThAl_2$ (experimentally 4·164 Å) and the c-axis of ThAl (experimentally 4·19 Å) had to equal the a-axis of $ThAl_2$ (experimentally 4·393 Å). So there has been a deformation of the hexagonal cell. The length of the a-axis of the ThAl cell can be calculated as follows: it has to be at least $\frac{1}{3}$ times the long diagonal of the $ThAl_2$ cell base (10·15 Å). However, the axis has to be even longer because we must replace one Al-Al distance in it by a Th-Al distance. If one uses the distances Al-Al and Th-Al as they are found in $ThAl_2$ then a is calculated as $a_{ThAl} = \frac{1}{2}\,10{\cdot}15\,(1 + 3{\cdot}28/2{\cdot}54) = 11{\cdot}6$ Å, while 11·45 Å is found experimentally.

In ThAl the "$ThAl_2$ cells" had their normal neighbours in two directions viz. in the original c-direction and in one of the a-directions. In the compound Th_3Al_2 the cells have only maintained their normal stacking along the c-direction. This c-direction coincides with the tetragonal c-axis of Th_3Al_2 If one looks therefore along this axis one sees "rods of $ThAl_2$ cells". Where the $ThAl_2$ cells in their original lattice possessed aluminium neighbours then are now flanked on all four sides by thorium atoms. Each thorium in its turn serves as a neighbour of four "$ThAl_2$ cells". Th_3Al_2, viewed along its tetragonal axis, thus shows a mosaic pattern of rhombs and squares, being respectively the nearly undeformed $ThAl_2$ cells ($a = 4{\cdot}25$ Å and $c = 4{\cdot}22$ Å compared with

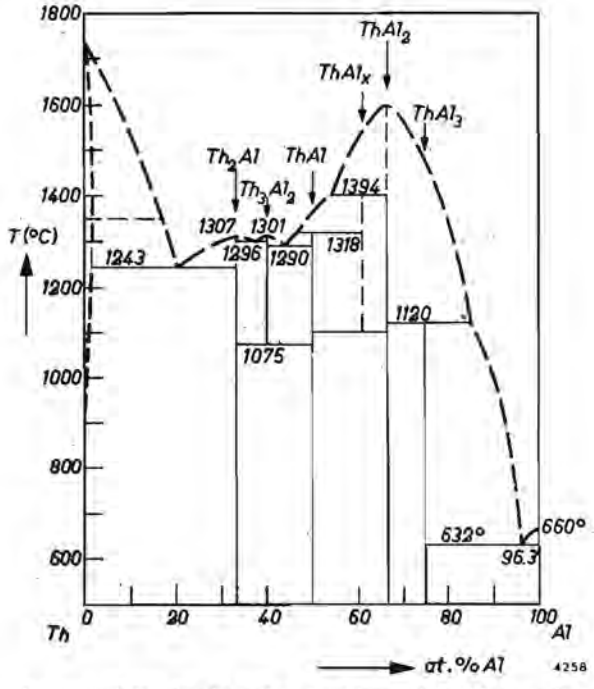

Fig. 14. Phase diagram of the Th-Al system as proposed by Murray, but slightly modified with respect to the composition of the $ThAl_x$ phase.

$a = 4{\cdot}39$ Å and $c = 4{\cdot}16$ Å in pure $ThAl_2$) and the pseudo-cubic "b.c.c. thorium cells" (with $a = 4{\cdot}22$ Å and $a' = 4{\cdot}25$ Å compared to 4·11 Å found for real b.c.c. thorium by Chiotti [10]). The $ThAl_2$ cells have only two thorium atoms in common per pair.

To sum up it may be stated that the structures of ThAl and Th_3Al_2 with respect to that of $ThAl_2$ take the position of a "layer structure" and of a "fibre structure", respectively.

4.4. *Conclusions*

The phase diagram of Grube and Botzenhardt of fig. 2 can now be extended. The present state of affairs is given by fig. 14. The thermo-analytical work on which this diagram is based was carried out by Miss Murray [22]. Our own observations, already partly communicated [18][19], where nowhere in contradiction. A point not yet fully elucidated is the composition and structure of the compound which has been called "Th_2Al_3" by Murray. Therefore this phase in fig. 14 is purposely called $ThAl_x$ and is, by reference to the speculative estimation of the composition in sec. 4.2, marked by the broken line at the site of $Th_{12}Al_{19}$. An important fact is further that neither Murray nor we ever obtained indications that the Th-Al compounds might possess detectable homogeneity ranges.

5. Binary system Ce-Al

5.1. *Introduction*

Since in the literature [5][6] the phase diagram, and even the structures of two of its compounds, $CeAl_2$ and $CeAl_4$ [7] already appeared to be well known, the original aim of our work was only to make some X-ray diagrams of the remaining compounds in order to be able to identify the phases in subsequent ternary compositions. This, however, proved to be less simple than expected, and after some abortive attempts this system also became the object of a systematic investigation. The results thus obtained deviated very much at some points from the data found in the literature. Though the results had already been published [23], they will be briefly described again in the next section.

5.2. *Results*

Just as for the system Th-Al, it seems useful to give an overall view of the possible compounds of cerium and aluminium. Table VIII therefore assembles the old results of Nowotny [7] and the newer X-ray data obtained by us. The compounds Ce_2Al found by Vogel [5] in 1912, and Ce_3Al_2 [6] which in 1943 was substituted for Ce_2Al and Ce_3Al, were sought in vain. On the other hand the compound Ce_3Al was rediscovered, and found to exist in two modifications:

TABLE VIII
Data of the compounds in the system Ce-Al

compound	structure: system	structure: space group (Intern. Tables): H.M. symbol	structure: space group (Intern. Tables): Schoenflies symbol	structure: space group (Intern. Tables): no.	type	lattice constants (Å)	"moles" per unit cell	atomic sites: cerium	atomic sites: aluminium	value of param.
$CeAl_4$ (low-temp. phase)	tetr.	$I4/mmm$	D^{17}_{4h}	139	$BaAl_4$ $D1_3$	$a=4{\cdot}374$ $c=10{\cdot}12$	2	$2a$: (0,0,0) $(\frac{1}{2},\frac{1}{2},\frac{1}{2})$	$4e$: (0,0,z) (0,0,$\bar{z}$) $(\frac{1}{2},\frac{1}{2},\frac{1}{2}+z)$ $(\frac{1}{2},\frac{1}{2},\frac{1}{2}-z)$ $4d$: $(0,\frac{1}{2},\frac{1}{4})$ $(\frac{1}{2},0,\frac{1}{4})$ $(\frac{1}{2},0,\frac{3}{4})$ $(0,\frac{1}{2},\frac{3}{4})$	$z=0{\cdot}376$
$CeAl_2$	cub.	$Fd3m$	O^7_h	227	$MgCu_2$ $C15$	$a=8{\cdot}064$ $\pm$ 0·001	8	$8a$: (0,0,0) $(\frac{1}{4},\frac{1}{4},\frac{1}{4})$ $(\frac{1}{2},\frac{1}{2},0)$ $(\frac{3}{4},\frac{3}{4},\frac{1}{4})$ $(\frac{1}{2},0,\frac{1}{2})$ $(\frac{3}{4},\frac{1}{4},\frac{3}{4})$ $(0,\frac{1}{2},\frac{1}{2})$ $(\frac{1}{4},\frac{3}{4},\frac{3}{4})$	$16d$: $(\frac{5}{8},\frac{5}{8},\frac{5}{8},)$ $(\frac{5}{8},\frac{7}{8},\frac{7}{8})$ $(\frac{7}{8},\frac{5}{8},\frac{7}{8})$ $(\frac{7}{8},\frac{7}{8},\frac{5}{8})$ $(\frac{1}{8},\frac{1}{8},\frac{5}{8})$ $(\frac{1}{8},\frac{3}{8},\frac{7}{8})$ $(\frac{3}{8},\frac{1}{8},\frac{7}{8})$ $(\frac{3}{8},\frac{3}{8},\frac{5}{8})$ $(\frac{1}{8},\frac{5}{8},\frac{1}{8})$ $(\frac{1}{8},\frac{7}{8},\frac{3}{8})$ $(\frac{3}{8},\frac{5}{8},\frac{3}{8})$ $(\frac{3}{8},\frac{7}{8},\frac{1}{8})$ $(\frac{5}{8},\frac{1}{8},\frac{1}{8})$ $(\frac{5}{8},\frac{3}{8},\frac{3}{8})$ $(\frac{7}{8},\frac{1}{8},\frac{3}{8})$ $(\frac{7}{8},\frac{3}{8},\frac{1}{8})$	
CeAl	ortho-rhomb.	$Cmcm$?	D^{17}_{2h}?	63?		$a=9{\cdot}27$ $b=7{\cdot}68$ $c=5{\cdot}76$	8?			
α-Ce_3Al	hex.	$P6/mmc$	D^4_{6h}	194	Ni_3Sn DO_{19}	$a=7{\cdot}043$ $\pm 0{\cdot}002$ $c=5{\cdot}451$ $\pm 0{\cdot}002$	2	$6h$: $\pm(x,2x,\frac{1}{4})$ $\pm(2\bar{x},\bar{x},\frac{1}{4})$ $\pm(x,\bar{x},\frac{1}{4})$	$2d$: $\pm(\frac{1}{3},\frac{2}{3},\frac{1}{4})$	$x=0{\cdot}829$
β-Ce_3Al	cub.	$Pm3m$	O^1_h	221	Cu_3Au $L1_2$	$a=4{\cdot}985$ $\pm 0{\cdot}001$	1	$3c$: $(\frac{1}{2},\frac{1}{2},0)$ $(\frac{1}{2},0,\frac{1}{2})$ $(0,\frac{1}{2},\frac{1}{2})$	$1a$: (0,0,0)	

α-Ce_3Al

This intermetallic compound was stable below 230 °C. It was formed, very sluggishly indeed, from the modification stable above this temperature in rather a difficult, inert way. Mechanical work accelerated the transformation. The pure form was obtained by powdering — with the help of the apparatus of fig. 5 — the specimen which was quenched from the molten state. This powder was afterwards annealed for a prolonged period of time on temperatures up to 230 °C in a good vacuum. We obtained the following values:

$$a = 7{\cdot}043 \pm 0{\cdot}002 \text{ Å}$$
$$c = 5{\cdot}451 \pm 0{\cdot}002 \text{ Å}$$
$$c/a = 0{\cdot}774$$

By using the trial-and-error method the Ni_3Sn structure (see table VIII) was found. For the 44 observed reflexions (including the very weak ones) the parameter value of 0·829 for the cerium atoms showed very good agreement between the calculated and the observed intensities. The reliability factor $R \equiv \sum_{44}(|I_o - I_c|)/(\sum_{44} I_o)$ in this case was 14%. The value 0·829 was chosen for geometric considerations: the mutual distances of the cerium atoms equal each other in that case. The parameter x is found as one of the roots of the equation $1 - 6x + 6x^2 = \frac{1}{4}(c/a)^2$, where c and a are the lattice constants of the unit cell. The "ideal" value of $\frac{5}{6}$ (= 0·833) gave $R = 17\%$. The calculated values of spacings and intensities are compared with the observed ones in table IX.

TABLE IX

Observed and calculated spacings and intensities of powder reflexions of the compound α-Ce_3Al

hkl	d(Å)		I_{obs}	I_{calc}	hkl	d(Å)		I_{obs}	I_{calc}
	obs.	calc.	(arb. units)			obs.	calc.	(arb. units)	
100		6·10			311 }	1·617	1·615	8	6
001		5·45			113 }				
101	4·07	4·06	65	52	203	1·561	1·561	43	38
110	3·53	3·52	20	21	400		1·525	<2	6
200	3·05	3·05	55	60	222	1·482	1·479	37	43
111		2·958	<2	0	401	1·472	1·469	35	31
002	2·723	2·725	60	59	312		1·437	<2	1
201	2·666	2·661	235	248	213	1·427	1·427	3	3
102	2·498	2·488	3	3	320		1·399	<2	0
210	2·306	2·305	14	8	004	1·360	1·363	5	5
112	2·156	2·155	9	8	321 }	1·358	1·355	8	6
211	2·123	2·123	4	9	303 }		1·355		
300 }	2·031	2·033	38	32	410 }	1·330	1·331	8	10
202 }		2·033			402 }		1·331		
301	1·907	1·905	6	1	104 }		1·330		
003		1·817	<2	0	411		1·293	<2	1
220 }	1·759	1·761	48	42	114		1·271	<2	2
212 }		1·761			223		1·265	<2	0
103		1·741	<2	4	322 }	1·245	1·244	7	6
310		1·692	<2	0	204 }		1·244		
221		1·676	<2	0	313		1·238	<2	3
302	1·633	1·630	2	4	500		1·220	<2	1

The principal distances are

Ce — Ce	3·43 Å
Ce — Al	3·46 Å
Ce — Al	3·70 Å

β-Ce_3Al

This compound could be obtained in a practically pure state by annealing α-Ce_3Al powder at 500 °C during ½ hr in vacuo and quenching subsequently. The X-ray diagram showed 29 lines and indicated a Cu_3Au structure. Iandelli [24]) recently confirmed this. The lattice parameter determined by us is $a = 4{\cdot}985 \pm 0{\cdot}001$ Å, while Iandelli finds $a = 4{\cdot}980$ Å. The observed reflexions, together with the measured and calculated values of spacings and intensities are to be found in table X. The parameterless positioning of both kinds of atoms yields a value of $R \equiv (\sum_{29} |I_o - I_c|)/(\sum_{29} I_o) = 17\%$.

The distance Ce-Ce is equal to the Ce-Al distance, namely 3·525 Å.

The compound is formed from α-Ce_3Al at a temperature of ca 250 °C. In fig. 15 we have tried to demonstrate — using projections of both structures — the transformation from one structure to the other. Probably dislocations and stacking faults (cold work) play a prominent part. The heat effect can clearly be observed but often retardation occurs, particularly in the direction β-$Ce_3Al \rightarrow$ α-Ce_3Al. α-Ce_3Al melts congruently at 655 °C. Vogel [5]) found 614 °C.

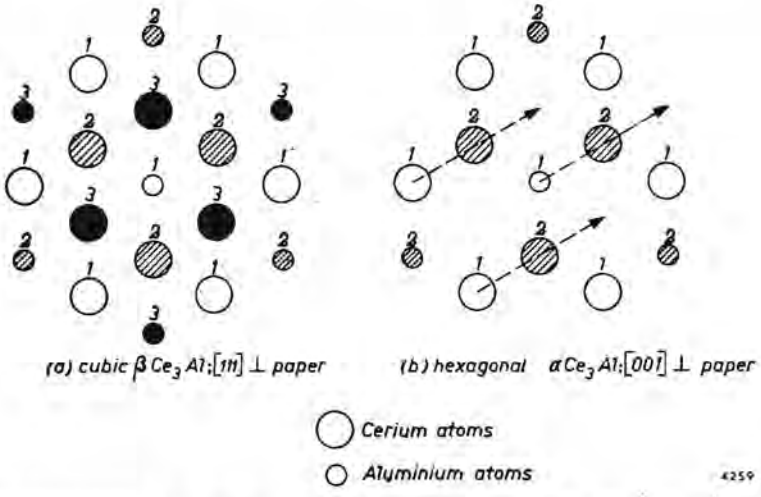

Fig. 15. The projections of the two structures of Ce_3Al. The numbers indicate the sequence of the layers. Layer 3 in fig. (*b*) coincides with layer 1. If this layer is shifted in the direction of the arrows the sequence becomes the same as that in fig. (*a*). The allotropic transformation is thus demonstrated, though actually a shifting of all the atoms of a layer simultaneously does not take place.

TABLE X

Observed and calculated spacings and intensities of powder reflexions of the compound β-Ce_3Al

hkl	d(Å)		I_{obs}	I_{calc}	hkl	d(Å)		I_{obs}	I_{calc}
	obs.	calc.	(arb. units)			obs.	calc.	(arb. units)	
100	4·97	4·98	62	74	330 / 411	1·172	1·175	7	5
110	3·52	3·52	57	53	311	1·144	1·144	70	54
111	2·878	2·878	363	358	420	1·115	1·115	65	52
200	2·493	2·493	186	240	421	1·088	1·088	8	6
210	2·230	2·230	36	51	332	1·063	1·063	3	4
211	2·031	2·035	28	40	422	1·017	1·018	46	36
220	1·760	1·763	142	178	430 / 500	0·9977	0·9971	3	4
300 / 221	1·661	1·662	19	22	510 / 431	0·9777	0·9777	8	5
310	1·577	1·577	14	10	333 / 511	0·9594	0·9594	48	32
311	1·503	1·503	177	153	432 / 520	0·9267	0·9258	7	7
222	1·439	1·439	51	51	521	0·9104	0·9102	4	3
320	1·381	1·383	9	9	440	0·8815	0·8813	13	10
321	1·330	1·332	15	12	441	0·8677	0·8678	2	3
400	1·247	1·246	23	25	531	0·8429	0·8427	47	25
410 / 322	1·210	1·209	11	10					

CeAl

This phase was obtained in a rather pure state by annealing the specimen — which was quenched from the molten state and afterwards powdered — for 5 days at 780 °C. The powder diagram showed, apart from the CeAl lines, only a few very weak lines belonging to the phase $CeAl_2$. The diffraction pattern of CeAl can be indexed on the basis of an orthorhombic unit cell with

$$a = 9{\cdot}27 \text{ Å}$$
$$b = 7{\cdot}68 \text{ Å}$$
$$c = 5{\cdot}76 \text{ Å}$$

Andelli [25]) suggested that CeAl should possess a "b.c.c. A_2-like structure" (by which the CsCl-structure is probably meant). The observations mentioned

TABLE XI

X-ray powder diagram of CeAl (Mo$K\alpha$)

The reflexions have been indexed on the basis of an orthorhombic unit cell

hkl	d(Å)		I_{obs} (arb. units)	hkl	d(Å)		I_{obs} (arb. units)
	obs.	calc.			obs.	calc.	
110	5·919	5·926	16	511	1·724	1·723	40
200	4·648	4·645	43	023	1·716	1·716	30
111	4·122	4·127	28	241	1·698	1·698	30
020	3·844	3·847	17	332	1·628	1·628	105
021	3·196	3·198	77	223	1·610	1·609	20
220	2·950	2·963	66	313	1·595	1·595	80
310+002	2·876	2·873+2·875	102	600	1·548	1·548	58
221	2·637	2·634	64	512	1·530	1·530	5
311+112	2·571	2·570+2·587	147	530	1·505	1·505	35
130	2·471	2·472	22	151	1·4677	1·4680	12
202	2·441	2·444	16	620+004+441	1·4362	1·4365+1·4376+1·4347	25
022	2·300	2·303	14	621+114	1·3943	1·3936+1·3971	25
222	2·061	2·063	5	602	1·3635	1·3633	25
312	2·031	2·032	24	043	1·3576	1·3578	20
330	1·970	1·975	45	351	1·3394	1·3402	35
421+132	1·876	1·879+1·874	25	532	1·3333	1·3332	30
041+113	1·824	1·824+1·824	45	513	1·3152	1·3146	8
510+402	1·812	1·806+1·807	20	710	1·3075	1·3079	12
240	1·777	1·777	10	314+622	1·2855	1·2857+1·2850	30

here give contradictory evidence. The observed reflexions and their corresponding spacings are given in table XI, while the spacings calculated on the basis of the unit cell given above are included for comparison. Allotropy of the compound was not observed either. The extinctions lead us to suspect a space group *Cmcm* (no. 63) or Cmc_2 (no. 36) — only reflexions with $h + k = 2n$ are found and of the $(h0l)$-reflexions only those with $l = 2n$. The compound melts with decomposition, giving a liquid and $CeAl_2$. The peritectic temperature was found to be 780 °C by Vogel [5]), 825 °C by Rolla c.s. [6]), and 845 °C by Van Vucht [23]).

$CeAl_2$

The $CeAl_2$ made by us was exceedingly brittle and could be readily powdered. It yielded a very beautiful diagram with Mo$K\alpha$-radiation. From a number of strong reflexions in the back-reflexion region a lattice constant $a = 8{\cdot}064 \pm 0{\cdot}001$ Å could be calculated. From some very weak reflexions in diagrams of CeAl which had been annealed for 1 hour at a temperature of 780 °C it was possible, though far less accurate, to calculate $a = 8{\cdot}036 \pm 0{\cdot}008$ Å. Wallbaum [26]) found $8{\cdot}055 \pm 0{\cdot}007$ Å and Nowotny [7]) thought he had found a range of homogeneity of the compound in which the lattice parameter varied from $a = 8{\cdot}106$ Å (stoichiometric) to $a = 8{\cdot}136$ Å (towards the CeAl side). The compound is said to melt at 1465 °C.

$CeAl_4$

This compound has at 1005 °C a transformation point between two allotropic forms. At 1250 °C it melts, with decomposition, giving a liquid and $CeAl_2$. Only the low-temperature modification seems to be found at room temperature with X-rays. For the investigation described here the compound was only of minor importance, therefore we did not try to add to the data pusblished by Nowotny [7]). He found for the lattice dimensions of the tetragonal compound

$a = 4{\cdot}374$ Å
$c = 10{\cdot}12$ Å

Iandelli [24]) found $a = 4{\cdot}383$ Å
$c = 10{\cdot}036$ Å

5.3. *Conclusions*

As a result of our investigations a new phase diagram can now be given. This is shown in fig. 16. To sum up, the changes amount to the following: Instead of the compound Ce_3Al_2, discovered in 1943 by Rolla et al. [6]) — which could not be confirmed — two allotropic modifications of Ce_3Al were demonstrated. One of these, α-Ce_3Al, is stable below 250 °C, the other, β-Ce_3Al, above this temperature. The compound $CeAl_2$, published by Vogel [5]) in 1912 was not found.

Again in this system it is interesting to relate the volume effects occurring in the formation of the various compounds from the elements. Since cerium at

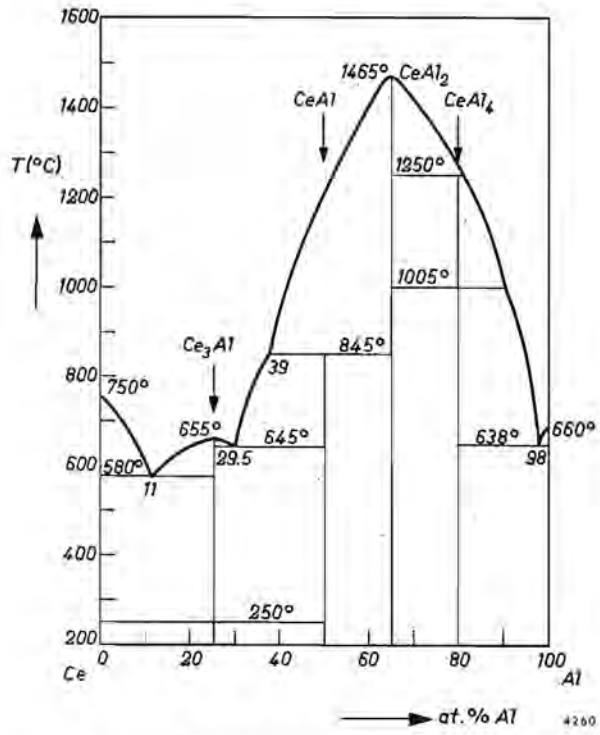

Fig. 16. Diagram of Vogel (1912), combined with our own results for compositions $\leqslant$ 50 atomic per cent Al.

room temperature can have two f.c.c. modifications (cf. sec. 2) — one at normal and one at high pressures — it is possible to define ΔV in two ways: one for ΔV with respect to the "small" (high-pressure) cerium, and one for ΔV with respect to the normal cerium. Both sets of values have been plotted in fig. 17. It must be remarked that evidently β-Ce_3Al contains the "big Ce" (in the figure the γ-modification) and α-Ce_3Al the high-pressure form (α-modification). Furthermore it appears that the volume effect does not change sign and thus resembles that in the Th-Al system, if α-Ce is taken as the standard. This might be an indication that the normal electronic configuration of cerium in its compounds with aluminium, at least in those that are stable at room temperature, is that of the high-pressure modification. Perhaps this is better expressed by saying, since in principle mixtures of the two kinds of cerium are possible, that the contracted cerium is there the major constituent. However, it appears that the volume effects in the systems La-Al and Pr-Al (lanthanum and praseodymium showing no such "allotropy" like cerium) are virtually identical with the broken line *I* in the figure; therefore such a conclusion is not justified.

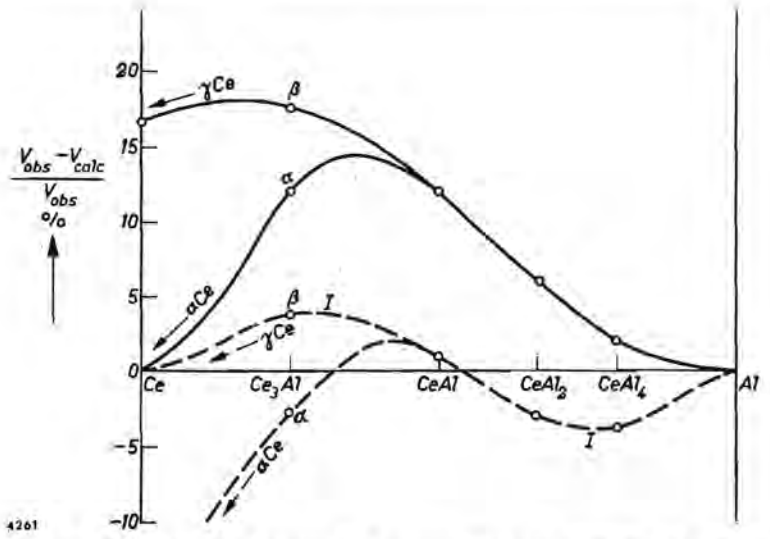

Fig. 17. The relative difference between the measured volumes (V_{obs}) and the volumes calculated by adding the atomic volumes of the elements Ce and Al (V_{calc}) for their various compounds. For the full curves the volume of Ce in the high-pressure α-modification (a = 4·85 Å) has been used to calculate. For the broken lines, the normal-pressure γ-modification (a = 5·165 Å) has been used.

6. Binary system Th-Ce

6.1. *Introduction*

At the start of this investigation no information was available from the literature. After publication of our own results [27]), however, it appeared that in a difficultly accessible report of the U.S. Atomic Energy Commission [28]) a remark was made that cerium and thorium were mutually completely soluble at room temperature. About four months after the appearance of our results they were confirmed and completed in an article on the same subject by Weiner, Freeth and Raynor [11]).

6.2. *Results*

All the compositions examined in this system at room temperature possessed the cubic close-packed f.c.c. structure. The lattice constant of the unit cell was determined as a function of the cerium content. These data are given in fig. 18, together with the values observed by Weiner et al. We have not tried to give the shape of the solidus though some preliminary experiments indicated the absence of a minimum. However, thanks to Weiner et al., it is possible now to show a phase diagram (fig. 19).

The lattice-parameter data given by Weiner et al. are more exact and numerous than those communicated by us. The interpretation of the data at the far thorium side, however, is very disputable. In a discussion of their paper [29])

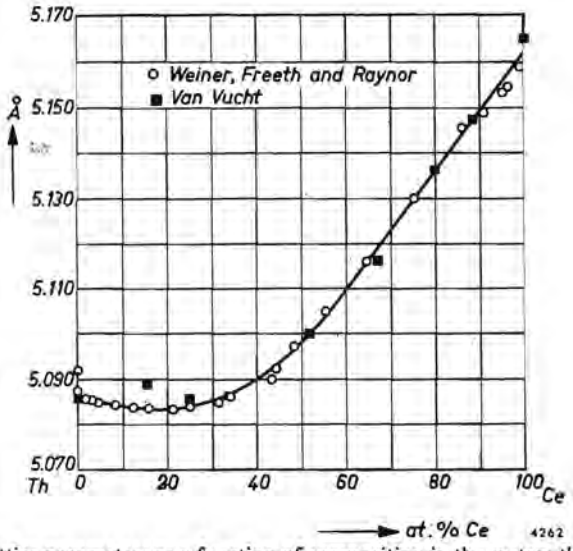

Fig. 18. Lattice parameters as a function of composition in the system thorium-cerium.

the possibility was pointed out that the steep fall of the lattice-parameter curve at this side might be ascribable to a scavenging action of the cerium for impurity atoms, e.g. dissolved hydrogen. The general behaviour of the lattice parameter

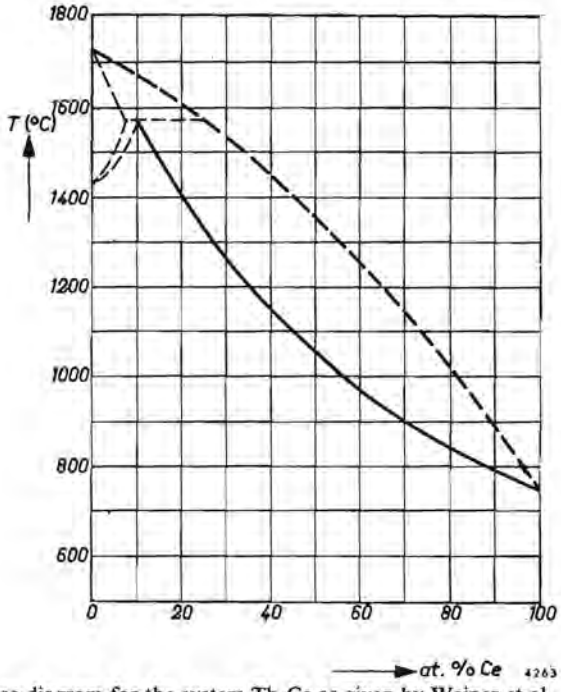

Fig. 19. Phase-diagram for the system Th-Ce as given by Weiner et al., but slightly modified towards the Ce side in accordance with our own experiences.

is explained by all authors on the basis of the occurrence of a new electronic configuration of the dissolved cerium atoms, the same configuration that is caused by a pressure rise or a temperature decrease. In this picture one should expect for the curve at the thorium side a tangent with a slope to intersect the 100%-Ce axis just at the parameter value for the small cerium $a = 4{\cdot}85$ Å. Weiner et al. stated in their reply [30]) that the steep fall was real and did not occur, for example, in the thorium-lanthanum system. Furthermore they denied the presence of hydrogen in their specimens.

6.3. *Conclusions*

Thorium and cerium are completely miscible in the f.c.c. phase. An important part of the phase diagram is now known, due to the work of Weiner et al. [11]). In the light of the next section their view of the diagram is reproduced with slight modifications at the cerium side.

7. The element cerium

7.1. *Introduction*

Various investigators have reported that cerium possessed a transformation point rather close to its melting point. These transformation points varied considerably, just like the given melting points, as shown in table XII. In connection with the phase diagram of Th-Ce and the remark [29]) about the possibility of cerium — like thorium — having perhaps the b.c.c. structure just below its melting point, a cursory investigation was dedicated to this subject.

TABLE XII

List of melting points and transformation points of cerium, as found by various authors

melting point (°C)	transformation point (°C)	author(s)
815	710	J. Loriers [39]), 1948
	740±10	
795	700	D. H. Ahmann [32]), 1950
785	—	D. Peterson et al. [33])
804	754	F. H. Spedding and A. H. Daane [34]), 1954.
750	695	J. H. N. van Vucht [23]), 1957

7.2. *Experimental*

For the X-ray work, a Unicam high-temperature camera was used in which the specimen in the form of a polished cube was placed on a rotating alundum table. Just below this the thermocouple was fixed. The specimen was thus placed in the centre of a sphere, formed by two halves separated by a slit. The halves of the sphere could be heated up to 1200 °C. The whole was placed in a vacuum. The X-rays found their way through a narrow window in the shape of a ring, covered by a thin foil of aluminium. On the outside of this window the film cassette was placed. Walls and top of the evacuated part of the camera were water-cooled. The vacuum reached (while pumping) was of the order of 10^{-4} - 10^{-5} mm Hg. This once caused the series of experiments to be interrupted in order to file off the oxide formed on the specimen. The exposure time was always ½ hr, working with unfiltered Cu*K*-radiation.

7.3. *Results*

We started our first series of experiments, after an exposure at room temperature, with an exposure at a temperature just below the transformation point found earlier (695 °C). Apart from the lines of the cerium f.c.c. phase, given in table XIII some rather weak reflexions were observed that could not be found in the room-temperature radiograph. These were identified as Ce_2O_3 lines. They were still present in the room-temperature pattern of the last column, but had disappeared after the removing of the oxide skin. Some other lines were found that had to be ascribed to platinum metal precipitated on the specimen. The first run consisted of exposures at three temperatures increasing from 690 °C to 720 °C. The line pattern of f.c.c. cerium, given in table XIII, became, compared with the oxide lines, continually weaker. In particular the intensity of the (200) reflexion decreased abnormally. Therefore the specimen was cooled down to room temperature in order to file off the skin formed by the reaction of the metal with the diluted gases in the camera.

In the second run (table XIV) we observed a broadening of all lines. We measured at temperatures increasing from 735 °C up to 770 °C, where the specimen, after some little time of exposure, melted down. The specimen was found still partly upright but was very much deformed. The metal had attacked the small Al_2O_3 table seriously. Therefore the experiment was repeated, using this time a thin plate of CeO_2 in order to protect the Al_2O_3. The result is given in table XV. After opening the camera this time the cerium specimen proved to be deformed again. Now no chemical attack of any extent had taken place, though the CeO_2 plate had blackened. The radiograph, taken at room temperature, showed line widening; the picture taken at 770 °C, however, did not. The picture at room temperature after the hot exposures showed again stronger oxide lines and a nearly extinguished cerium pattern of which the (200) was especially weak.

TABLE XIII

Lines of the f.c.c. Ce phase, observed at various temperatures

$10^3\sin^2$ (Cu$K\alpha$) / *hkl*	room temp.		690 °C		705 °C		720 °C		room temp.	
	obs.	calc. $a=5{\cdot}159$ Å	obs.	calc. $a=5{\cdot}156$ Å	obs.	calc. $a=5{\cdot}170$ Å	obs.	calc. $a=5{\cdot}145$ Å	obs.	calc. $a=5{\cdot}119$ Å
111	67·3	66·9	67·6	67·0	67·0	66·6	67·4	67·3	68·6	68·0
200	88·9	89·2	89·3	89·3	88·9	88·8	89·2	89·7	91·0	90·6
220	178·2	178·4	178·2	178·6	177·0	177·6	179·7	179·4	181·6	181·2
311	245·3	245·3	245·2	245·6	243·1	244·3			247·6	249·2
222	267·7	267·6	268·4	268·0	267·9	266·5				
lattice constant	5·16±0·02 Å		5·16±0·02 Å		5·17±0·01 Å		5·15±0·01 Å		5·12±0·02 Å	
remarks			(200) weak		oxide lines growing in intensity at the cost of f.c.c. Ce lines					

First run with first specimen. After cooling, the specimen was freed from oxide by filing. Then it was replaced on the alundum table for the second run.

TABLE XIV

Powder reflexions of the f.c.c. Ce phase in the second run

$10^3\sin^2\theta$ Cu$K\alpha$ / *hkl*	735 °C		755 °C		770 °C	
	obs.	calc. $a=5{\cdot}168$ Å	obs.	calc. $a=5{\cdot}198$ Å	obs.	calc. $a=5{\cdot}228$ Å
111	68·8	66·7	65·9	65·9	66·7	65·1
200	90·7	88·9	89·5	87·9	86·9	86·1
220	175·7	177·8	174·2	175·8	172·1	173·7
311	242·6	244·4				
222						
lattice constant	5·17±0·03 Å		5·20±0·03 Å		5·23±0·03 Å	
remarks	all f.c.c. Ce lines were strong but very broadened					

The broadening of the lines is probably due to a deformation of the specimen. After exposure at 770 °C the specimen melted in the camera and poured onto the thermo-couple.

TABLE XV

Lines of the f.c.c. Ce phase; third run

$10^3\sin^2\theta$ Cu$K\alpha$ / *hkl*	room temp.		770 °C		room temp.	
	obs.	calc. $a=5{\cdot}155$ Å	obs.	calc. $a=5{\cdot}272$ Å	obs.	calc. $a=5{\cdot}137$ Å
111	67·5	67·0	65·2	64·1	67·0	67·5
200	90·1	89·3	85·4	85·4	87·4	90·0
220	177·0	178·6	169·3	170·9	183·5	180·0
311	246·2	245·6	232·8	235·0	247·1	247·5
222			259·0	256·3		
lattice constant	5·16±0·03 Å		5·27±0·02 Å		5·14±0·03 Å	
remarks	lines broadened				lines weak, oxide lines stronger	

The new specimen was now placed on a cerium oxide plate. The specimen did not melt completely but proved afterwards to be in a very deformed state.

7.4. *Discussion*

It was evident immediately that from 690 to 770 °C only one phase — the f.c.c. phase — of cerium had been found. Anyway there was no evidence that at these temperatures any other phase of cerium was stable.

The results seem to agree with the work of Dialer and Rothe [31]). These authors believe that at higher temperatures the normal f.c.c. cerium lattice with $a = 5{\cdot}152$ Å is transformed into a f.c.c. phase with $a = 5{\cdot}136$ Å. The latter parameter was observed with a cerium specimen that had been melted (they did not mention how or in what kind of crucible this had been done). Furthermore they indexed erroneously some oxide reflexions as — otherwise forbidden — reflexions of the f.c.c. cerium lattice).

The attack on the Al_2O_3 table by cerium can have been caused only by a chemical reduction:

$$Al_2O_3 + Ce \rightarrow Ce \text{ oxide} + Al,$$

where the aluminium goes into solution in the cerium metal. The lattice constant therefore decreases from $5{\cdot}16 \pm 0{\cdot}02$ Å to $5{\cdot}12 \pm 0{\cdot}02$ Å (table XIII, room temperature) which is in agreement with the lattice parameter found for cerium in the two-phase region Ce-Ce_3Al, where a value $a = 5{\cdot}116$ Å [23]) was found. If this or a similar process (e.g. contamination of the specimen by Pt) is indeed to be held responsible for the small lattice parameter of the cerium specimen after heating, then the lattice parameter at high temperatures (e.g. 770 °C: $5{\cdot}23 \pm 0{\cdot}03$ Å) will be found to be too small. Thus the fact that at 690 °C a lattice-parameter value is found that is virtually equal to the value at room temperature (before heating) becomes meaningless as a criterion if it is used to deduce a phase transformation. (Besides, a degassing process, i.e. a loss of hydrogen by the first specimen which was not previously degassed, might result in a small lattice-parameter decrease.)

These assumptions were confirmed by the experiment in which the cerium specimen was placed on a CeO_2 base. Now we found both at 770 °C and at room temperature afterwards a larger lattice parameter, viz. $5{\cdot}27 \pm 0{\cdot}02$ Å and $5{\cdot}14 \pm 0{\cdot}03$ Å, respectively.

Summarizing it may be said that, under the conditions obtaining in the high-temperature camera used, we were unable to observe any clear phase transformation. In this connection it is doubtful whether the halting point, observed earlier in thermo-analytical experiments, was not due to reactions with foreign materials, e.g. crucibles. The great variation of the temperatures given by diverse investigators may be explained in this way.

7.5. *Contracted f.c.c. phase of cerium*

As mentioned in sec. 2, the f.c.c. cerium modification which is stable at room temperature can change under influence of pressure or temperature or both into a different form with the same crystal structure but in which the atoms possess a smaller radius. The length of the cell edge decreases from 5·16 Å to 4·85 Å, the radius of the cerium atoms from 1·83 Å to 1·71 Å. One might say that the contracted state corresponds to cerium with a valency of four and that the nor-

mal room-temperature modification agrees with trivalent cerium. With this property cerium occupies an exceptional position in the sequence of the rare earth metals. (In this sequence from La to Lu cerium indeed is too small, be it only 0·01 Å.) Its exceptionality is also expressed in the lattice dimensions of the intermetallic compounds: Iandelli [24]) nowhere finds a well-fitting value of the cerium-compound dimensions between the analogous lanthanum and praseodymium compounds. The values for cerium are always too small. One might assume that this is caused by an admixture of a fraction of "small atoms". Already the presence of 8% of atoms with $r = 1{\cdot}71$ Å causes, if distributed at random in the lattice of the "large atoms", a decrease of the average radius from 1·84 Å to 1·83 Å (using Vegard's law). In fact this would mean that the equilibrium

$$Ce_{large} \rightleftarrows Ce_{small}$$

at room temperature and 1 atm pressure does not lie totally over to the left-hand-side. This situation, as far as the entropy is concerned, is more probable than one in which all Ce atoms possess the electronically expanded structure. Besides, there is the possibility that the "small" state of cerium is stabilized by some foreign atoms present as impurities in the room-temperature metal.

In some of the alloys described in this paper it is possible to discern this "atomic isomery" of cerium. There are two modifications of the compound Ce_3Al. The α-form, stable below 250 °C, contains cerium with a radius of 1·71 Å, calculated from the Ce-Ce distance. The β-modification, stable above 250 °C, is 7% more voluminous and contains cerium of which the interatomic distance indicates a radius of 1·77 Å. Here it seems that, like in the high-temperature form, an already appreciable part of the cerium atoms, under the influence of the aluminium atoms, is present in the "small state". When the temperature is lowered this proportion tends to increase. Then, however, a state is suddenly reached where a lower energy level is produced if the Ce_3Al transforms into the hexagonal modification. It would be interesting to compare the behaviour in thermal expansion of the intermetallic compounds of cerium with the corresponding La and Pr compounds.

The shape of the curve of fig. 18, where the lattice parameters of thorium-cerium alloys are given suggests that the first cerium atoms that are dissolved in the f.c.c. thorium lattice adopt the electronic configuration belonging to the "quadrivalent" form. This occurs under the influence of the forces — exerted as compressive forces on the cerium atoms — that keep the thorium atoms together in their lattice. These forces can be imagined as to be analogous to the forces exerted in the transformation of pure cerium metal [13]) [14]).

8. Ternary diagram Th-Ce-Al

8.1. *Introduction*

When the above three binary systems are used to build up the ternary diagram

the following question becomes very important: What is the extent of the homogeneity ranges of the various phases? A single-phase region, with a "finite" composition range in a binary boundary system, will extend into the ternary diagram as a region with a "finite" area. A "point-shaped" boundary phase, on the contrary, can propagate itself as a single-phase line into the ternary diagrams.

A priori one may expect that compounds formed by metals that differ greatly in atomic radius (except the interstitial compounds) exhibit very small stoichiometric differences. The fact that it was nearly impossible to obtain completely homogeneous metallographic specimens accords with very narrow one-phase regions. As for the Th-Al compounds neither Murray [22]) nor we were able to find indications for stoichiometric variations.

If, starting from such a "point"-shaped binary single-phase, the ternary system is entered, then one can use two ways of maintaining a single phase. The first one is obvious and consists of the substitution of one kind of atom in the binary compound by the atoms of the new element. This is free from difficulties only if radius and chemical nature of the atoms in question do not differ too widely. One can picture as a second method a substitution of one kind of atom, by atoms that may differ in volume and nature, and a simultaneous creation of vacancies or interstitially placed atoms of the third kind. It might be possible, for example, that, if one replaces some thorium atoms of a Th-Al compound by somewhat larger cerium atoms, the homogeneous state is stabilized by omitting an aluminium atom here and there. In the first case the single-phase line in the ternary diagram is parallel to one side of the triangle, in the latter case not.

8.2. *Results*

A review of the compositions examined is given in table XVI. Each X-ray diagram obtained was compared with those of the binary compounds and the elements. The percentage of the detected phases was estimated from the intensities of the line patterns in the diagrams and from metallographic experiments. The latter were, however, rather difficult because of the chemical reactivity of the specimens, during polishing, with respect to air and aqueous solutions. Furthermore the brittleness caused numerous pits and cracks, from metal grains falling out of the metallographic cross-sections. Nevertheless in most cases we were successful, albeit with some trouble, in establishing a certain number of phases.

The lattice dimensions in table XVI have been calculated from in part rather poor diagrams that always exhibited a multiphase composition. In spite of many precautions, we always found lines of the oxides (and sometimes of the carbides) of thorium and cerium or mixtures, which indeed is not surprising with these getter materials.

8.3. *Discussion*

On the basis of the mutual solubility of cerium and thorium, as found in

TABLE XVI

Samples of ternary composition in the diagram Th-Ce-Al

no.	composition atomic percentage			treatment of sample	X-ray diagram **)			polished cross-section		
	Th	Ce	Al		% phase 1	% phase 2	% phase 3	% phase 1	% phase 2	% phase 3
1*a*	52·1	15·3	32·6	melted in A-arc furnace, crushed, 1 hr 500 °C vac.	100 Th_2Al	—	—	—	—	—
1*b*				sintered in high vac., crushed, 1 hr 500 °C vac.	90 Th_2Al	5 Th	5 $CeAl_2$	—	—	—
2*a*	58·3 (7)	8·3 (1)	33·3 (4)	melted in A-arc. furn., crushed	100 Th_2Al	—	—	95	5 dendr. (oxide?)	—
2*b*				treated as 2*a*, then 1 hr 500 °C vac.	100 Th_2Al	—	—	—	—	—
3*a*	50·0 (6)	16·7 (2)	33·3 (4)	melted in A-arc furn., crushed	100 Th_2Al	—	—	90	8 dendr.	2 at grain boundaries
3*b*				as 3*a* + 1 hr 800 °C vac.	100 Th_2Al	—	—	—	—	—
4*a*	33·3 (4)	33·3 (4)	33·3 (4)	*) 1 hr 500 °C high vac.	70 Th_2Al $a=7·65$ $c=5·84$	30 α-Ce_3Al	—	—	—	—
4*b*				not annealed	very diffuse and unclear			—	—	—
5*a*	16·7 (2)	50·0 (6)	33·3 (4)	1 hr 500 °C high vac.	35 Th_2Al	55 α-Ce_3Al	10 CeAl	—	—	—
5*b*				not annealed	very diffuse and unclear			—	—	—
11	25 (1)	50 (2)	25 (1)	not annealed	75 Th_2Al	20-25 α-Ce_3Al $a=7·11$ $c=5·33$	0-5% Th (?) $a\approx5·19$	60 grey	35 white	5 dark spots
12	12·5 (1)	62·5 (5)	25 (2)	1 day 500 °C high vac., then quenched	40 Th_2Al	55-60 α-Ce_3Al $a=7·09$ $c=5·42$	0-5 % Th (?)	65 eut. grey-white	35 white	—
13	6·25 (1)	68·75 (11)	25 (4)	1 day 500 °C high vac., quenched	10 Th_2Al	90 α-Ce_3Al $a=7·06$ $c=5·44$	—	95 dark grey	5 white	—
14	66·7 (8)	8·3 (1)	25 (3)	1 hr 500 °C high vac.	90 Th_2Al $a=7·61$ $c=5·87$	10 Th(Ce) $a=5·078$	—	90 white	10 dark at grain boundaries	—
21	25 (1)	25 (1)	50 (2)	1 day 500 °C high vac., quenched	20 Th_2Al $a=7·626$ $c=5·810$	40 ThAl	40 CeAl	70 white	30 grey + dark	—
22	37·5 (3)	12·5 (1)	50 (4)	two days 500 °C high vac.	0-5 % CeAl?	80 ThAl	20 $ThAl_2$	90 white	9 grey	1 black?
23	12·5 (1)	37·5 (3)	50 (4)	1 hr 500 °C high vac., two days 400 °C high vac.	60 CeAl 90 CeAl	40 $CeAl_2$ 10 $CeAl_2$	— —	— 30 white	— 60 grey	— 10 dark
31	40 (2)	40 (2)	20 (1)	1 hr 500 °C high vac.	60 Th_2Al $a=7·634$ $c=5·814$	10 α-Ce_3Al	30 Th (Ce) $a=5·09$	60 white	30 grey	10 dark
32	5 (1)	75 (15)	20 (4)	1 hr 500 °C high vac.	—	30 α-Ce_3Al $a=6·96$ $c=4·93$ 30 β-Ce_3Al $a=4·93$	40 Th(Ce) $a=5·13$	85 white	5 grey	10 dark
41	75 (15)	15 (3)	10 (2)	1 hr 500 °C high vac.	30 Th_2Al $a=7·611$ $c=5·897$	—	70 Th(Ce) $a=5·08$	70 white	30 grey	—
42	15 (3)	75 (15)	10 (2)	1 hr 500 °C high vac.	—	40 α-Ce_3Al	60 Th(Ce) $a=5·11$	40 white	60 grey	—
51	12 (1)	12 (1)	76 (6)	1 hr 500 °C high vac.	90 $ThAl_3$	10 $ThAl_2$	—	90 white	10 grey	—

*) All further specimens have been melted in the argon-arc furnace and crushed.

TABLE XVII

Lattice constants of the various compositions with Th_2Al structure

Composition	a	c	V	c/a
	Å	Å	Å^3	
$Th_{16}Al_8$	7·616	5·861	340·0	0·770
$Th_{14}Ce_2Al_8$	7·621	5·835	338·9	0·766
$Th_{13}Ce_3Al_8$	7·626	5·813	338·1	0·762
$Th_{12}Ce_4Al_8$*)	7·606	5·860	339·0	0·770

*) The last composition is the overall composition of a non-homogeneous specimen.

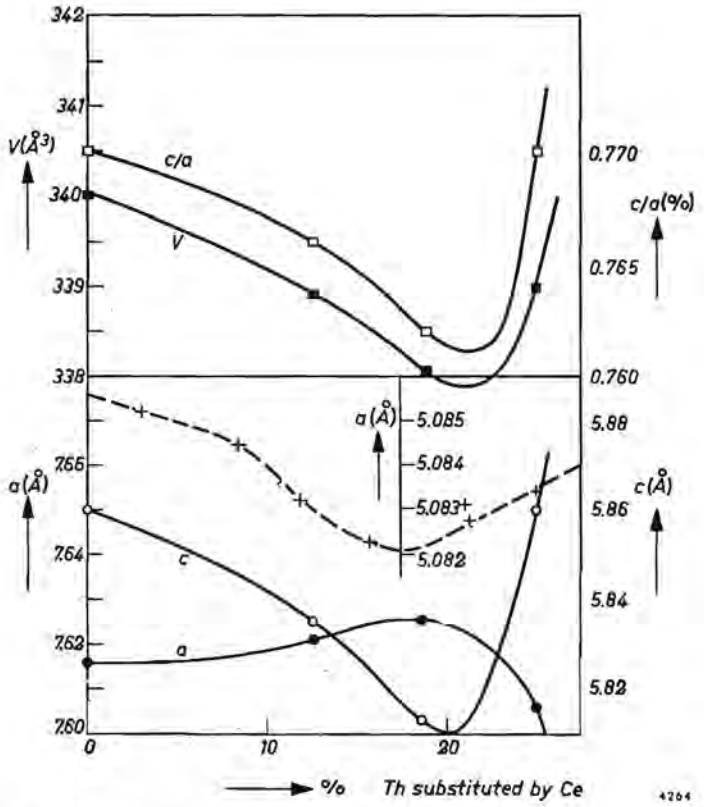

Fig. 20. Lattice parameters, volume and c/a of the tetragonal Th_2Al cell plotted against the percentage of cerium atoms substituting for thorium atoms. Compare with the conduct of the f.c.c. thorium lattice: broken line (data of Weiner et al.).

sec. 6, we expected these atoms to be able to act as each other's substituents in their compounds with aluminium as well. This has now been proved experimentally. The substitution is observed best in the compound Th_2Al. While retaining the $CuAl_2$ structure this compound appears to be able to exchange some 20%

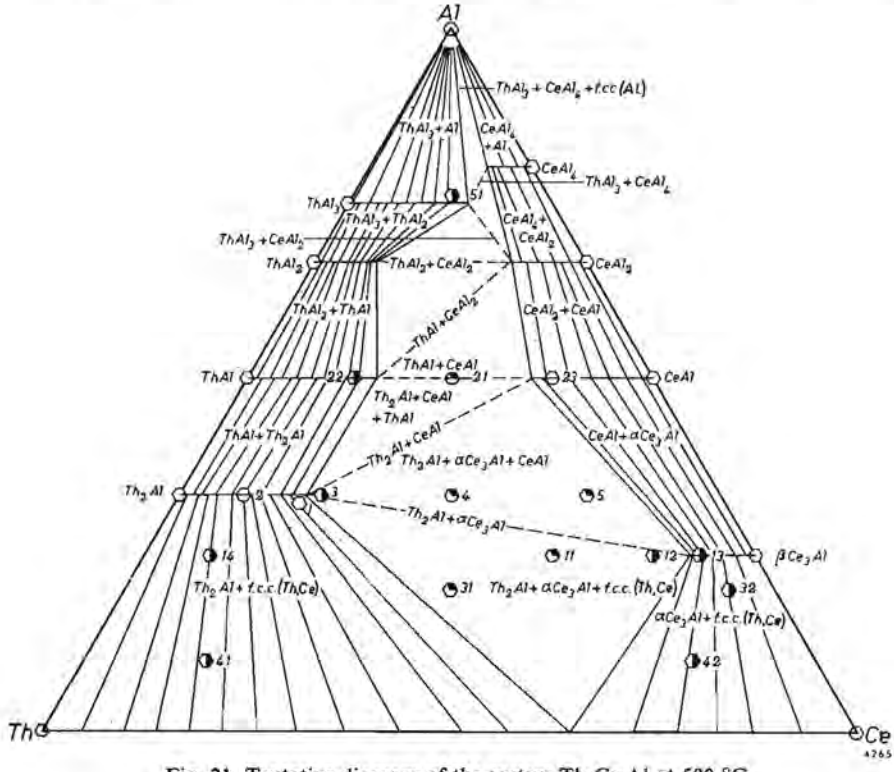

Fig. 21. Tentative diagram of the system Th-Ce-Al at 500 °C.

of the thorium atoms for those of cerium. Apparently the substituted atoms are distributed without long-range order over the thorium sites, for we never observed super-lattice lines. It is not known if this substitution involves a deviation of the Al occupation. The behaviour of the lattice dimensions of the tetragonal Th_2Al, while substitution is proceeding, is illustrated in table XVII and fig. 20. For comparison, fig. 20 shows the influence of the corresponding substitution in the f.c.c. thorium lattice [11]). It is interesting to see that in this type of compound — depending mainly on size relationship ($r_{Th}/r_{Al} = 1{\cdot}25$) according to Raynor [36]) — much less thorium can be replaced by cerium than might be expected from the consequences of this substitution observed in the f.c.c. lattice of pure thorium. This might indicate that in this type of compound the electronic properties play their role as well. The minima of V_{Th_2Al} and a_{Th} in fig. 20 practically coincide, which means that all is well as long as cerium is

substituted as a quadrivalent ion, but that this procedure abruptly comes to a halt as soon as the normal — though geometrically better fitting — trivalent cerium atoms try to substitute for the quadrivalent thorium atoms.

The transformation point of the compound Ce_3Al, which for the pure state lies at about 225 °C, seems to rise quickly when thorium is built in. Only the hexagonal (= low-temperature) phase was found in the specimens quenched from 500 °C. In the pure Ce_3Al specimens, on the other hand, we rarely succeeded in getting significant amounts of the α-phase in this way.

The tie-lines shown in fig. 21 are only schematic. The lattice parameter of the f.c.c. Th(Ce) phase found in various samples does not indicate with sufficient certainty the composition of this phase. It is not known how much aluminium is dissolved in this f.c.c. phase and what influence this process has on the dimensions.

The sample compositions were so chosen that from few specimens as much as possible could be learned about interesting binary sections and possible ternary compounds. As far as the latter were concerned the results of the investigation were negative.

8.4. *Ceto*

The getter Ceto, as it is made in the factory by sintering a mixture of Th and $CeAl_2$ powder, is lying — in composition — very near to the line Th_2Al — "Ce_2Al" (point 1 in fig. 21). The X-ray diagram shows that the sintering reaction never goes to completion. A small amount of both components of the mixture always remains unchanged. The part that reacted took on the $CuAl_2$ structure, in which the aluminium sites were occupied by a mixture of thorium and cerium atoms in a ratio of about 4 : 1, the copper sites being occupied by aluminium.

REFERENCES

1) A. Leber, Z. anorg. Chem. **166**, 16-26, 1927.
2) G. Grube and L. Botzenhardt, Z. Elektrochem. **48**, 418-425, 1942.
3) H. Bückle, Z. Metallk. **37**, 43-47, 1946.
4) G. Brauer, Naturwissenschaften **26**, 710, 1938.
5) R. Vogel, Z. anorg. Chem. **75**, 41-57, 1912.
6) L. Rolla, A. Iandelli, G. Canneri and R. Vogel, Z. Metallk. **35**, 29-42, 1943.
7) H. Nowotny, Z. Metallk. **34**, 22-24, 1942.
8) A. J. C. Wilson, Proc. phys. Soc. Lond. **53**, 235-244, 1941.

[9]) W. I. James and N. E. Straumanis, Acta cryst. **9**, 376, 1956.
[10]) P. Chiotti, J. electrochem. Soc. **101**, 567, 1954.
[11]) R. T. Weiner, W. E. Freeth and G. V. Raynor, J. Inst. Met. **86**, 185-188, 1957.
[12]) F. Trombe, Rev. Métall. **53**, 1-36, 1956.
[13]) A. W. Lawson and Ting-Yuan Tang, Phys. Rev. **76**, 301-302, 1949.
[14]) A. I. Likhter, Yu. N. Ryabinin and L. F. Vereshchagin, J. exp. theor. Phys. Moscow **33**, 610, 1957.
[15]) F. H. Spedding and A. H. Daane, J. Metals **6**, 504-510, 1954.
[16]) J. Loriers, C. R. Acad. Sci. Paris **226**, 1018-1019, 1948.
[17]) J. D. Fast, Z. anorg. allg. Chem. **241**, 42-56, 1939.
[18]) P. B. Braun and J. H. N. van Vucht, Acta cryst. **8**, 117, 1955.
[19]) P. B. Braun and J. H. N. van Vucht, Acta cryst. **8**, 246, 1955.
[20]) J. R. Murray, J. Inst. Met. **84**, 92-96, 1955.
[21]) A. F. Andresen and J. A. Goedkoop, Acta cryst. **8**. 118, 1955.
[22]) J. R. Murray, Report AERE M/R 2665.
[23]) J. H. N. van Vucht, Z. Metallk. **48**, 253-258, 1957.
[24]) A. Iandelli, paper presented at Symp. on Phys. Chem. of Met. Sol. and Interst. Comp., N. P. L. Teddington, June 1958.
[25]) A. Iandelli, Atti X° Congr. Inter. Chem. **2**, 688, 1938.
[26]) A. Wallbaum, Z. Kristallogr. **A103**, 147-148, 1940.
[27]) J. H. N. van Vucht, Philips Res. Repts **12**, 351-354, 1957.
[28]) H. A. Saller and F. A. Rough, U. S. Atomic Energy Commission Publ. 1955, (B.M.I.-1000).
[29]) J. H. N. van Vucht, J. Inst. Met., Bull. **4**, 94-95, 1958.
[30]) R. T. Weiner, W. E. Freeth and G. V. Raynor, J. Inst. Met., Bull. **4**, 106-107, 1958.
[31]) K. Dialer and W. Rothe, Z. Elektrochem. **59**, 970, 1955.
[32]) D. H. Ahmann, Report of the U.S. Atomic Energy Comm. AECD-3205, 1950.
[33]) D. Peterson, W. Lyon and W. H. Keller, Report CT-2952, 1945.
[34]) F. H. Spedding and A. H. Daane, J. Metals **6**, 504-510 1954.
[35]) K. Dialer and W. Rothe, Z. Elektrochem. **59**, 970, 1955.
[36]) G. V. Raynor, Progress in Metal Physics, Butterworths Scientific Publications, London, 1949, Vol. 1, p. 1.
[37]) Structure Reports, 1950, Vol. 13, p. 48.
[38]) E. Hellner, Z. anorg. Chem. **261**, 226, 1950.
[39]) J. Loriers, C. R. Acad. Sci. Paris **226**, 1018-1019, 1948.

CHAPTER 3

EQUILIBRIUM PRESSURES IN THE SYSTEM Th_2Al-HYDROGEN

Summary

For reasons of theoretical and practical importance pressure isotherms are measured of hydrogen in equilibrium with its solid solutions in the getter metal Th_2Al. From these measurements thermodynamic data are obtained, which permit of comparing the stabilities of the hydrogen solutions with those of other getter hydrides. The isotherm at about 225 °C shows three points of inflexion, at compositions of about $Th_8Al_4H_5$, $Th_8Al_4H_9$ and $Th_8Al_4H_{13}$. Those at $Th_8Al_4H_5$ and $Th_8Al_4H_{13}$ are considered as remnants of "plateaux" and indicate a tendency to phase-separation in the solid solution. The effect of replacing some of the thorium atoms in Th_2Al by cerium atoms is an increase of hydride stability, together with the appearance of real plateaux.

Zusammenfassung

Aus theoretisch und praktisch bedeutsamen Gründen werden Druck-Isothermen von Wasserstoff im Gleichgewicht mit seiner festen Lösung im Gettermetall Th_2Al gemessen. Aus diesen Messungen werden thermodynamische Daten gewonnen, die einen Vergleich der Stabilitäten der Wasserstofflösungen mit solchen anderer Getterhydride ermöglichen. Die Isotherme bei etwa 225 °C zeigt drei Wendepunkte bei den Zusammensetzungen von etwa $Th_8Al_4H_5$, $Th_8Al_4H_9$ und $Th_8Al_4H_{13}$. Diejenigen bei $Th_8Al_4H_5$ und $Th_8Al_4H_{13}$ werden als "Plateau-Reste" angesehen und zeigen eine Neigung zur Phasentrennung in der festen Lösung. Der Ersatz einiger der Thoriumatome in Th_2Al durch Ceratome hat ein Ansteigen der Hydridstabilität in Verbindung mit der Erscheinung eines echten Plateaus zur Folge.

Résumé

Vu leur interêt théorique et pratique on a mesuré des isothermes de pression d'hydrogène, en équilibre avec les solutions solides dans le getter métallique Th_2Al. Au moyen de ces isothermes on a calculé des données thermodynamiques, qui permettent la comparaison des stabilités des solutions solides d'hydrogène dans Th_2Al avec celles dans d'autres getters. Les isothermes d'une température d'environ 225 °C accusent trois points d'inflexion dans les compositions d'environ $Th_8Al_4H_5$, $Th_8Al_4H_9$ et $Th_8Al_4H_{13}$. Le premier et le dernier point d'inflexion sont considéré, comme des résidus de plateaux qui indiquent une tendance à une séparation de phases dans la solution solide. Le remplacement de quelques atomes de thorium par des atomes de cérium a donné lieu a une augmentation du stabilité des hydrures et a l'apparition de plateaux réels.

1. Introduction

Until rather recently it was the general opinion that the value of a getter was to be judged only from its behaviour with respect to hydrogen (sorption rate, residual pressure, sorption capacity). In the meantime this standpoint has been abandoned, though these properties remain important. The hydrides are always the least stable compounds that getters form with gases, and thermodynamically they therefore have the highest dissociation pressures. Particularly at temperatures where the sorption rates for the other gases become sufficiently large, the hydrogen-equilibrium pressure may be too high. In some applications, however, for example where oxide cathodes are concerned, a certain hydrogen pressure

may be desirable in the valve. For this purpose a selective getter is sought, one which binds oxygen, nitrogen and carbon and whose temperature determines a certain hydrogen pressure, for which it works as a buffer. Because of their practical importance, but also for theoretical reasons, equilibrium-pressure isotherms were measured for the ceto-like getter Th_2Al and for a number of isostructural alloys containing some cerium.

2. Literature

As early as 1923 Sieverts and co-workers measured equilibrium-pressure isotherms of a great number of metal-hydrogen systems such as those with iron, nickel, and including the interesting getter metals cerium [1]), zirconium and thorium [2]). The system palladium-hydrogen became the subject of numerous such measurements [3–6]) because of its theoretical interest. In recent years many reactor metals were studied this way, such as zirconium [7]), hafnium [8]), uranium [9]) and plutonium [10]). Titanium [11]) was studied because of its importance as a structural material in aircraft. Very recently the even-series metals of group V, namely vanadium [12]), niobium [13]) and tantalum [14]), were investigated. Only relatively few metal alloys have been studied so far in regard to their hydrogen-sorption properties: palladium-gold [15]), palladium-platinum [16]), uranium-zirconium [17]) and the compound ZrNi [18]). Furthermore Witte and co-workers made similar measurements with a number of alloys of metals that normally absorb only small amounts of hydrogen [19]).

The results obtained can be summarized as follows. There are metals that absorb hydrogen *endothermally*: with an increase in temperature the solubility of hydrogen increases. Many of them absorb only small amounts (copper, magnesium, aluminium, zinc, etc.), but the transition metals like iron, nickel, platinum can absorb amounts that are of practical interest. On the other hand there are metals that are able to absorb great quantities of hydrogen *exothermally*, forming true compounds, namely hydrides. One kind of hydride is salt-like and always virtually stoichiometric; this kind is formed by the alkali and the alkaline-earth metals. Then follow the metals of the lanthanide and the actinide transition groups with hydrides that largely retain a metallic character, for example CeH_2, metallic and non-stoichiometric (at higher hydrogen contents it becomes more salt-like, as in stoichiometric CeH_3). Then come the group-IV*a* metals titanium, zirconium, hafnium and thorium, also having very stable and stoichiometric hydrides, and subsequently the group-V*a* elements vanadium, niobium and tantalum, having less stable and mostly non-stoichiometric hydrides. Palladium may be considered to stand on the border between the endothermally and the exothermally absorbing metals because of its intermediately stable, non-stoichiometric hydrides. Alloying, in particular with members of the endothermally absorbing group, shifts the hydrogen-binding properties of the exothermic absorbers to the endothermal side. Lieser and

Rinck [20]), however, showed with an alloy of nickel and zinc that the combination of two endothermic absorbers can sometimes turn out to absorb exothermally. Libowicz, Hayes and Gibb [18]) showed that nickel alloyed to zirconium increased the number of hydrogen atoms that can be bound per zirconium atom from 2 to over 2·5 in the compound ZrNi.

If the hydrides are sufficiently stable, two-phase regions are always found between them and the mother metal, which contains very few hydrogen atoms. At higher temperatures these regions tend to become single-phase solid solutions. Decreasing stability of the hydrides means increasing equilibrium pressures and larger deviations from stoichiometry in the sense that less hydrogen can be bound. In general the critical temperature of the two-phase region decreases with decreasing stability of the hydrides.

In the single-phase regions, sufficiently far from any two-phase region, the hydrogen-equilibrium pressure appears to be proportional to the square of the hydrogen concentration in the metal. This clearly indicates that hydrogen in the dissolved state is present in monatomic form either as atoms or as ions (positively or negatively charged) and that the dissolved particles behave more or less as in an ideal solution, i.e. they do not interact and they obey Sieverts' law. The occurrence of two-phase regions (separation into two phases containing different amounts of hydrogen) indicates, however, that at lower temperatures the behaviour of the dissolved particles deviates more and more from that in an ideal solution, as has been pointed out by Lacher [21]) in a paper concerning the system palladium-hydrogen. He calculated with the aid of statistical mechanics the equilibrium-pressure isotherms, assuming a weak attraction between hydrogens in neighbouring lattice positions. Martin and Rees [22]) did the same thing for the system zirconium-hydrogen, taking into account the possible effects of the existence of vacancies in the zirconium lattice.

For the sake of completeness some recent literature is mentioned concerning the behaviour of the element thorium with respect to hydrogen. Thorium forms a very stable compound ThH_2 with a heat of formation of about -34 kcal per mole [23]), and some possibility to deviate from the stoichiometric composition, especially towards lower hydrogen contents [24]). At higher temperatures this compound dissolves in the thorium lattice to a considerable extent: at 800 °C some 25 at.% hydrogen are in homogeneous solution [25]). At room temperature the amount of hydrogen that can be homogeneously dissolved is negligibly small. Furthermore it is possible, at higher hydrogen pressures, to obtain a hydride that has a composition of approximately Th_4H_{15} [26]).

3. Experimental

The principles of the measurement of the equilibrium-pressure isotherms were as follows. Getter powder, placed in an evacuated vessel, was loaded stepwise with small amounts of hydrogen, merely by introducing the gas into the vessel

and allowing the getter to absorb it until equilibrium was reached. The hydrogen pressure directly above the getter was then measured. The corresponding hydrogen concentration in the getter was calculated from the weight of the getter and the pressure, temperature and volume data of the gas before and after absorption. Measurements were performed in two ways: (1) by keeping the temperature constant during the series of hydrogen additions and (2) by varying the temperature after each hydrogen addition. Figure 1 shows schematically the measuring sequence for each of these two methods.

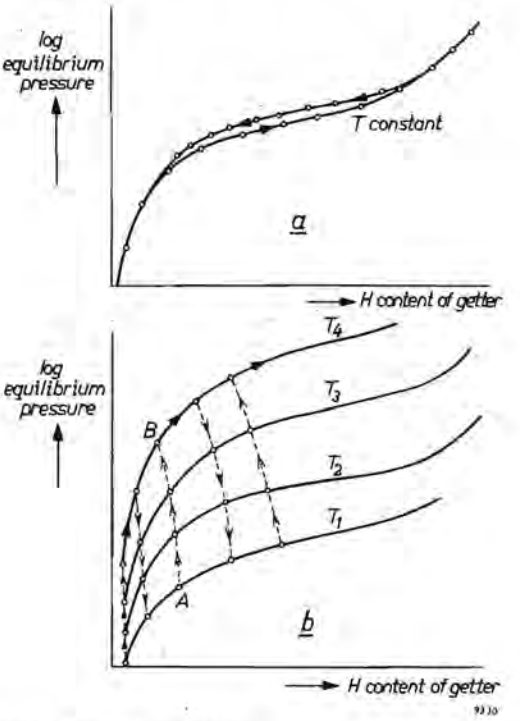

Fig. 1. Measurement of equilibrium pressure
(*a*) at constant temperature by adding or withdrawing small amounts of hydrogen,
(*b*) by varying the temperature after each addition of hydrogen; AB is a line of constant hydrogen content of the system.

The apparatus used is represented schematically in fig. 2. Specimens of 500 mg Th_2Al powder in a silica crucible were placed in the silica reaction vessel. After sealing, the vessel was evacuated carefully and the powder was degassed by heating the CrNi furnace to about 1000 °C. After cooling down to the desired temperature hydrogen was admitted from the calibrated dosing volume. Its pressure in this volume was measured by means of a two-legged silicone-oil manometer, the temperature by an ordinary mercury thermometer outside the

volume. After attainment of equilibrium the hydrogen pressure above the getter powder was measured by the Pirani gauge or, in some cases, by the Warmoltz ionization gauge or the oil manometer.

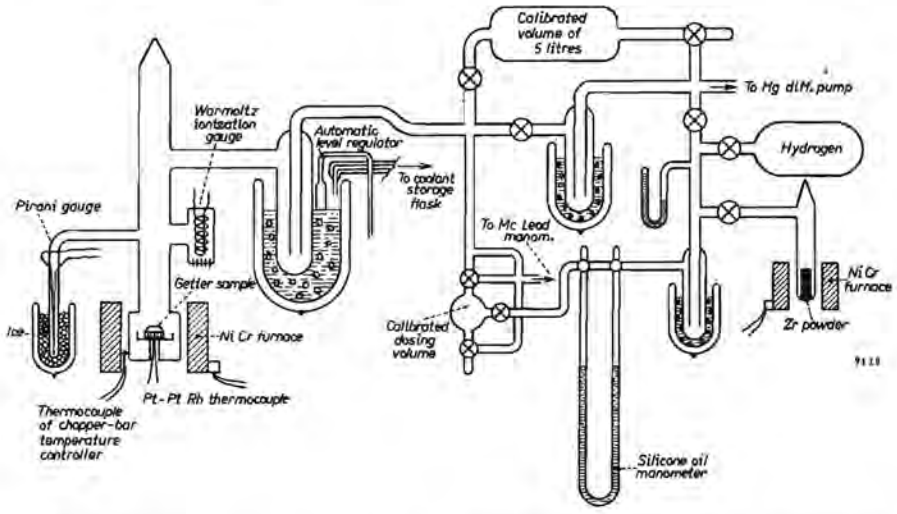

Fig. 2. Apparatus for measuring hydrogen-equilibrium pressures at various temperatures.

The getter metal was made in an argon-arc furnace as described previously [27]). The single-phase character of the specimen was checked by microscopical investigation of its polished (unetched) surface. The metal was then crushed under acetone in an agate mortar and sieved, until a grain size $< 50\ \mu$ was reached. For a further check on the single-phase character an X-ray diagram was taken. The hydrogen used, of the best industrial purity, was further purified by absorption in zirconium so as to remove all contaminants. When hydrogen was to be added to the getter the zirconium hydride was decomposed by heating it to about 900 °C.

It was not possible to bake out the apparatus after the getter specimen had been introduced, without making the whole set-up very complicated. This meant that during the course of an experiment, which for isotherms at lower temperatures sometimes lasted three weeks, measurable quantities of gases were slowly liberated from the walls. Particularly at low pressures, the precision of the measurements was limited by this inevitable phenomenon. By keeping the liquid-air trap filled night and day by means of an automatic device, the results became better. However, really satisfactory accuracy was obtained only by keeping the level of the coolant in the Dewar flasks at a constant height all the time. This was performed by means of the device shown in fig. 3.

Temperature measurements during the experiments were made by means of a thermocouple fixed outside the apparatus and just below the crucible containing the getter specimen, as shown in fig. 2. The true temperature of the powder was obtained by a calibration experiment; during this a second thermocouple was placed in the crucible, which was this time filled with quartz grains instead of getter powder (thus avoiding heat-producing reactions with gases), in a gas

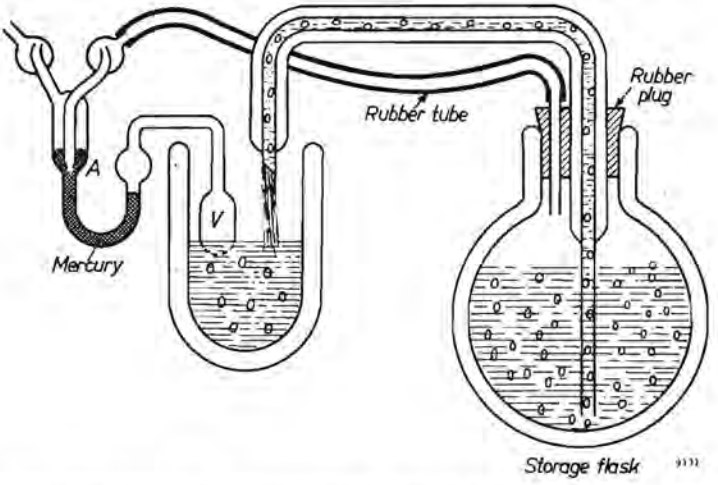

Fig. 3. Device for maintaining a constant coolant level. If the level becomes too low, the gas in *V* expands, causing the mercury to close the opening *A*. The boiling coolant in the storage flask (e.g. liquid nitrogen) then starts to build up a pressure that pushes the liquid upwards in the syphon. When the coolant level has risen sufficiently, the gas in *V* contracts because its temperature decreases, and the opening *A* is freed, so that it can release the nitrogen pressure in the storage flask. The syphon then ceases to work.

atmosphere comparable to that in normal experiments. Temperature regulation was performed by means of a chopper-bar temperature regulator, controlled by a thermocouple near the inner furnace wall (see fig. 2). In the isothermal experiments at lower temperatures, where equilibrium was attained very slowly, the above regulating apparatus was temporarily disconnected in order that the process of attaining equilibrium might be accelerated by manual control.

Pressure measurements were performed in three ways. During the preliminary pumping procedure use was made of an ionization manometer of a type described by Warmoltz [28]). Occasionnally this manometer was also used for the measurements of equilibrium pressures at temperatures lower than 250 °C, where they were too low for the Pirani manometer. Most of the equilibrium-pressure data were obtained with the latter instrument, which covered a range from 10^{-4} up to 10 torr. The Pirani gauge was calibrated for hydrogen before and after each experiment by means of a McLeod gauge of a type described by Jansen and Venema [29]).

The Pirani gauge, developed by R. W. P. de Vries, consisted of a glass tube of 7 mm diameter in which a platinum wire of 25μ was held at a fixed temperature ($\approx$ 150 °C, its resistance was then about 200 Ω). The outer wall was kept at 0 °C by placing a Dewar flask filled with melting ice around the Pirani gauge. The platinum wire was part of a Wheatstone bridge, of which the other three resistances (see fig. 4*a*) were kept at 0 °C in another Dewar flask. The Wheatstone bridge is fed by an amplifier (see fig. 4*c*), the input of which is connected

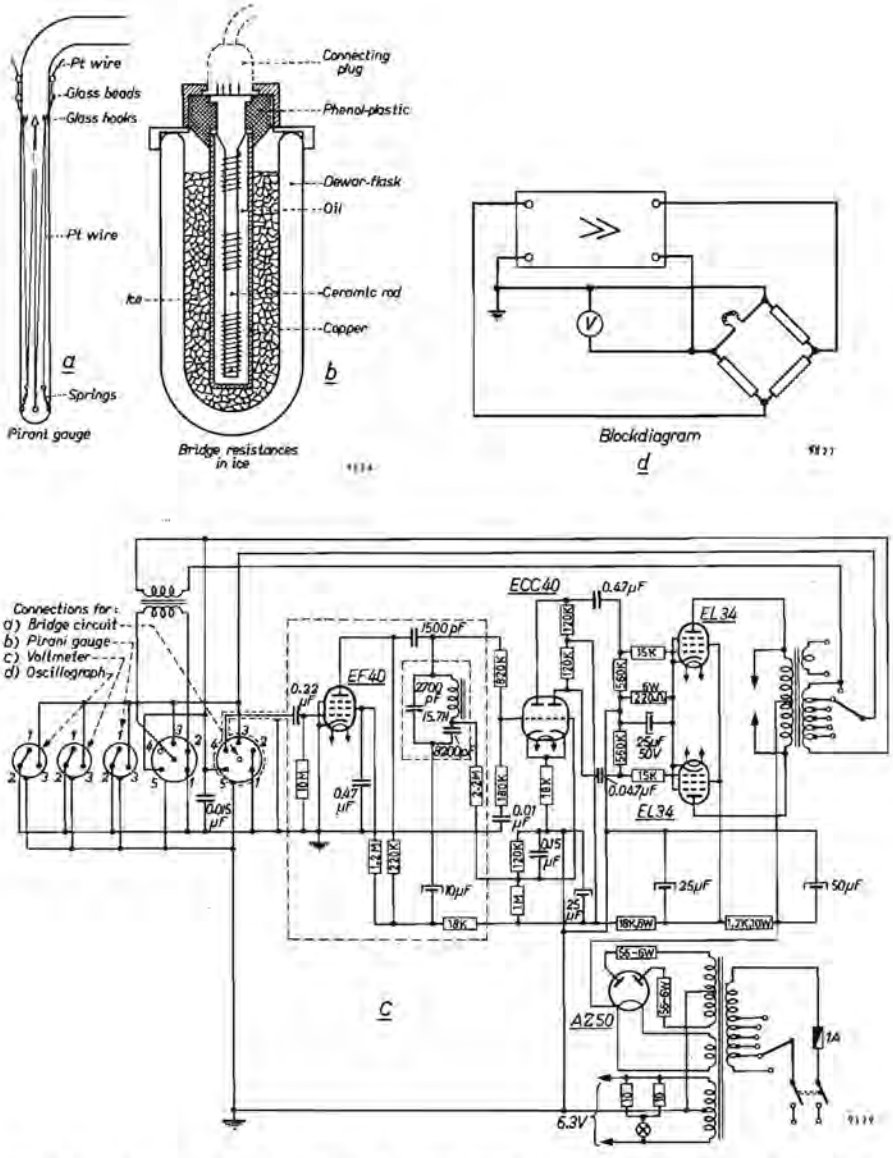

Fig. 4. Pirani gauge (*a*) with bridge (*b*) and power-supply circuit diagram (*c*). An electronic a.c. voltmeter completes the set-up (*d*).

to the zero branch of the bridge. Originally the bridge is out of balance, which causes the amplifier to oscillate with increasing amplitude. The Pirani wire becomes heated proportionally and in consequence changes its resistance. In this way the bridge approaches equilibrium, thereby decreasing its signal transfer. As soon as this transfer is equal to the reciprocal value of the amplification the amplitude no longer increases. Since the signal transfer of the bridge is determined by the temperature of the Pirani wire, it may be said that the amplitude automatically arrives at a value required to hold the Pirani-wire resistance at its pre-determined value. The voltage V over the wire could be read from a normal a.c. voltmeter or, if desired, automatically recorded. Its value was a measure of the energy required to keep the Pirani wire at a constant temperature, and therefore also of its loss of heat due to conduction through the gas plus a constant radiation loss. If T_w be the wire temperature and T_e the temperature of the glass envelope, then at zero gas pressure the voltage over the Pirani wire will be given by $V_0^2/R = a_w T_w^4 - a_e T_e^4$ where $a_w T_w^4$ and $a_e T_e^4$ are the emissions of the wire surface and of the glass wall respectively, and R is the constant resistance of the wire (which determines the value of the other three resistances in the bridge). Given now a pressure p in a region where heat conduction is a linear function of the pressure (this is the case when the mean free path of the molecules is of the order of the wire-wall distance), then the voltage indication will be given by

$$V^2/R = V_0^2/R + kp(T_w - T_e).$$

Here the factor k is the accommodation coefficient for heat transfer between the wire and the gas in question. For constant temperatures of wire and envelope the equation takes the form

$$V^2 = k_0 + k_1 p.$$

A typical calibration curve for hydrogen is shown in fig. 5.

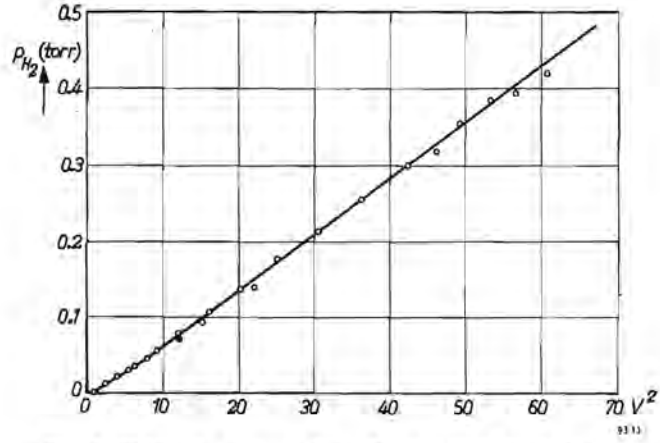

Fig. 5. Calibration curve of the Pirani gauge for hydrogen.

The third manometer, used only if equilibrium pressures exceeded 1 torr *), was the oil manometer already mentioned. The oil used was a silicone oil with very low vapour pressure, such as is commonly used in diffusion pumps. Its density was 1·06 g/cm³. Before use it was degassed by boiling in vacuum in the

*) 1 torr = 1 mm Hg

manometer. Because of the rather small quantities of getter powder available and the uncertainties in the values of V and p it was not practicable to extend the measurements to regions where a normal mercury manometer had to be used.

Initially the reproducibility of the measurements was very poor: equal amounts of the same specimen, measured at the same time in different apparatus, yielded different equilibrium pressures. It appeared, however, that this discrepancy did not occur if the powder specimen was saturated and subsequently degassed a few times before the measurement was started. Special attention was given to the possibility of hysteresis. Some experiments were therefore carried out in an apparatus in which it was possible to proceed also in the reverse direction along the isotherm, withdrawing known amounts of hydrogen, instead of admitting them. Within the limits of accuracy the isotherms thus produced coincided, at least for powders treated in the above way.

The hydrogen content of the getter was never measured directly, because of the practical difficulties of quenching the specimen. It was therefore calculated from the volumetric data, using calibration data from special runs without a getter, and allowing for the amount of oxide present, which was determined by chemical analysis. The specimens of Th_2Al always contained about 6% by weight of oxide, and the cerium-containing specimens about 1% more.

4. Results

As already mentioned in sec. 3, various methods and instruments were used to determine the equilibrium pressures. The data given in fig. 6 are the most reliable ones. The pressures above 1 torr, measured with the oil manometer, and those below 10^{-4} torr, measured with the Pirani gauge, correlate well. As regards the lower part of the diagram it must be remarked that here irreproducible phenomena always occurred. These are commonly encountered in these regions, by various investigators and for different metals. They are thought to be due to surface poisoning or contamination, or, more generally, to impurities at the crystal boundaries. Sometimes they are ascribed to irregularities, originating in the existence of a separate occluding system such as lattice defects. Here one is apt to think in the first place of dislocations. Sometimes, however, less-well-defined defects on a larger scale are meant, which were called "rifts" by Smith [30]). Hitherto it has not been possible to prove or disprove either surmise. The lower points in fig. 6 therefore do not pretend to represent true equilibria.

The isotherms do not show any kind of plateau, as might be expected if at these temperatures a second solid phase occurred. In a ternary system, such as this system strictly speaking is, the absence of a plateau does not necessarily imply that no new phase is formed. However, the temperatures of the isotherms are low compared with the melting point of the mother metal (1307 °C), which means that it is unlikely that aluminium and thorium atoms diffuse appreciably,

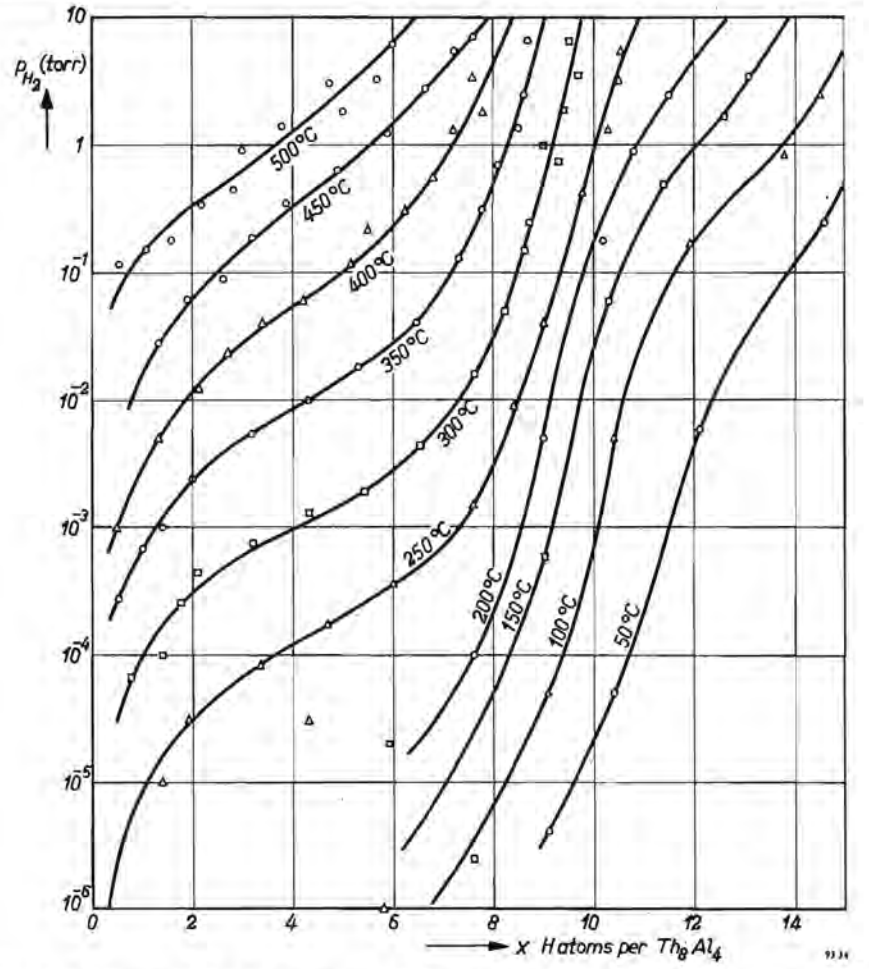

Fig. 6. Isotherms of the hydrogen equilibrium pressure above Th_3Al; $\log p_{H_2}$ is plotted against the composition of the hydride $Th_8Al_4H_x$.

for example to rearrange into a mixture of ThH_2 and aluminium. It therefore seems admissible to consider the system as quasi-binary. In that case, according to Gibbs' phase rule, the absence of a region of constant pressure in the isotherms may be interpreted to mean that the solid phase remains homogeneous, i.e. the dissolved hydrogen has not formed a precipitate in, nor any crust on, the metal.

If the data of fig. 6 are plotted on a log-log scale, it is seen that they obey fairly closely the simple law $c = kp^{\frac{1}{2}}$, up to a concentration c of approximately 4 hydrogen atoms per unit cell of Th_8Al_4. This law, which bears the name of Sieverts, requires that the hydrogen molecules in the gas phase are in equilibrium with single hydrogen particles in the metal, while the particles in each phase do not interact.

Writing the dissolution of hydrogen as follows:

$$H_{2\ gas} \rightleftarrows 2\ H_{metal},$$

equilibrium means that

$$\mu_{H_2\ gas} = 2\ \mu_{H\ metal}. \tag{1}$$

If the particles in both media behave as in an ideally diluted solution (i.e. if they obey the Henry-Sieverts' law), then at temperature T we may write:

$$\mu^0_{H_2 gas} + RT \ln (p_{H_2\ gas}) = 2\ \mu^0_{H\ metal} + 2\ RT \ln (x_{H\ metal}), \tag{2}$$

where $\mu^0_{H_2 gas}$ is the chemical potential at temperature T for hydrogen in the gas phase at $p = 1$ (atm), $\mu^0_{H\ metal}$ is a constant to be tabulated later for 25 °C, and $x_{H\ metal}$ is the concentration of H in the metal lattice in atoms per unit cell of Th_8Al_4. Equation (2) may be re-written:

$$\ln x_{H\ metal} = (\mu^0_{H_2 gas} - 2\ \mu^0_{H metal})/2RT + \tfrac{1}{2} \ln (p_{H_2\ gas}). \tag{3}$$

The first term on the right-hand side is a constant at a constant temperature, so that

$$(p_{H_2\ gas})^{\frac{1}{2}} = k\ x_{H\ metal}, \tag{4}$$

where

$$k = \exp \{(\mu^0_{H metal} - \tfrac{1}{2}\ \mu^0_{H_2 gas})/RT\}.$$

If the behaviour of the hydrogen in the metal is not ideal, k will depend on the concentration. In that case we have to extrapolate to zero concentration to find the value of the standard chemical potential at temperature T.

In fig. 7, k is shown as a function of x. Extrapolation to zero yielded the values plotted in fig. 8 against $1000/T$. From this graph it is seen that extrapolation to 298 °K seems to be admissible with reasonable accuracy. We then find

$$\mu^0_{H\ in\ Th_2Al} = -11{\cdot}6\ (\pm\ 0{\cdot}4)\ \text{kcal for } T = 298\ °\text{K}.$$

The slope of the line in fig. 8 gives the standard enthalpy of hydrogen dissolved in Th_2Al, for

$$d(R \ln k)/d(1/T) = d(\mu/T)/d(1/T) = \mu + (1/T)\{d\mu/d(1/T)\} = \mu - T(d\mu/dT) = \mu + Ts = h.$$

$$h^0_{H\ in\ Th_2Al} = -13{\cdot}9\ (\pm\ 0{\cdot}4)\ \text{kcal}.$$

The standard entropy $s^0_{H\ in\ Th_2Al}$ is then found from $\mu^0 = h^0 - Ts^0$, and has the value

$$s^0_{H\ in\ Th_2Al} = -8\ (\pm\ 1)\ \text{cal/deg for } T = 298\ °\text{K}.$$

The function $\mu_{H\ metal} - \frac{1}{2}\ \mu^0_{H_2 gas} = g$, the chemical potential (or partial molar free enthalpy), is obtained directly from the pressure data as $\frac{1}{2}RT \ln p_{H_2}$. Its

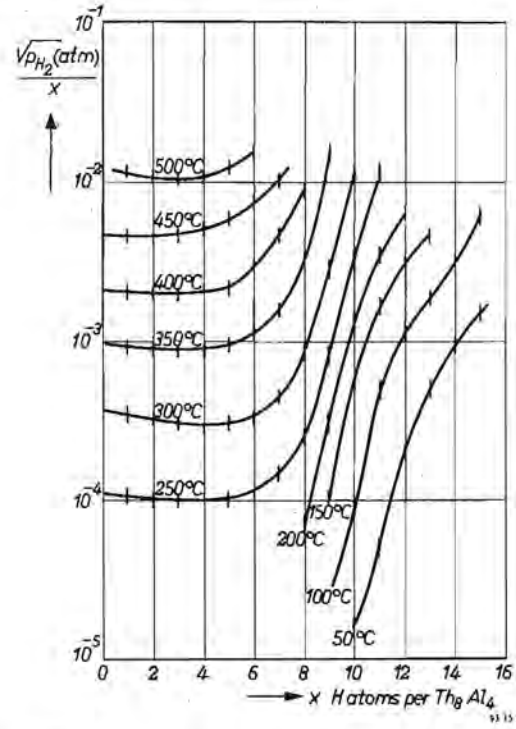

Fig. 7. The function $p^{\frac{1}{2}}/x$ plotted against x for various temperatures.

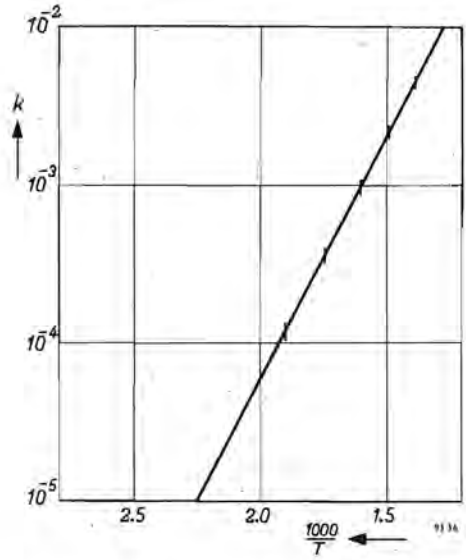

Fig. 8. Extrapolated values of $p^{\frac{1}{2}}/x$ plotted against $1000/T$.

values are compiled in table I, together with the functions

$$h = h_{\text{H metal}} - \tfrac{1}{2}h^0{}_{\text{H}_2\text{gas}}$$

and

$$s = s_{\text{H metal}} - \tfrac{1}{2}s^0{}_{\text{H}_2\text{gas}},$$

being respectively the partial molar enthalpy (or molar heat of solution) and the partial molar entropy; each function is expressed per 1 mole atomic hydrogen, i.e. N (Avogadro's number) H atoms or $\frac{1}{2}$ mole of dissolved gaseous hydrogen. The latter two functions have been evaluated from the temperature dependence of the measured equilibrium pressures. In fig. 9, values of $\log p_{\text{H}_2}$

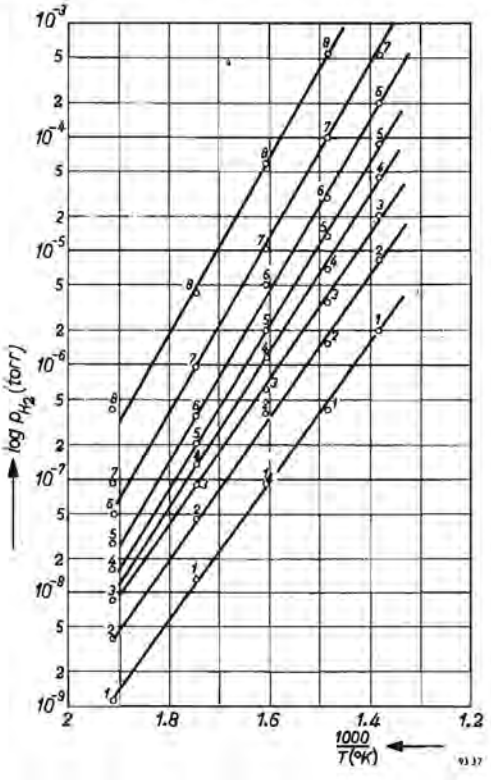

Fig. 9. Equilibrium pressures (logarithmic) plotted against $1000/T$ in the system Th_2Al-H_2.

at constant hydrogen concentrations are plotted against $1000/T$. The slopes of these lines are the partial heats of solution per mole H_2. This follows directly from eq. (2), which can be written as

$$\ln (p_{\text{H}_2\text{ gas}}) = (2\,\mu_{\text{H metal}} - \mu^0{}_{\text{H}_2\text{gas}})/RT. \qquad (2a)$$

Differentiating both sides with respect to $1/T$ and taking h (which is also the

TABLE I. Thermodynamic data of solutions of hydrogen in the alloy Th_2Al

T(°K) \ x		1	2	3	4	5	6	7	8	9	10	11
523	p	$11{\cdot}2.10^{-9}$	$4{\cdot}08.10^{-8}$	$9{\cdot}0.10^{-8}$	$1{\cdot}58.10^{-7}$	$2{\cdot}7.10^{-7}$	$4{\cdot}9.10^{-7}$	$9{\cdot}6.10^{-7}$	$4{\cdot}0.10^{-6}$	$5{\cdot}7.10^{-9}$	$11{\cdot}2.10^{-4}$	$1{\cdot}9.10^{-2}$
	$10^4 p^{\frac{1}{2}}/x$	1·06	1·01	1·00	1·01	1·04	1·16	1·4	2·5	8·4	33·4	126
	g	− 9·5	− 8·8	− 8·4	− 8·1	− 7·8	− 7·6	− 7·2	− 6·4	− 5·1	− 3·5	− 2·1
	s	− 8·5	−10·0	−11·4	−13·5	−15·2	−17·0	−18·1	−19·3	−21·7		
	h	−13·9	−14·1	−14·5	−15·5	−16·3	−17·1	−17·3	−17·6			
	G	−10·5	−19·65	−28·3	−36·15	−44·4	−52·25	−59·6	−66·6	−72·5	−76·45	−79·2
	S	− 6·2	−15·3	−26·0	−38·5	−52·8	−69·3	−86·4	−105·3	−126·0		
	H	−13·9	−27·9	−42·6	−57·5	−73·2	−90·3	−107·2	−125·1			
573	p	$1{\cdot}3.10^{-7}$	$4{\cdot}21.10^{-7}$	$8{\cdot}0.10^{-7}$	$1{\cdot}35.10^{-6}$	$2{\cdot}1.10^{-6}$	$3{\cdot}7.10^{-6}$	$9{\cdot}5.10^{-6}$	$4{\cdot}2.10^{-6}$	$7{\cdot}4.10^{-4}$	$1{\cdot}45.10^{-2}$	
	$10^4 p^{\frac{1}{2}}/x$	3·6	3·3	3·0	2·9	2·9	3·2	4·4	8·1	30·2	120	
	g	−9·0	−8·3	−8·0	−7·7	−7·4	−7·1	−6·6	−5·7	−4·1	−2·4	
623	p	$9{\cdot}0.10^{-7}$	$3{\cdot}55.10^{-6}$	$6{\cdot}5.10^{-6}$	$11{\cdot}2.10^{-6}$	$2{\cdot}0.10^{-5}$	$5{\cdot}0.10^{-5}$	$10{\cdot}5.10^{-5}$	$6{\cdot}6.10^{-4}$	$2{\cdot}10^{-2}$		
	$10^4 p^{\frac{1}{2}}/x$	9·5	9·4	8·5	8·4	9·0	11·8	14·7	32·1	157		
	g	− 8·6	− 7·7	− 7·4	− 7·1	− 6·4	− 6·1	− 5·7	− 4·5	−2·4		
	G	−10·0	−18·0	−25·6	−33·0	−39·6	−46·2	−52·0	−57·6	−61·0		
673	p	$3{\cdot}95.10^{-6}$	$1{\cdot}58.10^{-5}$	$3{\cdot}6.10^{-5}$	$7{\cdot}0.10^{-5}$	$1{\cdot}4.10^{-4}$	$3{\cdot}0.10^{-4}$	$1{\cdot}0.10^{-3}$	$5{\cdot}3.10^{-3}$			
	$10^4 p^{\frac{1}{2}}/x$	19·9	19·9	20·0	20·9	20·9	28·9	45·2	91·1			
	g	− 8·3	− 7·4	− 6·8	− 6·4	− 5·9	− 5·4	− 4·6	− 3·5			
723	p	$1{\cdot}98.10^{-5}$	$8{\cdot}3.10^{-5}$	$2{\cdot}0.10^{-4}$	$4{\cdot}2.10^{-4}$	$8{\cdot}6.10^{-4}$	$2{\cdot}0.10^{-3}$	$5{\cdot}1.10^{-3}$				
	$10^4 p^{\frac{1}{2}}/x$	44·6	45·6	47·1	51·3	58·7	74·5	102				
	g	− 7·8	− 6·7	− 6·1	− 5·6	− 5·1	− 4·4	− 3·8				
	G	− 9·0	−16·2	−22·4	−28·5	−33·6	−38·5	−42·4				
773	p	$1{\cdot}7.10^{-4}$	$4{\cdot}4.10^{-4}$	$8{\cdot}5.10^{-4}$	$1{\cdot}7.10^{-3}$	$3{\cdot}6.10^{-3}$	$8{\cdot}6.10^{-3}$					
	$10^4 p^{\frac{1}{2}}/x$	130	105	97	103	120	155					
	g	− 6·6	− 6·0	−5·4	− 4·9	−4·3	−3·6					

p: pressure in atm

x: hydrogen content in atoms H per Th_8Al_4

g: $\mu_H - \frac{1}{2}\mu^0_H$ the Gibbs free energy in kcal per $\frac{1}{2}$ mole H_2; h is the partial heat content in kcal per $\frac{1}{2}$ mole H_2, and s the partial entropy in cal/deg per $\frac{1}{2}$ mole H_2.

G is the integral free energy of formation in kcal per mole $Th_8Al_4H_x$; H and S are the analogous integral functions of enthalphy and entropy respectively.

negative heat of evaporation of hydrogen from the metal, or the differential heat of solution in the alloy) to be constant in the observed temperature range, (2*a*) becomes

$$\frac{\mathrm{d}(\ln p_{H_2})}{\mathrm{d}(1/T)} = \frac{2h}{R}. \tag{5}$$

Equation (5) is in fact the Clausius-Clapeyron relation, and at the same time an example of Van 't Hoff's law

$$\frac{\mathrm{d}(\ln K_p)}{\mathrm{d}T} = \frac{H}{RT^2},$$

where for the one gaseous reaction partner $\ln K_p$ becomes $-\ln p_{H_2}$, and H becomes $2h$. The partial entropy s can be derived directly by plotting the measured p values on a log scale against T, since $\mathrm{d}g/\mathrm{d}T = -s$. This has been done in fig. 10. As can be easily verified from table I the agreement is reasonable, particularly since the s values were taken as constant throughout the temperature range.

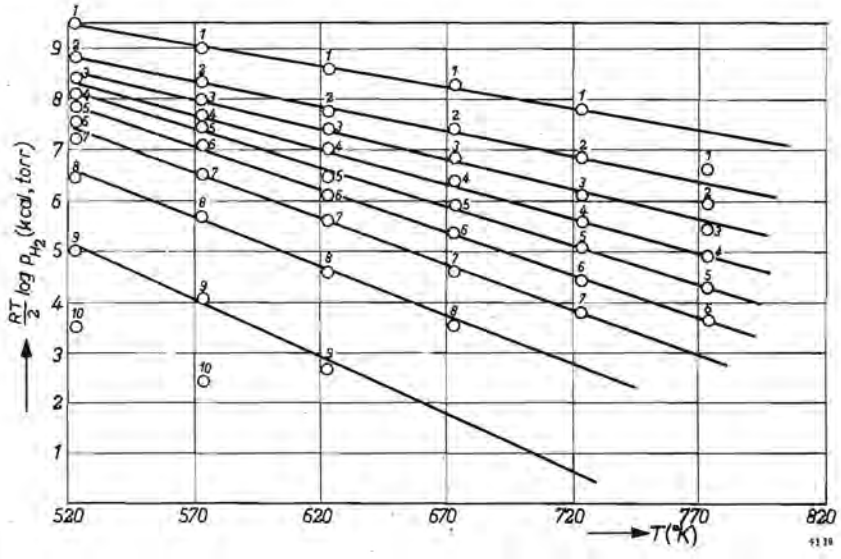

Fig. 10. Log p_{H_2} plotted against T for Th_2Al-H_2.

From the differential functions we may calculate the integral functions as follows, for example the free enthalpy

$$G_x = \int_0^x (\mu_H - \tfrac{1}{2}\mu^0_{H_2 gas})\,\mathrm{d}x,$$

where G_x is the free enthalpy of formation of one mole of $Th_8Al_4H_x$, with G_x taken at $x = 0$ to be zero as a reference point. These data are given in table I, together with

$$S_x = \int_0^x (s_H - \tfrac{1}{2} s^0_{H_2})\, dx)$$

and

$$H_x = \int_0^x (h_H - \tfrac{1}{2} h^0_{H_2})\, dx.$$

Here the number of cells of the solvent alloy has been kept constant ($= N$, Avogadro's number). The total number of atoms changes with x and amounts to $(12 + x)N$. It is also possible to keep the total number of atoms constant ($= N$), as is commonly done with substitutional solutions; then the functions above have to be divided by $(12 + x)$. This has been done for the free enthalpy at three different temperatures. The resulting values of this function, denoted here

$$G^* = \frac{1}{12 + x} \int_0^x (\mu_H - \tfrac{1}{2} \mu^0_{H_2})\, dx,$$

have been plotted against $x/(12 + x)$ (the atomic fraction of H) in fig. 11. The other possibility is to plot G_x against x. Thus only the G of a mixture of two separating phases lies on the common tangent of the minima in the G curve.

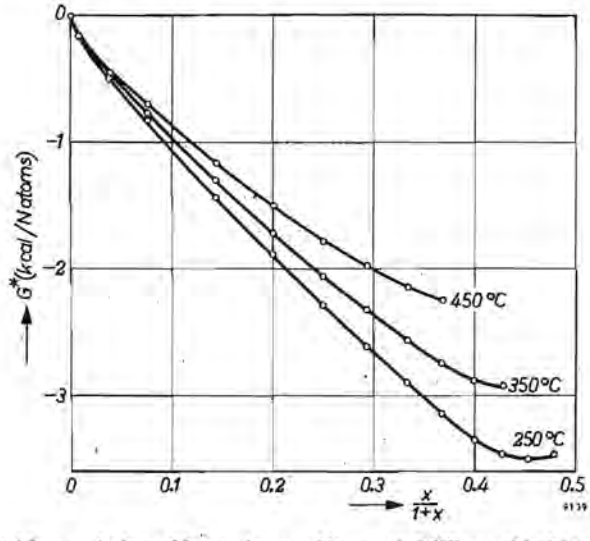

Fig. 11. Integral free enthalpy of formation per N atoms (of different kinds) totally in $Th_8Al_4H_x$ as a function of $x/(12 + x)$ for three temperatures.

which makes such a curve useful (in our case, for example, to estimate the nearness of a two-phase region).

It is possible, using the Duhem-Margules relation, to calculate from the partial functions of the hydrogen the corresponding partial functions for the alloy Th_2Al in the hydrogen solutions. This is omitted here, as it is deemed to be of no practical value. Nobody is interested in the change of the vapour pressure of Th_2Al upon dissolving some hydrogen in it, because, at the temperatures considered, the vapour pressure is very low. At higher temperatures it might become of interest, but then the above analysis is not applicable. The treatment of the system Th_2Al-H_2 as a binary system is inconsistent with adducing any significance to the thermodynamic potential of Th_2Al in this system. If the mobility of the atoms of the alloy is such that a vapour pressure of thorium and a vapour pressure of aluminium of any significance are to be expected above the hydride, the system has to be treated as a ternary one. It must then be expected that true equilibrium can be reached, and this will undoubtedly take the form of a phase separation into a mixture of ThH_2 and aluminium. In a later paper it will be shown that the presumption of the quasi-binary behaviour is justified.

5. Effect of cerium content

Some experiments similar to those described in the preceding sections for Th_2Al have been made with specimens of the compositions $(0{\cdot}875\ Th, 0{\cdot}125 Ce)_8Al_4$ and $(0{\cdot}75\ Th, 0{\cdot}25\ Ce)_8Al_4$. The first of these was fully homogeneous and of a structure identical with that of Th_2Al; the second one contained about 8 %

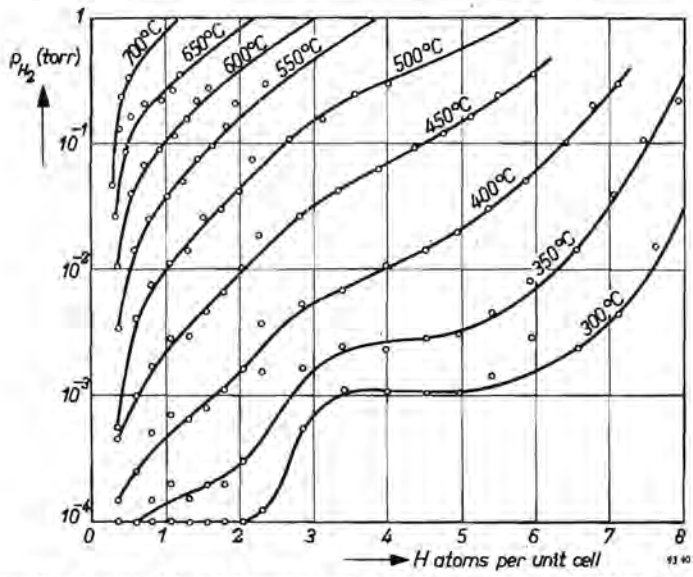

Fig. 12. Set of isotherms of the hydrogen equilibrium pressure above $(0{\cdot}875\ Th, 0{\cdot}125\ Ce)_8Al_4$.

of a second phase that virtually did not absorb hydrogen, and some 2% of a third phase as shown by metallographic observations (see previous paper [27]), table XVI). X-ray analysis showed that about 90% of the specimen of composition $(0{\cdot}75\ Th, 0{\cdot}25\ Ce)_8Al_4$ has also the same structure as Th_2Al.

The behaviour of these alloys with respect to hydrogen is illustrated in figs 12 and 13. The irregularities of fig. 12 are presumably partly due to difficulties in

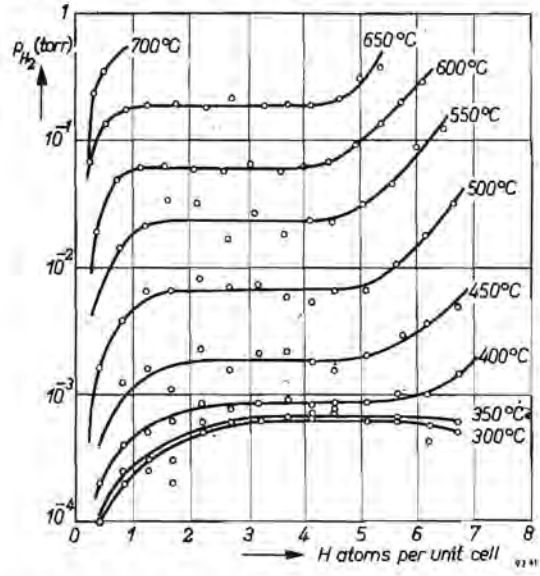

Fig. 13. Set of isotherms of hydrogen in equilibrium with $(0{\cdot}75\ Th, 0{\cdot}25\ Ce)_8Al_4$.

reaching the equilibrium state. The shapes of the lower isotherms, however, indicate the nearness of real plateaux, which means that the critical temperature of a two-phase region must lie somewhere near 200 °C. Furthermore the stability of the hydride appears to be somewhat higher when cerium is taken up in the lattice. This trend is continued in the properties of the second specimen, which is virtually of the composition of the getter Ceto. Table II compares the equilibrium pressures at room temperature (obtained by extrapolation) and the differential heats of solution per mole of hydrogen, both at the composition of 4 H per unit cell. Figure 13 shows clearly the occurrence of plateaux and, judging from their appearance, the continuous single-phase region must lie at a very high temperature.

6. Discussion of the results

The differential heats of solution of hydrogen in Th_2Al are seen to become more strongly negative with increasing hydrogen content. This has always been found, also from the older, less accurate data, and is an indication of a definite interaction between the dissolved atoms. Clearly the dissolving hydrogen atom

TABLE II

Equilibrium hydrogen pressures p at room temperature, obtained by extrapolation from above 350 °C, and differential heats of solution Q per mole H_2 for three isostructural getters

	p	Q
$Th_8Al_4H_4$	10^{-13} torr	31·0 (± 0·5) kcal
$(0{\cdot}875\ Th, 0{\cdot}125\ Ce)_8Al_4H_4$	10^{-15} torr	31·5 (± 0·5) kcal
$(0{\cdot}75\ Th, 0{\cdot}25\ Ce)_8Al_4H_4$	10^{-17} torr	31·8 (± 0·5) kcal

prefers the neighbourhood of other hydrogens already present. This does not necessarily mean that ordering must occur, but it predicts that at temperatures where the entropy becomes relatively less important, they tend to cluster. This implies that at lower temperatures we have to expect a separation into two phases, one with a small concentration of hydrogen, and one with the majority of the hydrogen in it. This behaviour is common in the exothermally occluding metals. Palladium, vanadium, niobium and tantalum all show this separation at the lower temperatures. Although no plateaux were encountered in the isotherms, a lower-lying two-phase region is thus predicted. In fact one might regard the points of inflection in the isotherms at $x = 4$ as the remnants of a plateau. In this connection it is interesting to note the existence of a second point of inflection at about $x = 12$.

The increase of the $p^{\frac{1}{2}}/x$ values of fig. 7 near zero as the concentration diminishes was found to change ultimately into a decrease by Kofstad, Wallace and Hyvönen in the case of tantalum and vanadium [12,14]). Therefore the extrapolation of the data obtained may be somewhat dubious. Data at the low hydrogen concentrations were always rather irreproducible, as different specimens were concerned. The consequence of a wrong extrapolation is an error in the integral thermodynamical functions, especially in the free enthalpy. Phenomena such as those observed by Kofstad et al. with tantalum, which were assumed to be caused by interstitial contaminations e.g. oxygen, were not found, and moreover they are unlikely here, because of the believed very small solubility of oxygen, nitrogen and carbon in Th_2Al.

The effects shown in fig. 7 at low hydrogen contents are directly connected with the changes in the heat of formation of the hydrogen solution. At higher concentrations the deviation of k can be explained as mainly the result of entropy changes.

Replacement of some thorium atoms in the Th_2Al lattice by cerium appears to yield a more stable hydrogen solution. It is possible that this is the direct result of the very stable hydrogen-cerium bond, manifesting itself particularly in the compound CeH_2.

REFERENCES

1) A. Sieverts and G. Müller-Goldegg, Z. anorg. Chem. **131**, 65-95, 1923.
2) A Sieverts and E. Roëll, Z. anorg. Chem. **153**, 289-308, 1926.
3) J. O. Linde and G. Borelius, Ann. Phys. Lpz. **84**, 747-774, 1927.
4) A. Sieverts and P. Zapf, Z. phys. Chem. **A 174**, 259-264, 1935.
5) L. J. Gillespie and L. S. Galstaun, J. Am. chem. Soc. **58**, 2565-2573, 1936.
6) P. L. Levine and K. E. Weale, Trans. Faraday Soc. **56**, 357-362, 1960.
7) C. E. Ells and A. D. McQuillan, J. Inst. Metals **85**, 89-96, 1956.
8) L. Espagno, P. Azou and P. Bastien, C. R. Acad. Sc. Paris **250**, 4353, 1960.
9) W. M. Albrecht and M. W. Mallett, J. electrochem. Soc. **103**, 404-409, 1956.
10) R. Mulford and G. Sturdy, J. Am. chem. Soc. **77**, 3449-3453, 1955.
11) G. A. Malkonian, Z. phys. Chem., Frankfurt **17**, 120-124, 1958.
12) P. Kofstadt and W. E. Wallace, J. Am. chem. Soc. **81**, 5019-5022, 1959.
13) S. Komjathy, J. Less-common Metals **2**, 466-480, 1960.
14) P. Kofstadt, W. E. Wallace and L. J. Hyvönen, J. Am. chem. soc. **81**, 5015-5019, 1959.
15) A. Sieverts and H. Hagen, Z. phys. Chem. **A 174**, 247-259, 1935.
16) A. W. Carson, T. B. Flanagan and F. A. Lewis, Trans. Faraday Soc. **56**, 363-370, 1960.
17) L. LaGrange, L. J. Dijkstra, J. M. Dixon and U. Merten, J. phys. Chem. **63**, 2035-2041, 1959.
18) G. G. Libowicz, H. J. Hayes and T. R. P. Gibb, J. phys. Chem. **63**, 76-79, 1958.
19) K. H. Lieser and H. Witte, Z. Elektrochem. **61**, 367-376, 1957.
20) K. H. Lieser and G. Rinck, Z. Elektrochem. **61**, 357-359, 1957.
21) J. R. Lacher, Proc. roy. Soc. **161 A**, 525-545, 1937.
22) S. L. H. Martin and A. L. G. Rees, Trans. Faraday Soc. **50**, 343-352, 1954.
23) M. W. Mallett and I. C. Campbell, J. Am. chem. Soc. **73**, 4850-4852, 1951.
24) R. E. Rundle, C. G. Shull and E. O. Wollan, Acta cryst. **5**, 22-26, 1952.
25) D. T. Peterson and D. G. Westlake, Trans.metall. Soc. AIME **215**, 444-447, 1959.
26) W. H. Zachariasen, Acta cryst. **6**, 393-395, 1953.
27) J. H. N. v. Vucht, this thesis, chapter 2, also Philips Res. Repts **16**, 1-40, 1961.
28) N. Warmoltz and E. Bouwmeester, Appl. Sci. Res. Sect. **B 2**, 273-276, 1952.
29) C. G. J. Jansen and A. Venema, Vacuum **9**, 219-230, 1959.
30) D. P. Smith, Hydrogen in Metals, University of Chicago Press, Chicago Illinois, 1948.

CHAPTER 4

X-RAY DIFFRACTION OF Th_2Al CONTAINING HYDROGEN

Summary

Room-temperature X-ray diffraction of hydrogen solutions in the intermetallic compound Th_2Al shows that, in compositions lying between $Th_8Al_4H_0$ and about $Th_8Al_4H_5$, a two-phase region occurs. From $Th_8Al_4H_5$ upward the hydrogen solutions remain homogeneous up to the saturation level corresponding to $Th_8Al_4H_{15.4}$. The volume of the unit cell increases monotonically, but the a-axis of the cell increases up to the composition $Th_8Al_4H_8$ and then decreases linearly on further hydrogenation until approximately the value of the original hydrogen-free compound is reached. Apart from a general discussion of the nature of the hydrogen-metal interaction, a model of the system here studied is proposed. This model implies an orderly, or a strong tendency towards an orderly, arrangement of the hydrogen atoms in the interstices of the lattice at half-saturation, i.e. in $Th_8Al_4H_8$.

Résumé

La diffraction des rayons X à la température ambiante de solutions solides d'hydrogène dans le composé intermétallique Th_2Al montre qu'il existe une région à deux phases entre les compositions $Th_8Al_4H_0$ et environ $Th_8Al_4H_5$. Depuis la composition $Th_8Al_4H_5$ jusqu'à la saturation $Th_8Al_4H_{15.4}$, les solutions solides restent homogènes. Le volume de la maille élémentaire tétragonale croît de manière uniforme, mais le paramètre a de la maille élémentaire cesse de croître une fois la composition $Th_8Al_4H_8$ atteinte, et diminue linéairement en hydrogénation progressive jusqu'à ce que la valeur du composé original sans hydrogène soit atteinte. Quelques généralités à propos de la nature d'interaction hydrogène-métal sont données, ainsi qu'une proposition de modèle du système étudié. Ce modèle implique l'ordre ou une tendance à l'ordre, des atomes d'hydrogène dans le réseau interstitiel d'une composition semi-saturée $Th_8Al_4H_8$.

Zusammenfassung

Die Röntgenbeugung von Wasserstofflösungen in der intermetallischen Verbindung Th_2Al zeigt bei Zimmertemperatur ein Zweiphasengebiet zwischen $Th_8Al_4H_0$ und ungefähr $Th_8Al_4H_5$. Von $Th_8Al_4H_5$ bis zur Sättigungszusammensetzung $Th_8Al_4H_{15.4}$ bleiben die Lösungen homogen und einphasig. Das Volumen der tetragonalen Elementarzelle nimmt monoton zu, die Länge der a-Achse der Zelle vergrössert sich aber nur bis zur Zusammensetzung $Th_8Al_4H_8$ und nimmt dan beim Weiterhydrieren linear ab, bis der ungefähre Wert der ursprünglichen wasserstofffreien Zelle erreicht ist. Es wird nicht nur die Art der Wechselwirkung Wasserstoff-Metall besprochen, sondern auch ein Modell für das untersuchte System vorgeschlagen. Dieses Modell impliziert eine Ordnung oder starke Neigung zu einer Ordnung, bei der sich die Wasserstoffatome bei halber Sättigung, d.h. beim $Th_8Al_4H_8$, auf Zwischengitterplätzen befinden.

1. Introduction

Recently [1]) it was shown that Th_2Al absorbed hydrogen up to a maximum of nearly 16 hydrogen atoms per unit cell of Th_8Al_4 at room temperature and that, at least at 300 °C and above, homogeneous solutions were formed, according to the absence of plateaux in the isotherms. It seemed of interest to know where this hydrogen was located and what its influence was on the metallic

structure. The absence of a second phase at the said temperatures was surmised on the presumption that the diffusion of thorium and aluminium atoms in the lattice was too slow to give rise to a new arrangement (if energetically favourable) in the form of some ternary hydride or of a separation into a thorium hydride and aluminium. First this had to be verified, and then — in case of true homogeneity — the effect of an increasing hydrogen content, for example, a gradual deformation, had to be studied. Both effects ought to be observable with X-rays because they concerned the siting of the heavier atoms thorium and aluminium. There was, however, no possibility of determining in this way the exact positions of the hydrogen atoms in the cell, because of their lack of scattering power compared to that of the thorium and aluminium atoms.

2. Experimental

Powder specimens of fine-grained ($< 35\ \mu$) Th_2Al were degassed by heating them to 900 °C in a vacuum. After the pumping off of the liberated gases and cooling down to room temperature, a measured amount of hydrogen was absorbed by the metal powder. The volume of the hydrogen was measured in a glass bulb previously calibrated with water. The pressure was measured with an oil manometer (see ref. [1]), fig. 1). The temperature was measured outside the bulb by a normal mercury thermometer. After hydrogen absorption the powder was annealed for about 4 hours in the closed volume at such a temperature that the hydrogen equilibrium pressure amounted to $\approx 10^{-2}$ torr. This temperature was found by cycling slowly from room temperature to 700 °C and back a few times. Thus special care was taken that the specimens were homogeneous.

After homogenization and cooling down to room temperature the apparatus was filled with nitrogen at slightly more than atmospheric pressure. A ground glass joint was now opened, the excess pressure causing an outward streaming of nitrogen that prevented ingress of air. It was now possible to lift the silica crucible, containing the specimen, with the help of an angling line, to just below the opening, where it could be reached by a glass syringe. By means of the latter the powder was immersed in a protective solution of nitrocellulose in acetone without having been exposed to air. This slurry was pasted on a "Philips" diffractometer specimen holder in such a way that, after drying, the surface of the specimen was level and coincident with the axis of the diffractometer. The protective action of the dried binder ensured that the specimen was protected from oxidation for some weeks. The hydrogen content of the specimens was calculated from the volumetric data and the known weight of metal powder, taking into account the oxide content determined by chemical analysis.

X-ray diagrams were made, using copper $K\alpha$ radiation over the largest possible diffraction angle. With the help of the reflections at low angles the diagram was indexed. The reflections at the higher reflection regions served to

calculate the cell dimensions. Where possible, back reflections were used. For different specimens it was often necessary to use different reflections: displacements of the reflections sometimes involved merging of a given line with another or with an oxide line; also the diffuseness of some lines made these unsuitable. For calculations the method of the least squares was used.

3. Results

After the results of the pressure measurements of hydrogen in equilibrium with its solid solutions in Th_2Al, described previously[1]), it was surprising to find that at room temperature a two-phase region existed: between a hydrogen content of 0 and about 5 atoms per Th_8Al_4 the specimens showed a mixture of two line patterns. These corresponded to phases that were isomorphous and differed

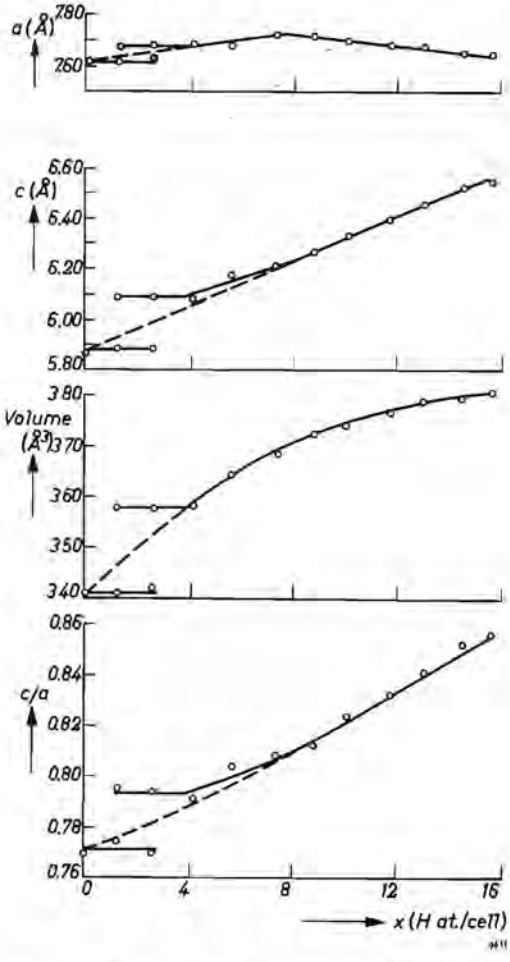

Fig. 1. Cell dimensions as a function of hydrogen content of $Th_8Al_4H_x$ at room temperature.

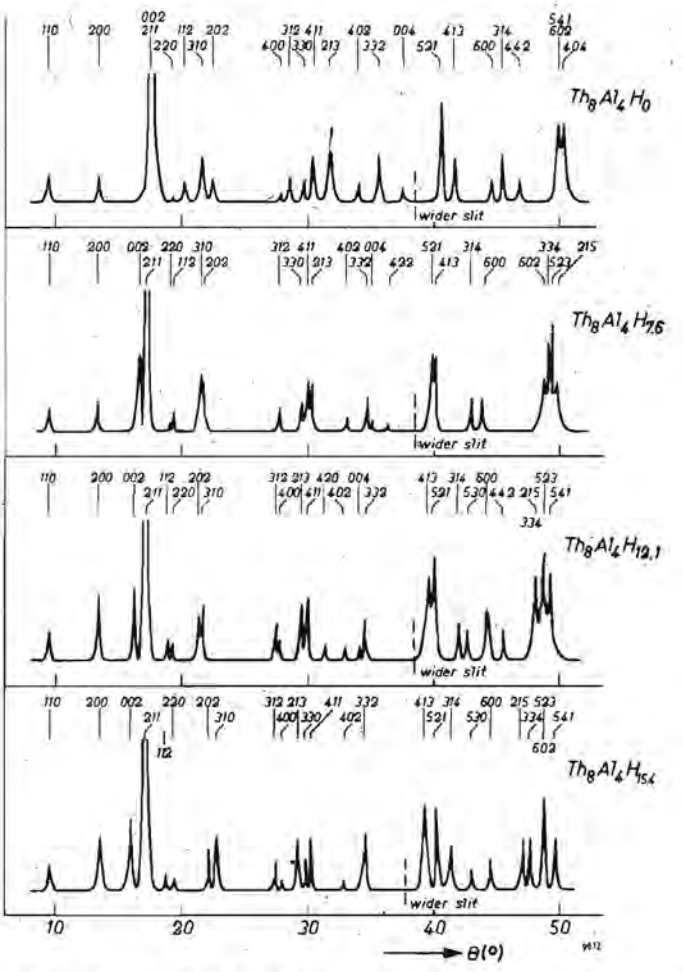

Fig. 2. X-ray diagrams of $Th_8Al_4H_x$ for $x = 0$, $x = 7{\cdot}6$, $x = 12{\cdot}1$ and $x = 15{\cdot}4$.

only in spacings. The diagram of fig. 1 therefore gives in this region two sets of data, corresponding to the coexisting phases. Understandably the determination of the cell dimensions was less exact in these mixtures, particularly where the specimen contained only a small proportion of the phase to be measured. However, the data of the two coexisting phases proved to be fairly constant, as must be expected for a binary equilibrium state. As fig. 1 shows, the hydrogen content of the original phase cannot be increased measurably at room temperature — judging from the lack of expansion — without the formation of a new phase. Apparently this new phase is able to dissolve homogeneously very large amounts of hydrogen. Its reflections stay nicely sharp over the whole range (see fig. 2) and allow precise spacing determinations. The c-axis of this phase increases monotonically until it reaches a saturation value of 112 % of the value for pure Th_2Al.

The length of the *a*-axis, however, behaves peculiarly: its original increase appears to change abruptly into a decrease. It is remarkable that the maximum length of the *a*-axis occurs at a content of about 8 atoms hydrogen per unit cell. The effects are smaller than the changes in length of the *c*-axis but very distinct. Since no discontinuity is found in the cell volume — in fact it appears to be possible to extrapolate it through the two-phase region (broken line in fig. 1) back to the original hydrogen-free phase — it is likely that at this point a small change of slope occurs in the *c*-axis curve as well. This, however, could not be measured with enough certainty, as the points in the left-hand part of the curve show.

TABLE I

Measured cell dimensions for the composition $Th_8Al_4H_x$

composition $Th_8Al_4H_x$	a(Å)	c(Å)	c/a	V(Å^3)
$x = 0$ raw material degassed at 900 °C	7·6157	5·8610	0·7695	340·5
$x = 1·3$ phase 1 (80%)	7·6121	5·8863	0·7738	341·0
$x = 1·3$ phase 2 (20%)	7·6653	6·0877	0·7945	357·9
$x = 2·6$ phase 1 (43%)	7·6298	5·8708	0·7695	341·8
$x = 2·6$ phase 2 (57%)	7·6684	6·0825	0·7932	357·6
$x = 4·1$ 92% phase 2 (only a trace of phase 1)	7·6780 ±0·0003	6·0731 ±0·0003	0·7905	358·3
$x = 5·6$	7·6857	6·1664	0·8930	364·0
$x = 7·3$	7·7051	6·2020	0·8073	368·4
$x = 8·7$	7·7068	6·2581	0·8122	372·2
$x = 10.0$	7·6909	6·3237	0·8225	373·9
$x = 11.6$	7·6758	6·3834	0·3813	376·5
$x = 13·0$	7·6645	6·4442	0·8400	378·6
$x = 14·4$	7·6404	6·5034	0·8515	379·3
$x = 15·4$	7·6324	6·5305	0·8555	380·2

Overall homogeneity was difficult to obtain, particularly in the region up to 8 hydrogen atoms per unit cell. This was found during the numerous preparations. Obviously in this region some extra hindrance was encountered by the

hydrogen in its attempts to attain by diffusion a uniform distribution in the specimen. This uniformity could only be presumed on the basis of diffraction diagrams that did not change any more with repetitions of the annealing process. However, it is still quite possible that the inner regions of the grains contained a considerably smaller concentration of hydrogen; such regions, deep in the grains, would make no observable contribution to the X-ray diffraction pattern. This effect directly gave rise to an extra uncertainty in the concentration data and is related to the troubles met in getting reproducible equilibrium-pressure values of hydrogen above the metal, as described earlier [1].

4. Discussion

The results show three different features, each of which will be discussed separately, namely the two-phase region, the expansion in general, and the anomaly in the expansion.

4.1. *Two-phase region*

The occurrence of a two-phase region is not in contradiction with the results of the equilibrium-pressure measurements; it is indeed valuable as a supplementary datum.

From the absence of a plateau in the 300 °C isotherms it was concluded that at this temperature no two-phase region existed. This was only justified if a rearrangement of the thorium and aluminium atoms did not occur. It has been shown that such a rearrangement does not occur, so the system Th_2Al-H_2 is in fact quasi-binary. Furthermore, if the room-temperature two-phase region found with X-rays represents an equilibrium state, then we have now defined a temperature region (though a rather wide one) in which the critical temperature of the two-phase region must lie. Above this point it is now possible to identify the points of inflection in the isotherms of the hydrogen equilibrium pressure (see ref. [1]), fig. 6), as being the rudiments of lower-lying plateaux. The question then arises of the ideal composition of each phase. Obviously one of the phases is Th_2Al, which is apparently able to dissolve homogeneously a quantity of hydrogen that increases with temperature. The second phase has been found to have a composition at room temperature of somewhere between 4 and 5 hydrogen atoms per unit cell, but in view of the comparative proximity of the critical point, where the compositions of both phases become equal, it is likely that it possesses a composition that deviates considerably from the ideal (stoichiometric) one. In accordance with the apparently small hydrogen content of the first phase at room temperature and the position of the point of inflection at approx. 4 hydrogen atoms per unit cell, as well as the fact that the room-temperature composition of the second phase is about 5 hydrogen atoms per cell, it must be concluded that the two-phase region in the T-x diagram has a very asymmetrical form. The shape of the curve, with the length of the a-axis as the

ordinate (cf. fig. 1), leads us to suspect that the composition with 8 hydrogen atoms per unit cell represents some special point and could be associated with the unknown ideal composition of the compound in question. This new phase would then possess a very broad homogeneity range, not only to the right-hand (excess hydrogen) side, but to the hydrogen-defective side as well.

4.2. *Volume expansion*

Fom fig. 1 it is seen that the volume of Th_2Al increases monotonically with the hydrogen content. The result of inserting hydrogen in a metallic lattice is not always expansion: sometimes contraction occurs. There proves to be no correlation between this size effect and the sign of the heat of reaction. Geometrical factors are more likely to play a role, for example the space needed for the hydrogen atom, which is nearly always sought in the interstices of the metallic lattice.

It has been commonly accepted that the hydrogen particle, dissolved in the metal, does not stay purely atomic. The interaction of metal and hydrogen is of the kind that a chemical bond is formed. The question arises as to whether this bond is ionic, homopolar or metallic in character. Representatives of each kind have been sought and found. The homopolar bond seems to occur, for example, in copper hydride and in some other, often metastable hydrides, some of which are gaseous. The two other kinds are of more importance for metallurgy: both can yield stable hydrides. The ionic bond is assumed to exist in the alkali-metal hydrides, for example in LiH. Here hydrogen is present as a negative ion H^-. This has been proved by Moers [1]) by electrolysis of molten lithium hydride, during which hydrogen was evolved at the anode. This hydride, like all those of the alkali and the alkaline earth metals, has plainly salt-like, heteropolar properties: the electrical resistance of the crystals is very high and the appearance is white. Upon hydriding the volume change is always negative.

The metallic bond seems to be best represented by the hydrides of hydrogen solutions of palladium and tantalum. The stabilities are not as great as those of the salt-like hydrides but they are also exothermically formed. The theory of the metallic bond can be best demonstrated briefly by discussing the alloying of hydrogen with palladium. This transition metal is believed to have room for an additional 0·6 electrons per atom in the 4*d* orbital, as results of magnetic susceptibility and electrical resistance measurements on its alloys with gold suggest. It is assumed that hydrogen, when it dissolves in palladium, donates its electron to fill up the *d* band. This would explain why the absorption of hydrogen is completed at the composition $PdH_{0.6}$. It must be remarked, however, that this "ultimate" composition is easily exceeded at higher pressure and at lower temperatures [2]), so that the composition PdH is reached, which is in accordance with a palladium having all its octahedral holes [3]) occupied. (In the other f.c.c. metals hydrogen is found to occupy the tetrahedral holes). Nickel is also believed to have 0·6 hole in its *d* band and was found to yield (endothermically,

however) a hydride of composition $NiH_{0.7}$ [4]). Lieser and Witte [5]) have attributed the weak and mostly endothermic hydrogen dissolution in metals like silver, copper and their alloys, in the Laves phases $MgCu_2$, $MgZn_2$, $MgAl_2$, $MgSi_2$ and their homogeneous mixtures, and also in alloys of nickel with zinc and copper, to the decrease of free energy caused by the polarization of the electron gas. This has to be conceived as a refinement of the above picture.

That hydrogen is present as protons in the lattice of these metallic solutions was shown already in 1930 by Coehn [6]) for palladium. When an electric direct current flowed through the solution, he found that the hydrogen migrated in the direction of the current. The transport number, very difficult to measure because of the outnumbering electrons, pointed, according to Wagner and Heller [7]), who compared it with the diffusion rate in a zero electric field, to only a fraction of the unit charge. Therefore they concluded that only part of the hydrogens were present as protons, the electrons participating in the conduction band. Lately Wesolowski c.s. [8]) performed a similar experiment with the radioactive (β-ray decay) isotope tritium ^3H in tantalum, with the same result. The hydrides of palladium and tantalum are good electrical conductors and retain their metallic appearance, but are hard and brittle. The volume is increased with respect to the original metals.

It is tempting to attribute the volume increase, and in the case of the alkali metals the decrease, directly to the addition of electrons to, or withdrawal of electrons from, the electron gas. The proton has no electron cloud and is therefore virtually dimensionless; only its positive charge is of influence (but probably only in the small interstices) on the metal-metal spacings. Judging from the volume that the hydrogen atoms require in titanium, the tetrahedral interstices of which are increased from the size corresponding to spherical particles of radius 0·35 Å to that for particles of 0·46 Å, thorium would have to swell only about 6 vol %; in actual fact the increase is 29 %. If the expansion is attributed to the volume increase of the electron gas we can estimate its extent by considering the compressibility κ of the mother metal. Thus, with a value of κ more than twice as large for thorium as for titanium, the above behaviour becomes partly comprehensible. On the other hand, when the salt-like hydrides are formed, it is clear that with the diminution of the electron gas, although H^- ions are formed that have a radius of about 1·5 Å, the nett effect is a shrinkage (which also will be larger, the larger the compressibilities). Figure 3 gives the volume increase of various elements, arranged according to mass number. It shows the various columns of the Periodic System (broken lines). It is also seen that several members of the lanthanide group seem to stand on the verge between the swelling and the shrinking metals, indicating that some kind of mixed bonds, or combinations of the two kinds, are possible. (The homopolar copper hydride is conspicuous as an extraordinary case.)

Libowitz and Gibb [9]), after a suggestion from Dialer, showed that in the

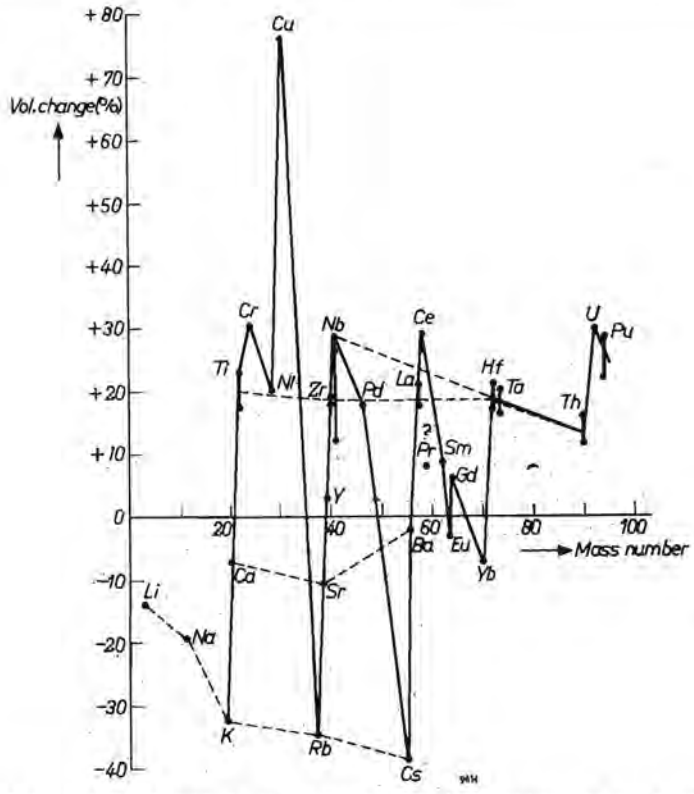

Fig. 3. Relative volume changes, in % per metal atom, upon addition of one hydrogen atom to the metal lattice, for metals arranged according to mass number. Where a range of hydride compositions is possible, i.e. with titanium, zirconium, etc., the mean value is given by the point of intersection of the broken line with the line corresponding to the range of the volume change. The broken lines connect the metals making up a certain sub-group in the periodic table.

hydrides of most of the elements of the groups IIIa (Sc, Y, La) and IVa (Ti, Zr, Hf, Th) including the lanthanide and the actinide series, H^- anions can be assumed to exist with a radius of $1{\cdot}29 \pm 0{\cdot}05$ Å. They calculated the nuclear spacings, using cation radii of the rare gas configuration and implying that the surplus electrons take part in a weak metallic bonding (for example: ThH_2 should be constituted of a cation Th^{4+}, two anions H^- and an "electron gas" of the remaining two electrons per thorium). This conception, too, is oversimplified since the remaining electrons are thought to take up no room, and above all it is not valid for those hydrides where proton migration has been found to occur. Particularly in those hydrides of hydrogen solutions where high mobilities of hydrogen are observed it is likely that the metallic bond predominates. Taking the two states of hydrogen H^- and H^+ as the extremes, it is possible to think of another way of combining the ionic with the metallic character, namely a resonance between these two states. Temperature decrease stabilizes the H^-

state, temperature increase opens up more possibilities for the H^+ state because of the open levels at the Fermi surface. And, if we assume that diffusion of the hydrogen atoms from interstice to interstice in the metallic lattice can only take place (at temperatures where this lattice is rigid and poor in vacancies) by jumping as a proton, we may get a full picture for the intermediate hydrides. Thus it is possible to have a salt-like character and a rapid diffusion of hydrogen in the same hydride, which is brittle at low temperatures but has more metallic character at higher temperatures.

4.3. *Anomalies in the expansion*

It does not seem too absurd to assume that at temperatures above the critical one, the cell constants vary as represented by the broken lines in fig. 1. This simplified situation will be the subject of this discussion.

At first sight the most striking point in the results is that expansion is nearly uniaxial: the maximum change in length of the *a*-axis is only one third of the change of the *c*-axis at that point. The ratio of the total change in the two directions is particularly large because the *a*-axis shrinks again to nearly the same value as in pure Th_2Al. The second point is the anomalous behaviour of the *a*-axis and, in connexion with this, the composition at which the anomaly occurs. Neither the uniaxial deformation nor the anomalous behaviour of the *a*-axis is unique.

Some anisotropy may be expected in a tetragonal lattice. Even the close-packed hexagonal lattice of zinc, consisting of one kind of atoms, shows such an anisotropic, nearly uniaxial dilatation in the *c*-direction upon heating. Even the cubic (f.c.c., $a = 5{\cdot}08$ Å) isotropic lattice of thorium, where, upon hydriding, the hydrogen atoms are placed in the regular tetrahedral holes, deforms in such a way that a tetragonal ThH_2 results instead of the normal cubic CaF_2-type hydride. For some unknown reason two edges of the tetrahedra are increased and the other two decreased, although they are crystallographically equivalent. Expansion then occurs in only one direction: from 5·08 Å to 5·80 Å, while in the other directions (perpendicular to the first one) there is slight contraction from 5·08 Å to 5·03 Å. Titanium, zirconium and hafnium have also hydrides XH_2 of a deformed CaF_2-type. This behaviour does not fit into the picture of Libowitz and Gibb, for only particles too small for the interstices they occupy could be imagined to give anisotropic effects; spherically symmetric ions that fit well could harly do so. Yakel [10]) believed the deformation to be due to an electronic ordering process, but then in the sense that homopolar, directional binding forces are beginning to take part, possibly admixed to the more symmetric forces of the ionic and metallic type, working on an H^- or an H^+ ion respectively. He showed for TiH_2 that the deformation disappeared at a definite temperature (310 °C), where a transformation of the low-temperature tetragonal unit cell into the cubic CaF_2-type modification could be observed, but where no effect

could be found in the variation of the cell volume. Another way to obtain cubic hydrides of these metals is to withdraw some hydrogen from the stoichiometric dihydrides [11, 12, 13]).

Anomalies in the expansion as a result of hydrogenation have been previously found also for some rare-earth metals. Cerium and lanthanum, which like thorium are cubic-close packed, form normal (undeformed) calcium-fluoride type dihydrides. Hydrogen is occluded in the tetrahedral holes, and causes a considerable increase in the lattice parameter. It is possible to increase the hydrogen content beyond the point where all the tetrahedral holes are occupied, thus surpassing the composition XH_2. Holley et al. [14]) found that from that point on hydrogen addition is accompanied by a lattice-parameter decrease, while the hydride stays homogeneous and cubic. In this second process hydrogen is believed to fill up the octahedral holes. It must be emphasized that the volume of the hydride (the end point is the hexagonal BiF_3-type trihydride) decreases too, which is different from our case. But the point is that the maximum of the lattice parameter corresponds with the stoichiometric composition of an intermediate hydride. In connexion with this it must be remarked that Streck and Dialer [15]) observed a point of inflexion between CeH_2 and CeH_3 in the hydrogen pressure isotherms, similar to that found with $Th_8Al_4H_{13}$.

In discussing the properties of the Th_2Al-hydrogen solution it is useful to study the host lattice and look for the interstices that are able to accommodate a hydrogen. Figure 4 shows the structure of Th_2Al in perspective, in order to demonstrate the tetrahedral holes. There are 16 that are crystallographically equivalent, and 4 of a different kind. In view of the maximum attainable composition of 16 hydrogen atoms per unit cell of Th_8Al_4, we assume that the 16 equivalent tetrahedra are occupied. The tetrahedra are similar to those found in f.c.c. thorium, but they are arranged in pairs in such a way that each couple has one plane in common, namely the plane parallel to the base of the cell, and they are slightly deformed. To explain the behaviour of fig. 1 (the original increase and subsequent decrease of the *a*-axis and the location of the rather sharp point where increase changes into a decrease) we might think of the following process. Up to a concentration of 8 hydrogen atoms per unit cell the hydrogens are randomly distributed over the 8 "double holes", in the sense that each single particle occupies one "double hole". From this concentration onward, each newly added hydrogen atom forms a doubly occupied "double hole". The change in size accompanied by the occupation of a double hole by two hydrogen atoms can be judged from the experimental data of fig. 1. The *c*-axis increases considerably and the expected Poisson contraction of the *a*-axis is obviously practically compensated by an expansion in the latter direction, as is demonstated by the fact that at saturation the length of the *a*-axis is virtually equal to that of the hydrogen-free metal. The initial linear increase and subsequent decrease of the *a*-axis in fig. 1 is supposed to be due to the initially increasing and eventually

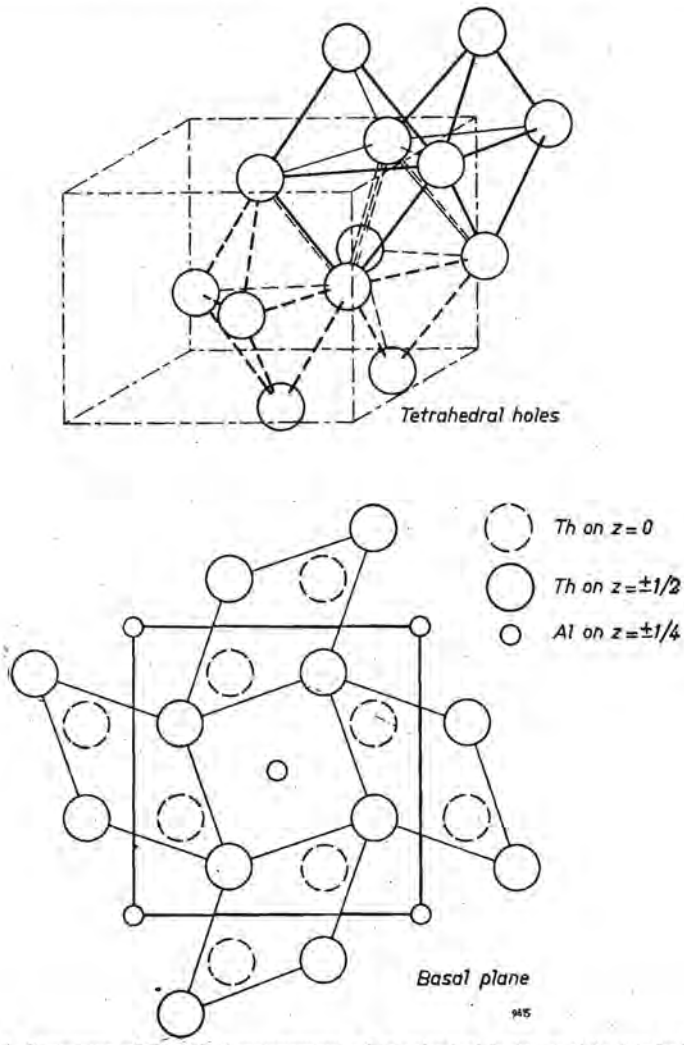

Fig. 4. Structure of Th_2Al. Arrangement of tetrahedral holes as "double holes".

decreasing possibility for the hydrogen atoms to vibrate from one partner of a "double hole" into the other. Such a vibration mode implies that the hydrogen atom remains for a finite time in the common plane of the tetrahedra. Logically the three thorium atoms in this plane are then forced somewhat away from each other which means an extra expansion of the *a*-axis. As the double holes are filled one by one with a second hydrogen atom this vibrational mode is lost and the extra expansion is reversed stepwise. Each occupied double hole will contribute equally to the overall expansion; thus the behaviour in fig. 1 is accounted for. Naturally we obtain the same result if we merely assume that a single hydrogen, placed in a "double" hole, causes an elongation of both axes, while two hydro-

gens together in a "double" hole, cause only the *c*-axis to expand. Then the effect also exists at temperatures at which the vibrational modes of the hydrogens are largely suppressed. The above explanation implies that at half saturation the hydrogens are strongly ordered in the common plane (which is unlikely because of geometrical reasons) or, if they vibrate from one half of the "double hole" to the other, that they are seemingly located nearer to the common plane at half saturation than at full saturation.

Besides this rather speculative explanation, which accounts for the point where the anomaly occurs, the possibility remains that the behaviour observed is due to two simultaneous processes of opposite sign: normal expansion, but then nearly uniaxial, and a simultaneous non-linear contraction that is not coupled specially to composition. It is, however, not easy to find any theoretical basis for such a process.

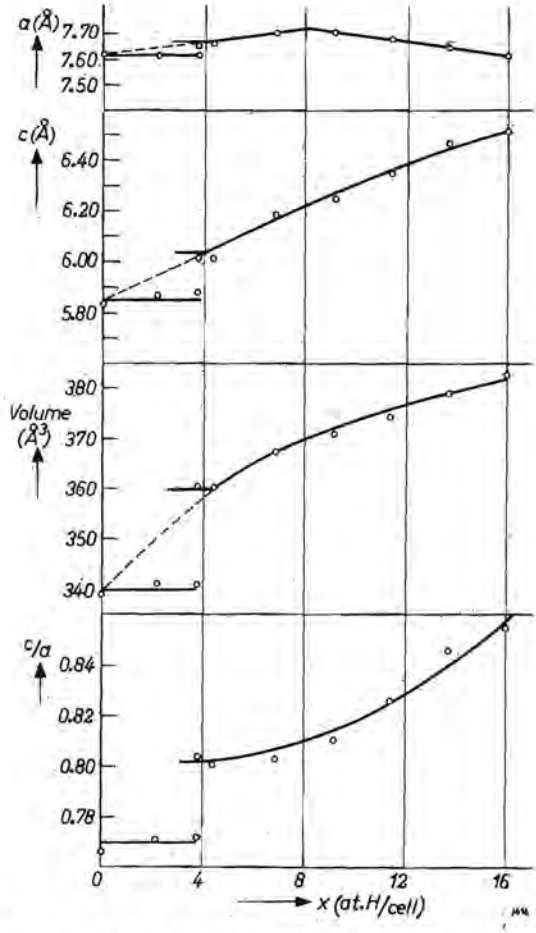

Fig. 5. Cell dimensions of (0·875 Th, 0·125 Ce)$_8$Al$_4$H$_x$ as a function of hydrogen content.

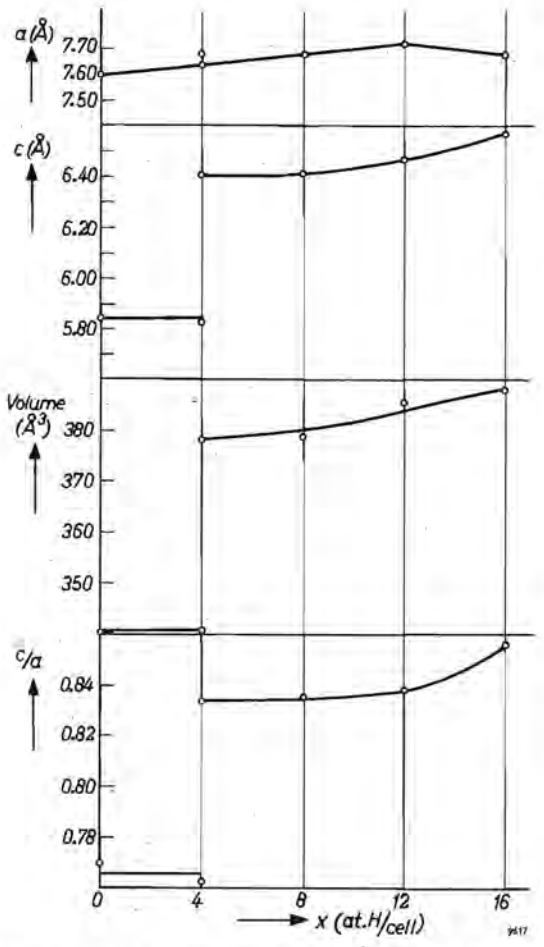

Fig. 6. Cell dimensions of (0·75 Th, 0·25 Ce)$_8Al_4H_x$ as a function of x.

5. Influence of cerium

For the sake of completeness similar measurements have been made with (0·875 Th, 0·125 Ce)$_8Al_4$–H (see fig. 5) and for (0·75 Th, 0·25 Ce)$_8Al_4$–H (fig. 6). The oxide content and the presence of traces of other phases, in particular in the latter specimen, vitiated an exact determination of the hydrogen content. Nevertheless it is clear that the behaviour of the lattice does not change essentially with cerium content. The behaviour of the a-axis of (0·75 Th, 0·25 Ce)$_8Al_4$ deviates somewhat, which might be in accordance with the expectation that in the neighbourhood of a cerium atom the occluded hydrogen particle has a more anionic character and cannot migrate.

REFERENCES

1) J. H. N. van Vucht, this thesis chapter 3.
2) K. Moers, Z. anorg. Chem. **113,** 201-230, 1920.
3) P. L. Levine and K. E. Weale, Trans. Far. Soc. **56,** 357-364, 1960.
4) J. E. Worsham Jr., M. K. Wilkinson and C. G. Shull, Phys, and Chem. of Solids **3,** 303-310, 1957.
5) B. Baranowski and M. Smialowski, J. phys. Chem. Solids, **12,** 206, 1960.
6) K. H. Lieser and H. Witte, Z. Elektrochem. **61,** 367-376, 1957.
7) A. Coehn and W. Specht, Z. Physik **62,** 1-31, 1930.
8) C. Wagner and G. Heller, Z. phys. Chem. **B 46,** 242-249, 1940.
9) J. Wesolowski and others, Bull. Acad. pol. Sci. serie des sciences chimiques **9,** 651-655, 1961.
10) G. G. Libowitz and T. R. P. Gibb, J. phys. Chem. **60,** 510, 1956.
11) H. L. Yakel, Acta cryst. **11,** 46-51, 1958.
12) S. S. Sidhu, L. Heaton and D. D. Zauberis, Acta cryst. **9,** 607-614, 1956.
13) V. V. Sof'ina, Z. M. Azarkh and N. N. Orlova, Sov. Phys. Cryst. **3,** 544-550, 1958.
14) L. Espagno, P. Azou and P. Bastien, C. R. Acad. Sci. Paris **250,** 4353, 1960.
15) C. E. Holley Jr., R. N. R. Mulford, F. H. Ellinger, W. C. Koehler and W. H. Zachariasen, J. phys. Chem. **59,** 1226-1228, 1955.
16) R. Streck and K. Dialer, Z. anorg. Chem. **306,** 141-158, 1960.

CHAPTER 5

NEUTRON DIFFRACTION AND PROTON MAGNETIC RESONANCE OF DEUTERIUM AND HYDROGEN SOLUTIONS IN Th_2Al

Summary

Room-temperature neutron-diffraction diagrams of powder samples of $Th_8Al_4D_8$, $Th_8Al_4D_{12}$ and $Th_8Al_4D_{15\cdot4}$ indicate that a dissolved hydrogen atom occupies a crystallographically sixteenfold position. This is situated in 8 pairs of tetrahedral holes; each couple of tetrahedra has one plane in common. The four other tetrahedral holes are less likely. For the non-saturated specimens a random occupation of these holes agrees best with the experiment. At 95 °K no orderly arrangement of hydrogen in $Th_8Al_4D_8$ has been found. Proton-magnetic resonance measurements have been made with specimens of compositions $Th_8Al_4H_8$, $Th_8Al_4H_{12}$, $Th_8Al_4H_{15\cdot4}$ and $Th_8Al_4H_{\approx8}D_{\approx8}$, at room temperature and downwards as far as 77°K. At room temperature the non-saturated specimens show "motional narrowing" of the resonance peaks, due to rapid interstitial diffusion of the protons. The fully saturated specimens yield broad lines. The second moments of these lines and also those of the low-temperature lines of $Th_8Al_4H_8$ and $Th_8Al_4H_{12}$ are in agreement with the neutron-diffraction results. Also these experiments failed to give evidence of an orderly arrangement of hydrogen in $Th_8Al_4H_8$.

Résumé

Les diagrammes de diffraction neutronique de poudres de $Th_8Al_4D_8$, $Th_8Al_4D_{12}$ et $Th_8Al_4D_{15\cdot4}$ indiquent, à la température ambiante, que les atomes d'hydrogène dissous occupent une situation cristallographique seize fois identique. Cette situation se retrouve dans 8 paires de sites interstitiels tétraédriques du réseau; chacun des deux tétraèdres ainsi couplés a une face en commun avec l'autre. L'occupation de quatre autres tétraèdres est moins probable. Quant aux échantillons non-saturés, une répartition aléatoire semble s'accorder le mieux avec les expériences. A 95 °K, on n'a trouvé aucune occupation d'hydrogène ordonnée dans $Th_8Al_4D_8$. Des mesures de résonance magnétique de protons ont été effectuées sur les préparations des compositions $Th_8Al_4H_8$, $Th_8Al_4H_{12}$, $Th_8Al_4H_{15\cdot4}$ et $Th_8Al_4H_{\approx8}D_{\approx8}$ à la température ambiante et au-dessous jusqu'à 77 °K. A la température ambiante, les échantillons non-saturés accusent un fort rétrécissement (motional narrowing) des raies d'absorption par suite de la diffusion rapide des protons dans le réseau interstitiel. Les échantillons complètement saturés donnent lieu à de larges raies. Les deuxièmes moments de ces raies, tout comme celles qui sont obtenues aux basses températures pour $Th_8Al_4H_8$ et $Th_8Al_4H_{12}$, s'accordent avec les résultats de la diffraction des neutrons. De cette manière non plus, on n'a pas obtenu de preuve formelle d'une disposition ordonnée des atomes d'hydrogène dans $Th_8Al_4H_8$.

Zusammenfassung

Die Neutronenbeugungsdiagramme von $Th_8Al_4D_8$–, $Th_8Al_4D_{12}$– und $Th_8Al_4D_{15\cdot4}$–Pulvern zeigen, daß bei Zimmertemperatur die gelösten Wasserstoffatome kristallographisch eine Sechzehnpunkt-Ordnung einnehmen. Diese Ordnung besteht aus 8 Tetraederlückenpaaren; je zwei Tetraeder haben eine Fläche gemeinsam. Vier andere Tetraederlücken sind weniger wahrscheinlich. Bei den ungesättigten Präparaten stimmt eine willkürliche Besetzung dieser Lücken mit den Experimenten am besten überein. Bei 95 °K wird beim $Th_8Al_4D_8$ bei der Besetzung durch Wasserstoffatome auch keine Ordnung gefunden. Protonenspin-Resonanzmessungen wurden bei Zimmertemperatur und bis zu 77 °K an Präparaten von $Th_8Al_4H_8$, $Th_8Al_4H_{12}$, $Th_8Al_4H_{15\cdot4}$ und $Th_8Al_4H_{\approx8}D_{\approx8}$ durch-

geführt. Bei Zimmertemperatur wurden für die ungesättigten Präparate wegen der schnellen Diffusion der Protonen im Zwischengitter sehr schmale Resonanzlinien („motional narrowing") erhalten. Die gesättigten Präparate zeigen breite Linien. Die zweiten Momente dieser Linien und ebenfalls der bei niedrigen Temperaturen erhaltenen Resonanzlinien von $Th_8Al_4H_8$ und $Th_8Al_4H_{12}$ stimmen mit den Meßergebnissen der Neutronenbeugung überein. Auch bei diesen Experimenten wird kein Beweis für eine geordnete Anordnung der Wasserstoffatome im $Th_8Al_4H_8$ gefunden.

1. Introduction

It was not possible by means of X-ray diffraction alone to decide where exactly the hydrogen particles were located in the Th_2Al lattice. Therefore resort was had to neutron diffraction. Neutrons are scattered quite differently from the way X-rays are. The latter, as is well known, are scattered by the electrons. Thus for X-rays the thorium atom has a scattering factor of about 90 times that of hydrogen, which means that it is quite impossible to detect hydrogen in a lattice containing thorium. Neutrons, however, interact with the atomic nuclei and also, because the neutron itself has a magnetic moment, with ions possessing a magnetic moment. The coherent neutron-scattering lengths for thorium, aluminium and hydrogen are $b_{Th} = 1{\cdot}01$, $b_{Al} = 0{\cdot}35$ and $b_H = -0{\cdot}38$ (10^{-12} cm) respectively. Hydrogen scatters neutrons mainly incoherently, which causes a large background, especially if the samples are polycrystalline. Therefore we preferred to use the chemically equivalent isotope deuterium instead, with $b_D = 0{\cdot}65$ (10^{-12} cm).

In addition another means of locating the hydrogen atoms was tried, namely the method of nuclear magnetic resonance or N.M.R. (here, proton-magnetic resonance, P.M.R.). This method of structure determination is based on the interaction of magnetic moments of nuclei, which is a function of their mutual separation.

In an external magnetic field H the energy levels of a proton-magnetic moment μ are given by

$$E = \pm \mu H.$$

The resonance condition when irradiated by electromagnetic waves is given by

$$\nu_L = 2\,\mu H/h.$$

The detection of this resonance occurs by a selective absorption of electromagnetic energy from an electronic oscillator. For isolated protons the resonance condition is very sharp. However, the magnetic fields arising from neighbouring spins in a crystalline sample cause a broadening of the resonance line. Another way of describing this method is by saying that the proton spins precess with Larmor frequency ν_L. Exchange of energy may take place between two spins, whose Larmor precessions are in phase. The description of this energy exchange

leads to the same expressions as given above. Since the local field of a neighbouring magnetic dipole is of the order of μ/r^3, the P.M.R. absorption will be shifted over plus or minus that field, depending on the sign of the proton spin. More remote protons give rise to a smaller shift, therefore a broadened absorption band is observed. The mean-square width of this band may thus supply information on the proton-proton distances occurring (cf. sec. 7). N.M.R. is specially suitable for the location of nuclei of ordinary hydrogen, because of the large magnetic moment of the proton.

Both series of experiments were conducted more or less in parallel. Neutron diffraction experiments were performed in Kjeller, Norway, at the J.E.E.P. reactor of J.E.N.E.R., in coöperation with Goedkoop and Bergsma. The P.M.R. measurements were made by Kroon and evaluated in cooperation with van der Stolpe in the Philips Research Laboratories. Results have been published elsewhere, partly in a rather abbreviated form [1,2]). Only the cerium-free getter material Th_2Al was studied.

2. Sample preparation

The deuterides $Th_8Al_4D_x$ were prepared as follows. Deuterium was obtained from D_2O by electrolysis, then purified by diffusion through a palladium tube and stored in glass bulbs. Analysis by a mass spectrometer revealed as the only significant contamination about 1 vol.% of normal hydrogen. Samples of Th_2Al powder (grain size $< 35\ \mu$) were degassed in a silica sample holder (fig. 1)

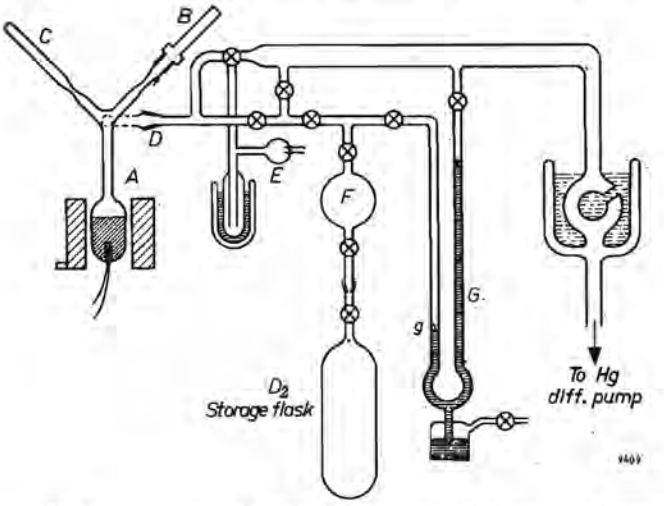

Fig. 1. Apparatus for the preparation of specimens for neutron diffraction and proton-magnetic resonance. *A* is a silica preparation vessel in a nickel/chromium furnace. *B* is the aluminium sample holder, with sealing-off glass capillary, for neutron diffraction. *C* is the hard-glass sample holder for the P.M.R. measurements. Rotation of this assembly is permitted by a ground-glass joint *D* (for the sake of clearness the plane of the three sample holders has not been sketched perpendicular to the paper.) *E* is a Penning-type ionisation gauge. *F* is a calibrated volume. *G* is a manometer with a fixed point (*g*) for the mercury meniscus in one leg.

for several hours at 800-900 °C in a vacuum of approximately 10^{-6} torr. After the sample had cooled down to room temperature the calculated amount of deuterium was added slowly. After absorption of the gas the powder was homogenized at 350 °C for one day and subsequently cooled slowly. In samples containing greater amounts of deuterium, in which the equilibrium pressure exceeded 10 torr, special care was taken that as good an equilibrium as possible was obtained at temperatures below 350 °C. Especially below 300 °C the inwards diffusion proved to be very slow. In order to reach maximum saturation these samples were cooled very slowly for more than a week from 350 °C down to room temperature. In accordance with these techniques samples were made of about 30 grams $Th_8Al_4D_8$, $Th_8Al_4D_{12}$ and $Th_8Al_4D_{15\cdot4}$ (i.e. saturated) for the neutron diffraction measurements. For P.M.R. we prepared samples of about 10 grams of $Th_8Al_4H_8$, $Th_8Al_4H_{12}$, $Th_8Al_4H_{15\cdot4}$ (saturated) and $Th_8Al_4H_{\approx 8}D_{\approx 8}$. The latter specimen was hydrogenated in the normal manner as far as $Th_8Al_4H_8$ then charged with deuterium to saturation at the lowest practicable temperature and finally homogenized. By means of a tilting arrangement the powder sample was transferred in vacuo to the sample holder. For the neutron diffraction this consisted of a thin-walled ($\approx$ 0·1 mm) aluminium cylinder, which was connected to the pumping apparatus by means of a fernico tube and a glass capillary. After filling, the capillary was sealed off. In the case of the P.M.R. samples silica powder, rendered specially dry to avoid protons that might originate in the adsorbed or chemically bound water, and which had been stored in a glass holder attached also to the tilting apparatus, was added to the gas-charged getter powder. Then the thin-walled hard-glass cylindrical sample holder was sealed off and the powders were mixed. The silica powder served to insulate the getter grains from one another: initially it was feared that the electromagnetic waves would not enter the inner grains of the sample because of the skin effect. Later on it was found that the natural oxide skin present at the grain surfaces was itself an effective insulator. The grain size was small enough to avoid line affection arising from skin effect in the grains.

3. Neutron diffraction; experimental

The diffractometer used has already been described by Goedkoop [3]. The wavelength of the neutrons, monochromatized by a lead single crystal, was found to be 1·026 Å. In front of the BF_3 counter Soller slits (0·25 mm wide, 200 mm long) were placed; the resolution is mainly determined by these slits.

Low-temperature measurements were carried out in a vacuum cryostat (fig. 2) designed by De Haan. It was necessary to design a special sample holder for use in the cryostat. The sample powder was transferred from the normal holder into the special one in a glove box filled with dry nitrogen gas. The holder was then fixed to the bottom of the inner cylinder of the cryostat. This cylinder was filled with liquid nitrogen (which could be pumped off). Temperatures were

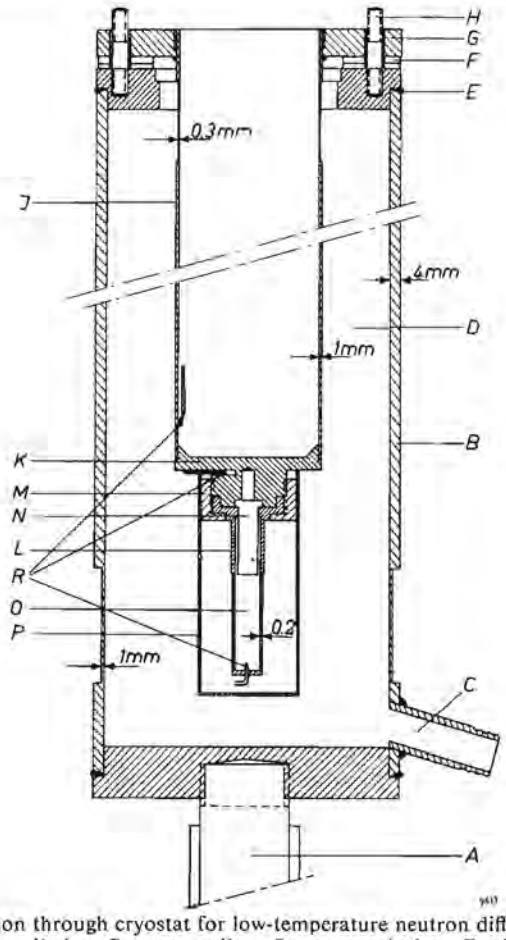

Fig. 2. Vertical section through cryostat for low-temperature neutron diffraction. *A*: support. *B*: aluminium outer cylinder. *C*: vacuum line. *D*: vacuum jacket. *E*: aluminium flange. *F*: pair of rubber washers. *G*: stainless steel flange. *H*: stud. *J*: stainless steel inner cryostat cylinder. *K*: brass bottom of inner cylinder. *L*: aluminium specimen holder. *M*: specimen-holder clamping nut. *N*: aluminium specimen-holder plug. *O*: specimen. *P*: thermal radiation shield. *R*: thermocouples.

measured with thermocouples at the top and bottom of the holder. The cylinder carrying the sample holder was surrounded by a vacuum. In the region traversed by the neutrons the wall of the aluminium outer cylinder was reduced to 1 mm. Around the specimen a thin thermal radiation shield was placed to promote a better temperature equilibrium.

4. Neutron diffraction; results

The diffraction diagrams, taken at room temperature, are shown in fig. 3. As in the diffraction of X-rays, small peak shifts are observed. Here, however, the peak intensities also change. New (superlattice) peaks do not appear.

Before the neutron diffraction peak intensities could be calculated it was

necessary to find out whether the parameters of the thorium and aluminium atoms underwent changes when the getter metal took up hydrogen. An analysis of the X-ray intensities revealed that the thorium parameter $x_{Th} = 0{\cdot}162$ might be considered as a constant throughout the hydrogenating process. Thus trial and error calculations were made, using the positions of Th at 8 (*h*): $\pm(x_{Th}, \frac{1}{2} + x_{Th}, 0)$; $\pm(\frac{1}{2} + x_{Th}, \bar{x}_{Th}, 0)$; $\pm(\frac{1}{2} + x_{Th}, x_{Th}, \frac{1}{4})$; $\pm(x_{Th}, \frac{1}{2} - x_{Th}, \frac{1}{4})$ with $x_{Th} = 0{\cdot}162$ and of Al at 4 (*a*): $\pm(0,0,\frac{1}{4})$; $\pm(\frac{1}{2},\frac{1}{2},\frac{1}{4})$. Since experimentally

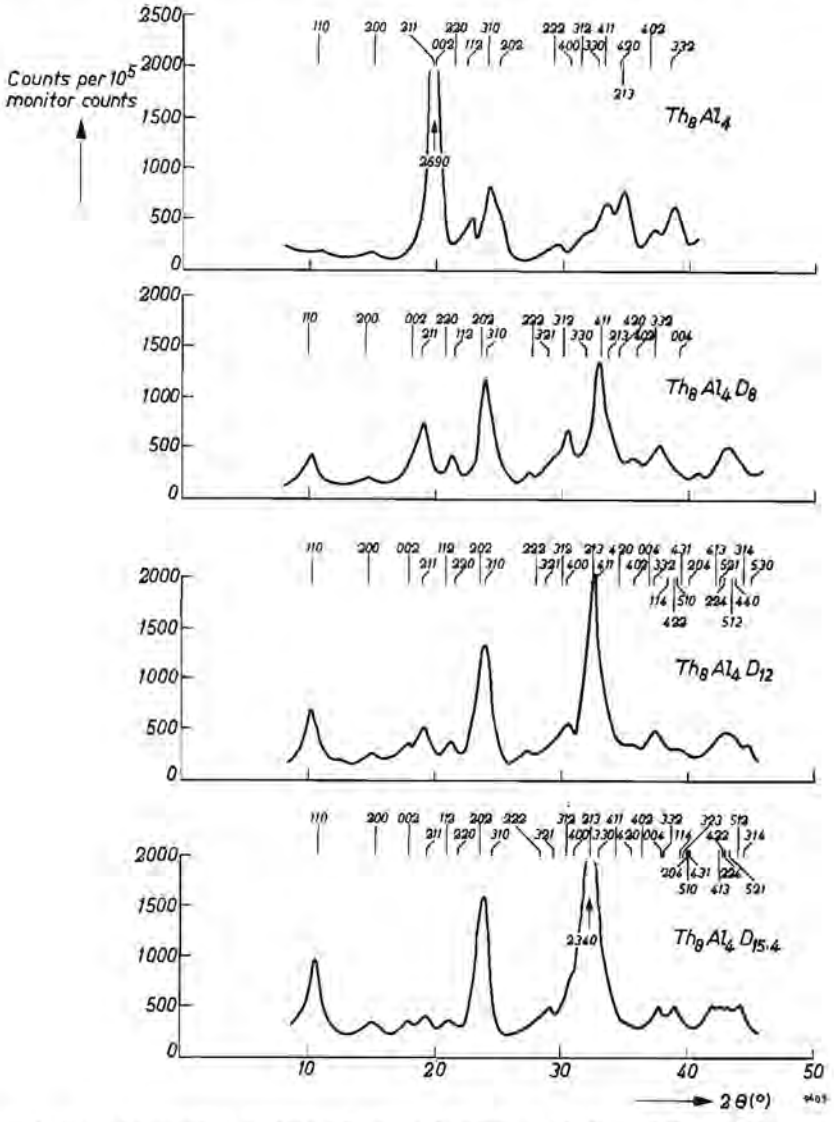

Fig. 3. Room-temperature neutron diffraction diagrams of Th_8Al_4 and three of its deuterium solutions.

the maximum content of hydrogen was always found to be close to 16 atoms per unit cell Th_8Al_4, the most likely place for the (here heavy) hydrogens was the sixteen-fold one: D at 16(*l*): $\pm(x_D,\frac{1}{2}+x_D,\pm z_D)$; $\pm(\frac{1}{2}+x_D,\bar{x}_D,\pm z_D)$; $\pm(\frac{1}{2}+x_D,x_D,\frac{1}{2}\pm z_D)$; $\pm(x_D,\frac{1}{2}-x_D,\frac{1}{2}\pm z_D)$, in the centres of the tetrahedra formed by the thorium atoms. As a second possibility, 4 of the deuteriums per cell might be situated in the somewhat smaller interstitial holes at $\pm(\frac{1}{2},0,\frac{1}{4})$ and $\pm(0,\frac{1}{2},\frac{1}{4})$. There are another three 16-fold positions in the space group *I* 4/*mcm*. These, however, were unlikely in view of the positions of thorium and aluminium.

Beginning with the deuterium-saturated specimen $Th_8Al_4D_{15\cdot4}$, the intensities showing best agreement were obtained with the parameters

$$x_D = 0{\cdot}368 \quad \text{and} \quad z_D = 0{\cdot}137$$

for all the 15·4 D atoms in the positions 16(*l*). The close agreement of calculated and observed values demonstrated in table I is somewhat spoiled by the values for the (211) reflexion. In the intermediate deuterides the deuterium atoms were now expected to occupy the same interstitial positions as above, though of course only some of them. Because of the peculiar effects of hydrogenation on the lattice parameters, as described and discussed previously [4], some ordering might be expected, in particular in such a way that, up to the composition $Th_8Al_4D_8$, at most one of a pair of two positions that differ in z only is occupied. This implies for the configuration at 8 D atoms per cell that all the "double holes" are half-filled arbitrarily in the upper or in the lower twin hole. Such a configuration is experimentally hardly distinguishable from a totally random distribution of 8 D atoms over the 16 available equivalent sites. In both cases the deuterium contribution to the structure factor has to be calculated as if these were 16 half-deuterium atoms at the 16 equivalent sites. If this is done for $Th_8Al_4D_8$ the closest agreement between observed and calculated intensities (see table III) is obtained when using the parameters

$$x_D = 0{\cdot}370 \quad \text{and} \quad z_D = 0{\cdot}125.$$

For $Th_8Al_4D_{12}$ the same trial-and-error method led to the values

$$x_D = 0{\cdot}370 \quad \text{and} \quad z_D = 0{\cdot}130.$$

For several order schemes for $Th_8Al_4D_8$ the peak intensities were nevertheless calculated, including the schemes that were not compatible with the space group of Th_2Al, purely to see what intensities extra peaks would have. Distributions thus calculated are given in table II. The reliability factors obtained were always larger than that for total disorder. The differences were not sufficient to exclude order totally but they made it unlikely. In particular short-range order remained possible, in addition to the special type of "half-order" discussed above. Goedkoop (private communication) calculated the diffuse scattering of the deuterium atoms and had to conclude that short-range order influenced the

TABLE I

Room-temperature neutron intensities observed and calculated

Th_8Al_4				$Th_8Al_4D_8$				$Th_8Al_4D_{12}$				$Th_8Al_4D_{15\cdot4}$			
hkl	2θ	I_c	I_o	*hkl*	2θ	I_c	I_o	*hkl*	2θ	I_c	I_o	*hkl*	2θ	I_c	I_o
110	10·9	2	—	110	10·8	31	25	110	10·8	211	195	110	10·9	334	320
200	15·4	7	4	200	15·2	9	7	200	15·3	38	28	200	15·5	55	55
211	20·1	130 } 149	149	002	18·8	21	26	002	18·4	69	69	002	18·1	52	51
002	20·2	19 }		211	19·4	46	53	211	19·4	67	115	211	19·6	18	82
220	21·9	7	8	220	21·6	6 } 25	21	112	21·4	62 } 87	86	112	21·2	50 } 77	80
112	22·9	15	21	112	21·8	19 }		220	21·6	25 }		220	22·0	27 }	
310	24·6	33	35	310	24·2	82 } 111	112	202	24·0	108 } 510	481	202	23·9	113 } 668	639
202	25·6	24	26	202	24·4	29 }		310	24·2	402 }		310	24·6	555 }	
321	29·9	1		222	28·8	0	—	222	28·6	0 } 45	69	222	28·6	0	36
222	30·0	0 } 16	19	321	29·2	5	—	321	29·2	45 }		321	29·6	75	88
400	31·3	4 }		400	30·8	27 } 39	54	312	30·6	37 } 205	185	312	30·7	23 } 280	270
312	32·0	11		312	30·8	12 }		400	30·8	168 }		400	31·2	257 }	
330	33·2	14	16	330	32·6	32		330	32·8	157		213	32·5	836	
411	33·8	39	36	411	33·2	35 } 174	168	213	32·8	531 } 842	915	330	33·2	220 } 1162	1226
420	35·2	8 } 52	46	213	33·4	99 }		411	33·2	119 }		411	33·6	106 }	
213	35·3	44 }		420	34·4	9		420	34·6	35		420	35·0	45	51
402	36·7	20	22	402	36·4	21	25	402	36·2	66	58	402	36·4	47 } 47	49
332	39·3	43	37	332	38·0	45 } 49	51	004	37·4	1 } 156	159	004	36·7	0 }	
				004	38·2	4 }		332	37·8	155 }		332	38·1	141 } 167	103
				510	39·6	2		114	39·0	13		114	38·4	26 }	
				422	39·6	0		422	39·5	2		323	39·6	130	
				114	40·0	1 } 13	—	510	39·6	15 } 104	83	422	39·7	3	
				431	40·0	0 }		323	39·6	68 }		204	40·0	3 } 159	145
				323	40·0	8		431	40·0	0		510	40·1	23	
				204	41·4	2		204	40·6	5		431	40·4	0	
				521	43·0	11						413	42·8	140	
				413	43·2	27 } 55	58					224	43·2	14	
				440	44·0	17 }						521	43·5	3 } 345	353
												512	44·4	37	
												314	44·7	0	
												440	44·8	151	

background of the diffraction diagrams in too small a way to be observable with the techniques applied.

A discrepancy, readily observed on reading table I, is the consistently low, calculated intensity for (211). The explanation for this is almost certainly the presence of unreacted material in the sample. From fig. 3 it is seen that (211) is by far the strongest peak in the Th_2Al diagram. It can easily be that an admixture of only 4·5% of Th_2Al is sufficient to account for the value observed for the intensity of the (211) peak in $Th_8Al_4D_{15\cdot4}$. It is understandable that this admixture can be found with neutron diffraction, although X-ray diffraction does not reveal any unreacted phase. The very large penetration depth of the neutrons makes it possible to look into the very heart of the metal grains, where deuterium may not have penetrated and to which X-rays cannot find their way because of absorption.

Another discrepancy, however, is the occurrence of a small scattering peak in the neighbourhood of 28°2θ in the diagrams of the deuterated specimens. Here there ought not to be a peak; accordingly its presence makes the observed intensities of the (222) reflection somewhat uncertain. An explanation for this peak is still lacking.

5. Low-temperature diffraction

For reasons of comparison with the P.M.R. experiments, which included measurements at temperatures between 77 and 293 °K, neutron diffraction at

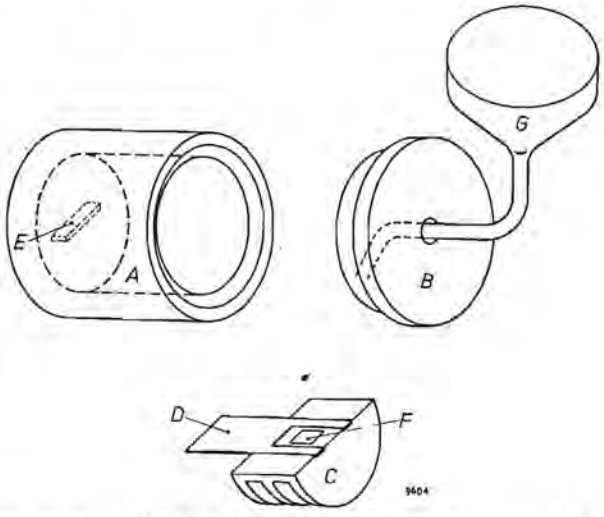

Fig. 4. The simple attachment for the Philips wide-range goniometer, used for low-temperature X-ray diffraction. *A*: polyfoam cylinder. *B*: polyfoam cover, which after closing is secured with adhesive tape. *C*: aluminium specimen holder with fins immersed in the coolant. *D*: polymethyl methacrylate (heat-insulating) plate to be clamped to the goniometer. *E*: hole through which *D* protrudes. *F*: powder specimen. *G*: funnel to pour the cooling liquid into *A*. A thermocouple may be fastened to *C* just below the specimen surface.

TABLE II

Schemes of order and disorder for 8 hydrogen or deuterium atoms, distributed over the available positions in a unit cell of Th_3Al_4 with results of neutron diffraction and P.M.R. calculations.

	schemes of order and disorder										
available positions	occupied positions										
$x, \frac{1}{2}+x, \pm z$	+	+	+	+	±	±	±	½(±)	(±)	±	±
$\frac{1}{2}+x, \bar{x}, \pm z$	+	+	−	−	±	0	0	½(±)	(±)	±	±
$\bar{x}, \frac{1}{2}-x, \pm z$	+	+	+	+	±	±	±	½(±)	(±)	±	±
$\frac{1}{2}-x, x, \pm z$	+	+	−	−	±	0	0	½(±)	(±)	±	±
$\frac{1}{2}+x, x, \frac{1}{2}\pm z$	+	−	+	−	0	±	0	½(±)	(±)	±	±
$x, \frac{1}{2}-x, \frac{1}{2}\pm z$	+	−	−	+	0	0	±	½(±)	(±)	±	±
$\frac{1}{2}-x, \bar{x}, \frac{1}{2}\pm z$	+	−	+	−	0	±	0	½(±)	(±)	±	±
$\bar{x}, \frac{1}{2}+x, \frac{1}{2}\pm z$	+	−	−	+	0	0	±	½(±)	(±)	±	±
$\frac{1}{2}, 0, \pm\frac{1}{4}$	0	0	0	0	0	0	0	0	0	0	±
$0, \frac{1}{2}, \pm\frac{1}{4}$	0	0	0	0	0	0	0	0	0	0	±
									4/8	8/16	8/20
	neutron-diffraction calculations										
reliability factor*) R (%)	16·9	—	—	—	—	—	—	16·3	16·3	16·3	16·0
superstructure lines (to be expected, but not observed)		001 s 111 m etc	202 s 301 m 103 w etc	not cal-cula-ted	001 m 111 m 210 w etc	not cal-cula-ted	not cal-cula-ted				
	proton magnetic-resonance calculations (experimentally: $S_2 = 7{\cdot}6$ gauss^2)										
second moment S_2 **) (gauss^2)	2·3	4·7	4·4	2·5	28·4	27·3	29·1	5·1	26·6	7·7	19·2

*) The reliability factors were calculated using the observed intensities at 95 °K of table IV.

**) The values of S_2 were calculated using the parameters $x_H = 0{\cdot}370$, $z_H = 0{\cdot}125$.

liquid-nitrogen temperatures was undertaken. This again made X-ray diffraction at this temperature necessary. The X-ray diffraction was performed using a simple attachment for the Philips wide-range goniometer as shown in fig. 4. By pouring-in liquid nitrogen a constant temperature of 83 °K was obtained, without the formation of even traces of ice on the specimen surface or on the outer wall of the specimen container. The X-ray diffraction served to ascertain that no change of configuration of the heavier atoms thorium and aluminium had taken place and allowed of detecting hydride separation taking place below room temperature. In particular the second point of inflexion in the hydrogen-pressure isotherms, between the compositions $Th_8Al_4H_8$ and $Th_8Al_4H_{16}$, seemed to indicate such a separation.

TABLE III

Lattice dimensions of some hydrogen solutions in Th_2Al at 83 °K and at room temperature

composition	unit cell dimensions						expansion (%) from 83 °K to 298 °K		
	a (Å)		c (Å)		V (Å^3)				
	83 °K	298 °K	83 °K	298 °K	83 °K	298 °K	a	c	V
$Th_8Al_4H_0$	7·608	7·616	5·839	5·861	338·0	340·0	+0·11	+0·38	+0·59
$Th_8Al_4H_8$	7·711	7·710	6·182	6·226	367·6	377·7	—0·02	+0·71	+0·67
$Th_8Al_4H_{12}$	7·667	7·680	6·397	6·402	376·1	377·7	+0·17	+0·09	+0·43
$Th_8Al_4H_{15\cdot4}$	7·620	7·640	6·541	6·536	379·8	381·5	+0·26	—0·07	+0·44

The results of the low-temperature X-ray diffraction are compiled in table III, in which the lattice parameters at 83 °K and at room temperature of the various hydrides are given. Noteworthy is the negative coefficient of thermal expansion of the c-axis at hydrogen concentrations above 8 H per unit cell. This phenomenon is another indication that $Th_8Al_4H_8$ is a distinct intermediate state in hydrogenation. The separation mentioned above was not observed; it is by no means certain whether this is due to quenching of the room temperature state. Neither was there any reason to revise the thorium parameter at this temperature. Furthermore the low-temperature neutron diffraction of $Th_8Al_4D_8$ dit not yield any new viewpoints. Long-range ordering evidently did not take place, for the diagram was nearly identical to that at room-temperature (fig. 5 and table IV).

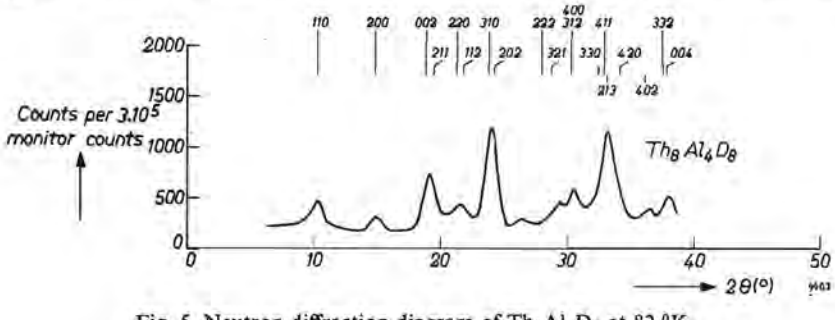

Fig. 5. Neutron diffraction diagram of $Th_8Al_4D_8$ at 82 °K.

TABLE IV

Neutron-diffraction intensities of $Th_8Al_4D_8$ powder at 95 and 82 °K compared to those at $T = 293$ °K

hkl	θ	I_{obs} T=293°K	I_{obs} T=95°K	I_{obs} T=82°K
110	5·4	103	97	85
200	7·6	25	35	30
002	9·4	286	308	294
211	9·7			
220	10·8	88	89	110
112	10·9			
310	12·1	360	396	378
202	12·2			
222	14·4	69	52	85
321	14·6			
400	15·4	255	208	159
312	15·4			
330	16·3	554	527	575
411	16·6			
213	16·7			
420	17·2			
402	18·2	93	99	90
332	19·0	158	182	187
004	19·1			

6. Proton-magnetic resonance; experimental

The apparatus used was designed and built by Kroon [5]). From "Ticonal X" a permanent magnet was constructed in such a way that a variable magnetic field could be obtained by varying the air gaps in the yoke by means of a synchronous motor. The maximum variation of the field strength was 290 gauss; the rate of variation could be chosen between 0·25 and 280 milligauss/sec. The maximum field strength was 4450 gauss, bringing the mean resonance frequency of the protons at about 17·2 Mc/s. Ih this field a cryostat was mounted in which it was possible to perform measurements down to the triple point of nitrogen. 63 °K. The specimen, surrounded by a R.F. coil of 12 turns, was placed in a copper tube inside the cryostat. The specimen container and the coil support had to be of a special hydrogen-free material. The container in our case was

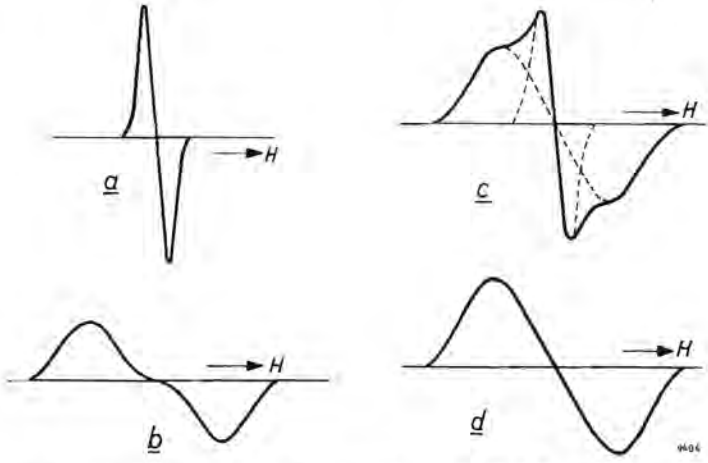

Fig. 6. Some examples of resonance lines obtained with the P.M.R. apparatus. *a*) "Motional narrowed" line. *b*) "Flat topped" line. *c*) "Mixed" line. *d*) Normal line.

hard glas, the coil support was a plastic named "Kell-F" *). The steady magnetic field was modulated by means of an A.F. oscillator that permitted of a full sweep of 30 gauss at a frequency of 230 c/s. This modulation made it possible to write directly the pseudo-derivative (for examples see fig. 6) on a potentiometric recorder. Detection of absorption of the radio-frequency signal in the coil around the sample was performed by an autodyne oscillator detector. A full description of the apparatus can be found in Kroon's thesis.

7. Proton-magnetic resonance; results

At room temperature $Th_8Al_4H_8$ and $Th_8Al_4H_{12}$ yielded very narrow resonance lines (see fig. 6*a*). This phenomenon is known under the name of "motional narrowing" and occurs when the thermal motion of the magnetic dipoles is so rapid that the time available for interaction is shorter than the time elapsing between two subsequent stages at which energy can be transferred. (This is only possible when the Larmor precession of the interacting nuclei is in phase.) At low temperatures this effect disappears and normally shaped broad lines were obtained. Figures 7 and 8 demonstrate these two cases, together with the transition at the temperature where the movement of the interstitial protons to adjacent interstices becomes slow enough. Another way of producing a broad resonance line is to fill up the interstitial holes. Then the speed of this movement is not altered but the number of protons that are able to move is decreased (evidently "interstitial vacancies" are necessary for proton diffusion). This is shown in fig.

*) Trade name of a product of Kellogg (polychloro-trifluoro-ethylene).

6*c*, where a room-temperature resonance line as obtained for $Th_8Al_4H_{15\cdot4}$ is reproduced. The line on analysis is found to consist of a broad line (caused by the immobile protons) and a small superimposed narrow line (due to the small fraction of protons that find a vacant neighbouring interstice). The same broadening was observed for the specimen $Th_8Al_4H_{\approx8}D_{\approx8}$ which was saturated but where only half of the hydrogen could be detected by this method, because the other half was the isotope deuterium having a quite different resonance frequency. In the latter case the broad line found was considerably smaller. The mean square width (which is usually called the second moment S_2) of the lines found for $Th_8Al_4H_{15\cdot4}$ and $Th_8Al_4H_{\approx8}D_{\approx8}$ was respectively about 18 and 5 gauss^2. At 77 °K the — then broad — line of $Th_8Al_4H_8$ had a width, measured between the points of maximum slope, of about 8 gauss and showed a peculiar shape which might be described as being somewhat flat-topped (see fig. 6*b*). The resonance line of $Th_8Al_4H_{12}$ at low temperature was of normal shape (fig. 6*d*), but its width was a function of the temperature (see fig. 8). Furthermore there was a difference from the $Th_8Al_4H_8$ line in respect of its transition from the narrow state to the broad one. For $Th_8Al_4H_{12}$ an intermediate state could be observed at about 230 °K where two lines of different character were superimposed, just like in the case of the saturated $Th_8Al_4H_{15\cdot4}$ at room temperature. At higher temperatures the narrow line grew at the cost of the broad one.

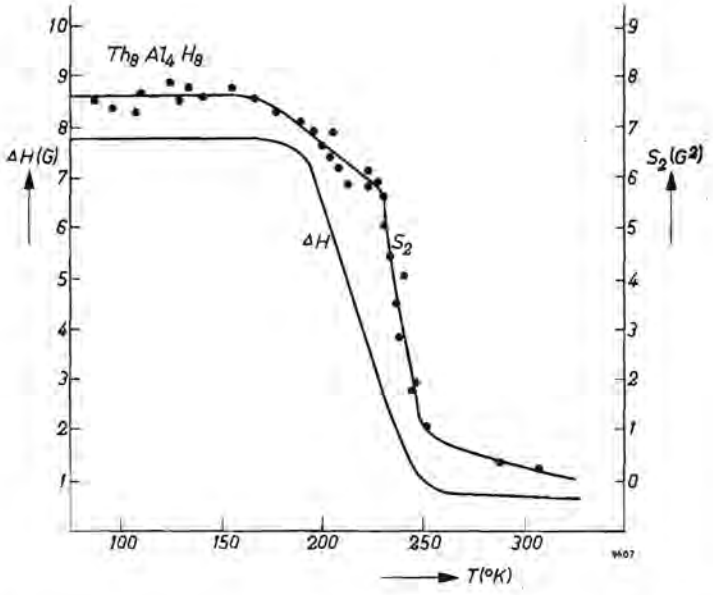

Fig. 7. Proton-magnetic resonance. Line width ΔH and second moment S_2 plotted against temperature for $Th_8Al_4H_8$.

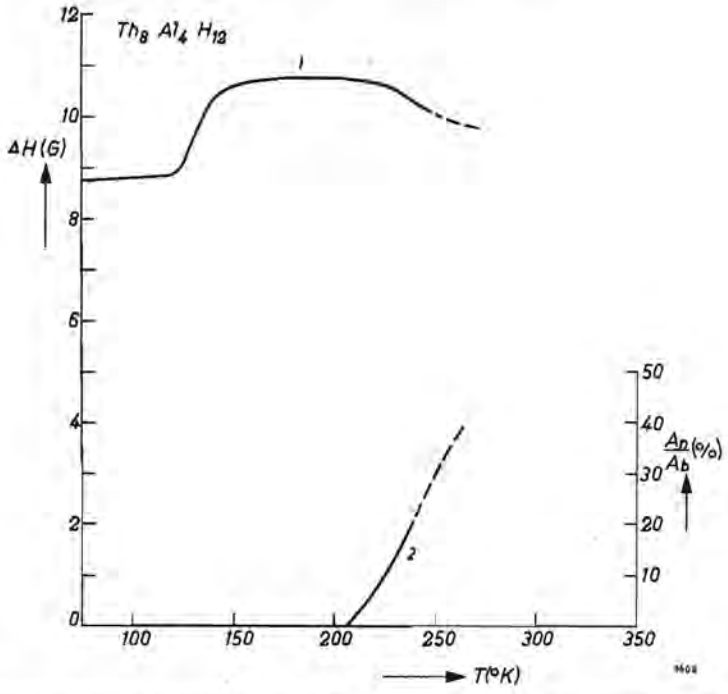

Fig. 8. Proton-magnetic resonance for $Th_8Al_4H_{12}$. 1) Line width ΔH plotted against temperature. 2) Ratio of the integrated areas of the narrow (A_n) and broad (A_b) lines plotted against temperature.

The results may be explained in the following way: At room temperatures in a non-saturated Th_2Al hydride the protons diffuse rapidly from interstice to interstice. They jump about 10^5 times per second. This is the case in $Th_8Al_4H_8$. At lower temperatures their kinetic energy decreases and gradually the number of protons able to diffuse (having at least an activation energy E_d) decreases until all protons are more or less immobile, i.e. a proton now jumps to a neighbouring hole only occasionally. (At 210 °K in $Th_8Al_4H_{12}$ the jump frequency is of the order of $2{\cdot}5.10^3$ sec^{-1}.) As the number of protons having the required energy E_d at the temperature T may be assumed to be given by the Boltzmann equation:

$$N(E_d) = N\exp(-E_d/kT) ,$$

it is possible to calculate E_d from the curve of fig. 7. In this way an activation energy for proton diffusion of 0·22 eV is found.

The flat top of the line at lower temperatures may indicate some degree of order. (This line shape is characteristic of a two-proton or perhaps a four-proton system). This state must be reached via a disordered one, in which the movement of the protons has already slowed down sufficiently to cause line broade-

ning. The behaviour of the line of $Th_8Al_4H_{12}$ seems to indicate a phase separation at these temperatures, presumably into $Th_8Al_4H_8$ and $Th_8Al_4H_{16}$.

The second moment S_2 can be measured by taking

$$S_2 = \int_{-\infty}^{+\infty} H^2 a(H) \mathrm{d}H$$

from the absorption curve observed. Its relation to the inter proton distances is given by Van Vleck's formula [6])

$$S_2 = \frac{6}{5} I(I+1) g^2 \mu_0^2 N^{-1} \sum_{j>k} r_{jk}^{-6} + \frac{4}{15} \mu_0^2 N^{-1} \sum_{j,f} I_f (I_f + 1) g_f^2 r_{jf}^{-6} ,$$

where the first term accounts for the nuclei at resonance, with I as their spin number ($\frac{1}{2}$ in the case of the proton), $g\mu_0 I$ as their nuclear magnetic moment (μ_0 is the nuclear magneton), N as the number of protons over which the sum is taken and r_{jk} as the length of the vector joining two protons j and k. The second term expresses the effect of non-resonant magnetic nuclei, in our case thorium and aluminium. Here again, I_f is the spin number of nuclei of species f, $g_f \mu_0 I_f$ is their magnetic moment, N their number in the system and r_{jf} the distance vector for two nuclei j and f.

The high negative power of the distance vector is the cause of a very rapid decrease of the effect of nuclei (non-resonant as well as resonant) beyond their nearest neighbours. In fact it is pointless to calculate in detail the contribution of nuclei at a distance of more than 5 Å. (Normally the rest of the lattice is considered as an isotropic continuum and its effect when not negligible can be accounted for by replacing the summations by an integral. This has been done applying the formula

$$\Delta S_{>r_0} = C \frac{4}{3} \pi \frac{N}{r_0^3} ,$$

where N is the number of protons per cm^3. C has the value 308 for H-H distances and 126 for Al-H.)

For the compositions $Th_8Al_4H_{15\cdot4}$ and $Th_8Al_4H_{\approx 8}D_{\approx 8}$ the second moment was calculated by means of the proton positions that were found in neutron diffraction with deuterides (see sec. 4 above). The results, considering their sensitivity to small changes of small distances, agreed quite well. For the first hydride we calculated an $S_2 = 17{\cdot}2$ gauss^2 while a value of $17{\cdot}8$ gauss^2 was measured; for the second ("mixed") hydride an $S_2 = 4{\cdot}5$ gauss^2 was calculated, presuming a random distribution of the protons over the above positions, which has to be compared with the measured value of $4{\cdot}8$ gauss^2. The measured S_2 value at 83 °K for $Th_8Al_4H_{12}$ was $10{\cdot}4$ gauss^2. With the parameters of sec. 4

above, and a random distribution of the 12 H atoms over the same 16 positions, we calculated 10·1 gauss^2.

For $Th_8Al_4H_8$ the second moment of 7·6 gauss^2 was measured at 80 °K. Table II shows the calculated values of the second moment for the various possible configurations of protons in this compound (ordered and disordered). In obtaining these values the parameters $x_H = 0{\cdot}370$ and $z_H = 0{\cdot}125$ were used, which had been calculated from the neutron-diffraction data, assuming a random distribution of 8 protons over the 16 equivalent holes. Other parameter values have also been tried but they led to unlikely configurations in view of the neutron diffraction results. As can be seen, the value for random distribution of 8 protons over the 16 equivalent positions agrees best. It would seem that P.M.R. is the most suitable technique to decide between the possible configurations left open by the diffraction results. The configuration in which each "double hole" contains one hydrogen (at random in the upper or the lower half), which was indistinguishable by diffraction from the normal random distribution, is now definitely ruled out by P.M.R. The total absence of the small distance of two protons in one "double hole" leads invariably to too small a value of S_2, whereas configurations with too many doubly occupied "double holes" yield values that are too large. The particularly small distances occurring if the four positions at $(\frac{1}{2},0,\pm\frac{1}{4})$ and $(0,\frac{1}{2},\pm\frac{1}{4})$ were available in a random distribution would cause the second moment to increase to such values that also this possibility must be rejected. This agrees with the neutron diffraction result obtained with $Th_8Al_4H_{15{\cdot}4}$, where the occupation of the 4 sites mentioned could definitely be ruled out, and certainly with P.M.R. measurements on the corresponding saturated hydride, where admission of the 4 additional places would lead to the exceedingly high value for S_2 of about 60 gauss^2.

8. Discussion of the neutron diffraction and P.M.R. results

The positive results of the neutron diffraction and the proton-magnetic resonance work can be summarized in two statements. The first is that the hydrogen has been proved to occupy the interstices which were already suggested previously [7]) on the basis of crystallographic evidence and of considerations concerning the observed saturation value of the hydrogen content (15·4 H per unit cell). The second is that at lower temperatures, after "freezing" (by quenching) the rapid motion of the hydrogen nuclei in the interstitial lattice, apparently no ordered configuration is reached; at least if the situation where four possible sites per cell remain unoccupied is not itself considered as some kind of order.

Neutron diffraction and P.M.R. also yielded a negative result: the seeming untenability of the explanation previously given [4]) for the changes in cell dimensions with H content. The failure to demonstrate any order at lower temperatures in $Th_8Al_4H_8$ nullifies the argument that at room temperature

a tendency to order should be responsible for the effects observed. However, if it is not true that in $Th_8Al_4H_8$ each "double hole" contains one H, the fact remains nevertheless that at this composition the number of half-filled "double holes" is at its maximum. The number per cell n, for a random distribution, is a quadratic function of the number of available hydrogen atoms per cell x

$$n = x - x^2/16 \ ,$$

which function is symmetrical, like the observed function of the tetragonal parameter a, but parabolic instead of "linear". Yet it seems not improbable that the properties of the a-axis must be explained by the change in its mean length in a mixture of $x^2/32$ doubly-filled "double holes" and $(16-x)^2/32$ vacant "double holes". These two extreme types, the vacant and the totally filled one, are found respectively in the hydrogen-free and the hydrogen-saturated Th_2Al. These particular compositions have a nearly identical length of the a-axis, which is the reason why the weak effect could be observed so beautifully. One might therefore estimate the length of the a-axis of a hypothetical, ordered $Th_8Al_4H_8$ (with strictly one H per "double hole") to be $a_0 + 2(a_{8H} - a_0)$. The parabolic shape of the a-function is assumed to have been lost due to experimental inaccuracies. Thus the experimental data of X-ray diffraction, and of neutron diffraction combined with those of P.M.R., might be reconciled.

As already pointed out, we failed to demonstrate order of the hydrogen nuclei in the interstitial lattice at the composition $Th_8Al_4H_8$. Long-range order is definitely ruled out by the neutron diffraction results. The partial-order schemes left open by these must be rejected in view of the P.M.R. results. However, it is necessary to make some remarks about the essential differences between the results of the two techniques. Neutron diffraction gives only long-range data, for example random distribution of H-ions, and additionally their parameters: $x = 0{\cdot}370, z = 0{\cdot}125$. It cannot give a conclusive answer if we suspect the H-ions to form pairs (clustering) or to avoid each other, and the parameters yielded have to be considered as mean values. Since we measure only effects due to the nearest environment of the proton (P.M.R "sees" a distance of only about 4 Å) around the proton, and weights the smaller distances very heavily) it becomes important to know how these mean values are obtained. The procedures leading to the P.M.R. results of Table II must therefore be examined in more detail.

Let us assume that the parameter $z = 0{\cdot}125$ for H atoms at random distributed over the tetrahedral holes in $Th_8Al_4H_8$ must be looked upon as being the linear mean value between a value for H atoms sited singly in "double holes" and the value for H atoms in doubly filled "double holes". The latter might be assumed to be 0·137 (the value found in the saturated hydride). For example, at a random distribution of 8 H over 16 holes (composition $Th_8Al_4H_8$) the parameter for H in the singly-filled "double holes" is then 0·113. For P.M.R. the

situation is then totally changed: the shortest distance of the protons has increased considerably, though some other distances may have become smaller. For the above example S_2 (calculated) changes from 7·7 to 5·0 gauss^2. To obtain the observed value of S_2 is only possible on the assumption that the number of "paired" protons is larger than that corresponding to the normal random distribution, i.e. that there is a preference for the paired occurrence. The situation in which all protons occur in pairs gives $S_2 = 26{\cdot}6$ gauss^2 (cf. table II), which illustrates that the excess number of pairs can only be small.

Apart from concluding that a paired occurrence of the protons is energetically favourable, we might imagine that such pairs occurred of necessity because of kinetic or trivial reasons. The most likely explanation, in our opinion, is a heterogeneity of the metal grains in the P.M.R samples, with an overall composition $Th_8Al_4H_8$, similar to the heterogeneity found with $Th_8Al_4D_{15\cdot4}$ in the neutron diffraction sample. Both heterogeneity troubles are due, or related, to kinetic phenomena such as were encountered earlier with the measurements of the hydrogen equilibrium pressures at temperatures below 250 °C.

REFERENCES

1) J. Bergsma, J. A. Goedkoop and J. H. N. van Vucht, Acta cryst. **14**, 223-228, 1961.
2) D. J. Kroon, C. van der Stolpe en J. H. N. van Vucht, Arch. Sci. **12**, 156-160, 1959.
3) J. A. Goedkoop, Ned. T. Natuurk. **19**, 140-141, 1957.
4) J. H. N. van Vucht, this theses, chapter 4.
5) D. J. Kroon, Line shape of proton magnetic resonance in paramagnetic solids, thesis, Amsterdam 1960; also Philips Res. Repts **15**, 501-600, 1960.
6) J. H. van Vleck, Phys. Rev. **74**, 1168, 1948.
7) J. H. N. van Vucht, this thesis, chapter 3.

CHAPTER 6

THE PROBLEM OF ORDER OR DISORDER OF HYDROGEN $Th_8Al_4H_8$

Summary

Theoretical considerations of the behaviour of hydrogen atoms in a system of paired interstitial holes in a metallic lattice lead to the conclusion that the occurrence of three points of inflexion in the pressure isotherms of hydrogen gas, in equilibrium with this system, necessarily means that, calculated per hydrogen atom, an occupation of the "double holes" by a single hydrogen atom is energetically more favorable than a double occupation.

Résumé

Considérations théoriques sur le comportement des atomes d'hydrogène dans un système de sites interstitiels accouplés dans un réseau métallique. Ces considérations mènent à la conclusion que la présence de trois points d'inflexion dans des isothermes de la pression du gaz d'hydrogène, en équilibre avec ce système, signifie incontestablement qu'une occupation des „sites doubles" par un seul atome d'hydrogène est énergétiquement plus favorable qu'une occupation double, les calculs étant effectués par atome d'hydrogène.

Zusammenfassung

Theoretische Überlegungen über das Verhalten von Wasserstoffatomen in einem System von paarweise angeordneten Zwischengitterlücken eines Metalles führen zu dem Schluß, daß das Auftreten von drei Wendepünkten in den Druckisothermen des mit diesem System im Gleichgewicht befindlichen Wasserstoffgases notwendigerweise darauf hindeutet, daß gerechnet pro Atom Wasserstoff eine Besetzung der „Doppellücken" mit nur einem einzigen Wasserstoffatom energetisch günstiger ist als eine Doppelbesetzung.

1. Introduction

The previous papers [1,2,3]) about the behaviour of hydrogen in the intermetallic compound Th_2Al have helped to build up a general picture of how and where the hydrogen atoms are bound by the getter metal. Measurements of hydrogen-equilibrium pressures at various temperatures yielded isotherms, some of which (in the neighbourhood of 225 °C) showed three points of inflexion, see fig. 1. Two of these, those at the approximate compositions $Th_8Al_4H_4$ and $Th_8Al_4H_{12}$, were considered to be remnants of plateaux, indicating two-phase regions at lower temperatures. This would imply that the composition $Th_8Al_4H_8$ had to be considered as an intermediate hydride. X-ray diffraction of Th_2Al containing hydrogen showed that at room temperature a phase separation did occur between $Th_8Al_4H_0$ and approximately $Th_8Al_4H_5$. However, neither at room temperature nor at 83 °K was a similar region found between $Th_8Al_4H_8$ and the saturation composition $Th_8Al_4H_{15\cdot4}$ that might correspond to the point of inflexion at approximately $Th_8Al_4H_{12}$. The behaviour of the cell dimensions with rising hydrogen content seemed to indicate that at the

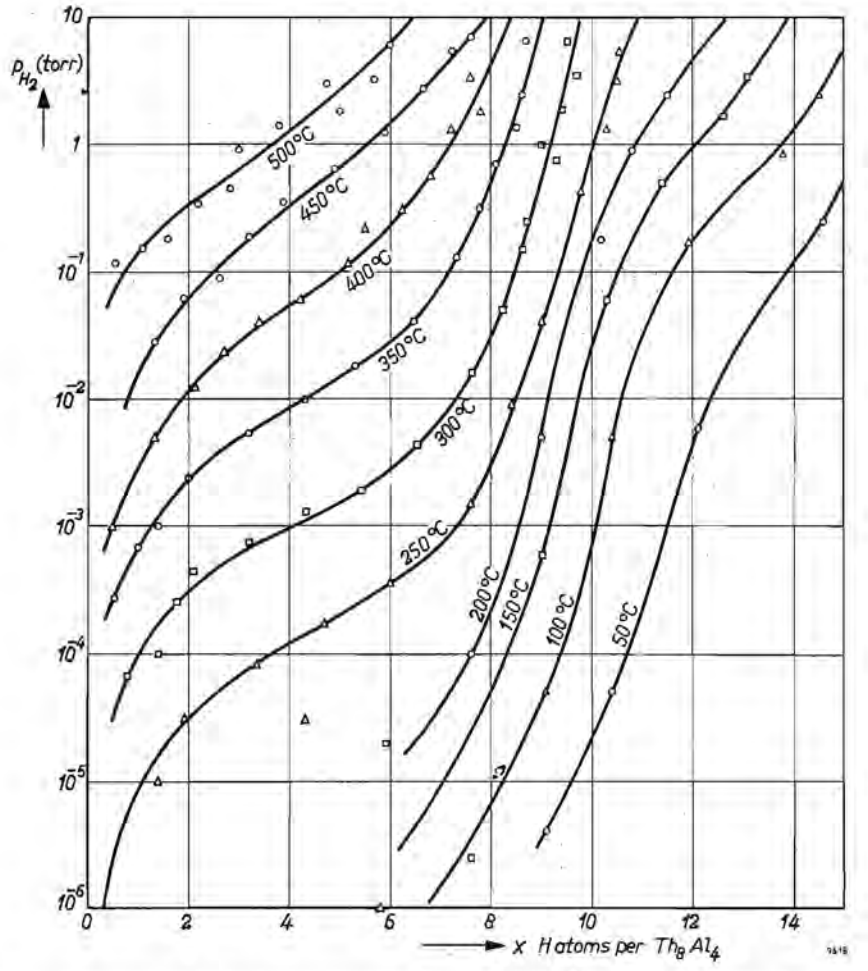

Fig. 1. Isotherms of the hydrogen equilibrium pressure [1]) above Th_2Al. Log p_{H_2} is plotted against the composition of the hydride $Th_8Al_4H_x$.

composition $Th_8Al_4H_8$ the hydrogen atoms were ordered, or had a strong tendency to order. The hydrogen atoms were presumed to occupy the 16 crystallographically equivalent interstitial holes in the unit cell of Th_8Al_4. These holes are ranged pair-wise and the order of the hydrogen atoms at half saturation was thought to consist of an occupation of each "double hole" more or less rigorously by one hydrogen. Neutron diffraction corroborated that the hydrogen atoms occupied the interstitial sites mentioned above and, together with proton-magnetic resonance (P.M.R.) measurements, yielded definite arguments that the four other interstitial holes were not occupied. For proving the special kind of order at the composition $Th_8Al_4H_8$, however, neutron

diffraction was not in principle an appropriate method. P.M.R. yielded only negative arguments for this expected kind of order, though the shape of the resonance lines for $Th_8Al_4H_8$ at 77 °K might be understood to represent some kind of order, and the behaviour of the resonance line of $Th_8Al_4H_{12}$ at decreasing temperature suggested a phase separation.

No additional experimental evidence for or against order of the hydrogen atoms at the composition $Th_8Al_4H_8$ was found. However, certain details obtained above concerning the behaviour of hydrogen in the interstitial lattice of Th_2Al permit theoretical considerations which convert the vague argument of the points of inflexion in the hydrogen equilibrium-pressure isotherms into a strong argument for a preference of the protons for single occupation of a "double hole".

2. Theoretical

The model used consists of the Th_2Al lattice, where protons can be placed in the 16 crystallographically equivalent tetrahedral holes that are coupled to 8 "double holes". We shall now derive an expression of $\ln p_{H_2}$ as a function of the number of hydrogen atoms per Th_8Al_4, using proton-proton interaction terms to obtain a value for the enthalpy.

If, like in a cubic close packed lattice, every tetrahedral hole has only equivalent neighbours (i.e. no direct neighbour has special advantages above the other ones) the interaction of the protons with the lattice can be described by a term

$$f\theta(1-\theta) \ ,$$

where θ is the fraction of holes occupied by a proton. In the lattice of Th_2Al each hole has one specially associated twin hole. There is likely to be a difference in energy between a pair of hydrogens in unassociated holes and a pair in a "double hole". Let us denote the energy of a single hydrogen in a "double hole" by a, and the energy of a pair of hydrogens in a "double hole" by $2b$. If q is the fraction of holes that are occupied and associated with a vacant twin, then the fraction of holes participating in doubly filled pairs is $\theta - q$ and the fraction of holes taking part in totally vacant pairs is $1-(\theta-q)-2q = 1-\theta-q$. Thus the enthalpy will be given by

$$H = f\theta(1-\theta) + aq + (\theta - q)b$$

and the Gibbs entropy by

$$S = -R\left\{\frac{\theta-q}{2}\ln\frac{\theta-q}{2} + \frac{1-\theta-q}{2}\ln\frac{1-\theta-q}{2} + q\ln\frac{q}{2}\right\}$$

for N (Avogadro's number) holes.

The Gibbs free energy

$$G = f\theta(1-\theta) + aq + b(\theta-q) + RT\left\{\frac{\theta-q}{2}\ln\frac{\theta-q}{2} + \frac{1-\theta-q}{2}\ln\frac{1-\theta-q}{2} + q\ln\frac{q}{2}\right\}$$

has to be a minimum with respect to q in order to find q at equilibrium:

$$\frac{\partial G}{\partial q} = 0 \ . \tag{1}$$

This equilibrium condition becomes

$$a-b = \frac{RT}{2}\left\{\ln\frac{\theta-q}{2} + \ln\frac{1-\theta-q}{2} - 2\ln\frac{q}{2}\right\}$$

or

$$\frac{(\theta-q)(1-\theta-q)}{q^2} = \exp\{2(a-b)/RT\} \ , \tag{2}$$

which is directly related to the equilibrium constant of the reaction:

1 doubly filled "double hole" + 1 vacant "double hole"
$\rightleftarrows$ 2 half-filled "double holes".

The expression for $\ln p_{H_2}$ can be obtained by differentiating G with respect to θ, for

$$\frac{dG}{d\theta} = \mu_{H \text{ in } Th_2Al}$$

and the condition for equilibrium with the gas phase is

$$\mu_{H \text{ in } Th_2Al} = \tfrac{1}{2}\mu_{H_2 \text{ gas}} = \tfrac{1}{2}\mu^0_{H_2} + \tfrac{1}{2}RT\ln p_{H_2} \ .$$

As (1) remains valid,

$$\frac{dG}{d\theta} = b + f(1-2\theta) + \frac{RT}{2}\ln\frac{\theta-q}{1-\theta-q} = C + \frac{RT}{2}\ln p_{H_2} \ ,$$

which shows that $\ln p$ against θ is symmetrical with respect to $\theta = \frac{1}{2}$. The points of inflexion in $\ln p_{H_2}$ are obtained by finding the extremes of

$$\frac{RT}{2}(d\ln p_{H_2})/d\theta = -2f + RT\frac{du}{d\theta} \ , \tag{3}$$

where

$$u = \tfrac{1}{2}\ln\frac{\theta-q}{1-\theta-q} \ .$$

In order to find $\frac{du}{d\theta}$ we convert the form

$$\frac{1-\theta}{\theta} = \frac{(1-\theta-q)+q}{(\theta-q)+q}$$

with the help of the equilibrium condition (2)

$$q = K\sqrt{(\theta-q)(1-\theta-q)}$$

(where $K = \exp\{-(a-b)/RT\}$)

to

$$\frac{K+\sqrt{\dfrac{1-\theta-q}{\theta-q}}}{K+\sqrt{\dfrac{\theta-q}{1-\theta-q}}} = \frac{K+e^{-u}}{K+e^{u}}$$

and differentiate with respect to u:

$$\frac{1}{\theta^2}\frac{\mathrm{d}\theta}{\mathrm{d}u} = \frac{K(e^u+e^{-u})+2}{(K+e^u)^2}$$

With

$$\theta = \frac{K+e^u}{2K+(e^u+e^{-u})} \tag{4}$$

we obtain

$$\frac{\mathrm{d}u}{\mathrm{d}\theta} = \frac{(2K+e^u+e^{-u})^2}{2+K(e^u+e^{-u})}$$

and, using (3),

$$\frac{RT}{2}(\mathrm{d}\ln p_{H_2})/\mathrm{d}\theta = -2f + RT\frac{(2K+e^u+e^{-u})^2}{2+K(e^u+e^{-u})}\,.$$

With constant RT and f this function is extreme when

$$2\ln\{2K+(e^u+e^{-u})\} - \ln\{2+K(e^u+e^{-u})\}$$

is extreme, thus

$$\frac{2(e^u-e^{-u})}{2K+(e^u+e^{-u})} - \frac{K(e^u-e^{-u})}{2+K(e^u+e^{-u})} = 0\,. \tag{5}$$

Since we find $(e^u - e^{-u})$ to be always a root of the equation it is clear that for $u = 0$, i.e. for $\theta = \frac{1}{2}$, a point of inflexion always exists in the curve of $\ln p_{H_2}$ against θ.

After division by $(e^u - e^{-u})$ eq. (5) becomes

$$e^u + e^{-u} = 2\sinh u = 2K - \frac{4}{K}\,.$$

The hyperbolic sine has a minimum value = 1 for $u = 0$. The function $K - 2/K$ is also equal to 1 for $K = 2$. Negative values of K are meaningless and for only

positive values $K - 2/K$ is monotonic from $-\infty$ to $+\infty$. Therefore for $K > 2$ we can obtain two more roots, i.e. two more different points of inflexion in $\ln p_{H_2}$. These points become coïncident for $K = 2$ and for $0 < K < 2$ they cease to exist; only the previously found point of inflexion at $\theta = \frac{1}{2}$ remains. If $K = 2$ and $u = 0$, the additional root of (6) leads to the same value of θ as already found for the point of inflexion that always occurs, so in fact the three points of inflexion merge at $\theta = \frac{1}{2}$ if K becomes 2. For each value of K where two values of u satisfy eq. (6), these values lie symmetrically with respect to the minimum at $u = 0$. This means that the corresponding points of inflexion must occur at values of $\theta = \frac{1}{2} \pm x$. The limit of x, for $K \rightarrow \infty$ is $\frac{1}{4}$.

3. Discussion

Summarizing the results of the previous section, we may conclude that at values of $K \leqslant 2$, i.e. for $b\text{-}a \leqslant RT\ln 2$ the curve of $\ln p_{H_2}$ against the number of hydrogen atoms per unit cell Th_8Al_4 has only one point of inflexion, lying at the concentration 8 H per unit cell. If $K > 2$, i.e. if the energy of a proton as a neighbour of another one in a "double hole" b exceeds that of a single proton by more than $kT\ln 2$, the $\ln p_{H_2}$ curve exhibits three points of inflexion. One of these again lies at 8 H/cell (now $(d\ln p_{H_2})/d\theta$ is a maximum here) and the other two lie at $(8 \pm x)$ H/cell. With increasing values of $b\text{-}a$ they move away on either side from the point 8 H/cell, initially rather rapidly, to the limiting positions at 4 H and 12 H/cell. Since experimentally three points of inflexion are found, which lie virtually at the compositions 4 H, 8 H and 12 H per cell it seems justified to conclude that a significant preference of the hydrogen atoms for half filled "double holes" exists. Temperature increase has the same effect as a decrease of $b\text{-}a$, namely a movement of the two extra points of inflexion towards the third one at 8 H/cell. This again has been found experimentally. It is rather remarkable that the minimum difference between b and a for the occurrence of three points of inflexion is found to be $RT\ln 2$.

Another remarkable point is that the general interaction energy f has no effect on the result as far as the number and the location of the points of inflexion in $\ln p_{H_2}$ are concerned. It must, however, be noted that the slope of $\ln p_{H_2}$ at these points is affected in accordance with eq. (3). This is demonstrated in fig. 2, where for varying relative values of K and f the curves of $(d\ln p_{H_2})/d\theta$ and $\ln p_{H_2}$ against θ are given schematically. It is seen that when a positive f dominates there is always a metastable region in the $\ln p_{H_2}$ curve, which gives rise to "plateaux" (figs 2*b*, 2*e* and 2*f*). If f is relatively small, or even negative, $(d\ln p_{H_2})/d\theta$ remains positive and, depending on the value of K (smaller than, equal to, or larger than 2) the cases represented by figs 2*a*, 2*c* or 2*d* will appear. Figure 2*d* is thought to represent the situation in the system Th_2Al-hydrogen at about 250 °C. The experimentally observed phase separation between

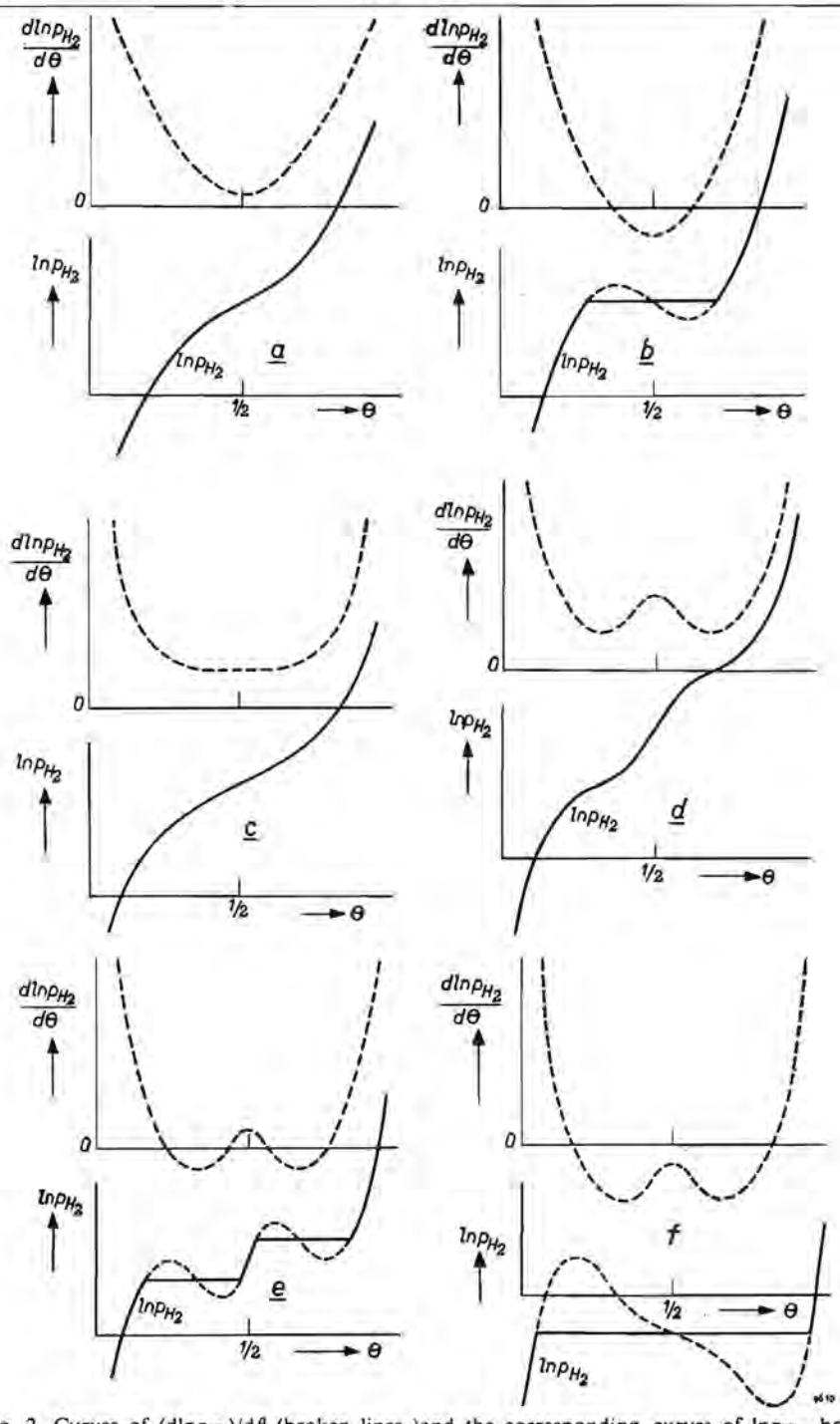

Fig. 2. Curves of $(d\ln p_{H_2})/d\theta$ (broken lines)and the corresponding curves of $\ln p_{H_2}$, both schematic, plotted against θ. a) $K < 2$, f small; b) $K < 2$, f large; c) $K = 2$, f small; d) $K > 2$, f small; e) $K > 2$, f of intermediate value; f) $K > 2$, f very large. "Small" for the parameter f means a small positive value or even negative values.

$Th_8Al_4H_0$ and $Th_8Al_4H_5$ at room temperature must also be attributed to this influence of f, and seems to be represented best by fig. 2*e*. However, the two-phase region at the other side of $Th_8Al_4H_8$, which has to be expected because of symmetry considerations, has not been found, unless the shape of the P.M.R. lines for $Th_8Al_4H_{12}$ at various temperatures is taken seriously as an indication for a phase-separation on a very small scale. On the other hand the schematical character of the energy and entropy started with, introduced the symmetry artificially. Therefore we are not too surprised to find that in this respect the experimental facts differ somewhat from the predicted ones.

4. Order in $Th_8Al_4H_8$; review of arguments

As a final, brief review of the main results and arguments we may start with the statement that the hydrogens in the interstitial lattice of Th_2Al strongly prefer the 16 equivalent holes per unit cell, arranged in 8 pairs of "double holes", and avoid the 4 other holes. This is fully sustained by the results of all the techniques applied. Considering the distribution of the protons over the 16 holes there are two results which positively indicate the tendency of the protons to occupy singly a "double hole", namely the shape of the hydrogen-equilibrium pressure isotherms, and the change of the unit cell dimensions. Neutron diffraction results positively exclude long-range order for the composition $Th_8Al_4H_8$ at lower temperatures, but are not able to yield evidence for or against a type of order in which the hydrogens occupy randomly the upper or lower half of the 16 rigorously half-filled "double holes". Proton-magnetic resonance was expected to prove the existence of such a type of order or at least a tendency to form this order. However, its results can only be used as arguments against this type of order, and may even be considered to indicate a tendency fo form paired protons in the "double holes". This inconsistency might be explained if it be assumed that the specimens of composition $Th_8Al_4H_8$ that were measured with P.M.R. contained for trivial reasons more doubly filled "double holes" than they ought to. In particular we might think of a heterogeneity of the hydrogenated metal grains, which means that at the composition $Th_8Al_4H_8$ there are regions in the grains where the number of hydrogen atoms exceeds 8 per unit cell. This difficulty in reaching homogeneity has been encountered more often already in investigations of this system and seems to be a likely explanation.

REFERENCES

[1]) J. H. N. van Vucht, this thesis, chapter 3.
[2]) J. H. N. van Vucht, this thesis, chapter 4.
[3]) J. H. N. van Vucht, this thesis, chapter 5.

CHAPTER 7

KINETIC STUDY OF THE REACTION OF Th_2Al WITH H_2

Summary

An analysis is given of an autocatalytic hydrogen-sorption process observed with getter powders. This kind of reaction is presumably caused by a layer of surface-poisoning oxide or nitride covering the metal grains. The layer is only very slowly permeated by hydrogen. Absorption really starts when enough hydrogen has passed to make the surface film crack under the strain of the expanding metal below. In addition some thoughts on thermal regeneration or the activation of getter powders are given.

Résumé

On analyse une réaction d'absorption d'hydrogène autocatalytique observée aux poudres de getter. Une telle réaction est probablement causée par un dépôt d'oxide ou de nitrure, couvrant les grains métalliques en empoisonnant leurs surfaces. Le dépôt n'est pénétré que très lentement. L'absorption essentielle ne commence qu'après le passage d'une quantité d'hydrogène assez grande pour faire crevasser le dépôt sous la tension du métal là dessous dilaté. Sont données aussi quelques idées sur le processus d'une régénération thermique ou d'une activation de poudres de getter.

Zusammenfassung

Es wird eine Analyse eines an Getterpulvern beobachteten autokatalytischen Wasserstoffabsorptionsvorgangs gegeben. Wahrscheinlich wird eine derartige Reaktion durch eine Schicht oberflächen-vergiftenden Oxyds oder Nitrids verursacht, die die Metallkörner umhüllt. Wasserstoff vermag die Schicht nur sehr langsam zu durchdringen. Die Absorption setzt erst dann richtig ein, wenn genug Wasserstoff eingedrungen ist, um die abschließende Schicht unter dem Druck des darunterbefindlichen, sich ausdehnenden Metalls aufzureißen.

1. Introduction; importance of surface layers

Gettering means the removal of gas from a closed volume. In practice this can be done by binding the gas to a surface, i.e. by producing a solid product of reaction that stays in place. This method always involves a heterogeneous reaction, as is the case with non-evaporating getters as well as with evaporating getters. It is also possible to getter homogeneously in the gas phase as is done by barium vapour during the flashing of a barium getter, or by titanium vapour in a titanium-ion pump. These last types of reaction, however, are of no interest here.

In a heterogeneous reaction the affinity of the reacting elements or compounds plays only a role of minor importance in determining its rate. The reaction products often build up a protecting layer, which impedes the reaction process, because such a layer can only be passed by slow diffusion. The layer

thickness grows at a rate equal to the reaction rate. The slow diffusion through the layer is the rate-determining step and is inversely proportional to its thickness. Thus such a diffusion-governed process follows a $\sqrt{t}$ law. The diffusion can consist of a movement of metal ions from the metal reaction-product boundary towards the gas phase or of anions in the opposite direction.

Sometimes the layer of the reaction product is not able to protect the underlying metal sufficiently. The reacting gas can now reach the metal surface by a mere gas diffusion, which is very rapid. The rate-determining process in such a reaction normally proceeds linearly with time. This is the case if the reaction product has a smaller volume than the metal from which it was formed. This rule was given by Pilling and Bedworth [1]).

As an example we may take barium; $V_{BaO}/V_{Ba} = 0{\cdot}66$ (here V is the molar volume). This means that, if a piece of barium oxidizes, the oxide skin produced is about 20% too small and will crack. Loriers [2]) suggested an extension of the rule on account of the oxidation mechanism of cerium. The oxide CeO_2 has a molar volume which is large enough to protect the metal: $V_{CeO_2}/V_{Ce} = 1{\cdot}15$. He found that between the CeO_2 layer and the metal a very thin layer of the suboxide Ce_2O_3 formed that rapidly oxidized further. This Ce_2O_3 also was large enough, with respect to the metal. However, it turned out that $V_{CeO_2}/\frac{1}{2}V_{Ce_2O_3} = 0{\cdot}89$. Therefore the thin Ce_2O_3 layer caused the thick outer CeO_2 layer to crack. The oxygen could reach the Ce_2O_3 very easily, and this presumably reacted in such a way that on one side CeO_2 was formed while on the other side Ce_2O_3 was produced from the metal.

It is easy to understand the importance of Pilling and Bedworth's rule if we consider getter reactions at lower temperatures (< 500 °C) where diffusion rates are usually small. At room temperature the reaction between a Zr-getter powder and gases like N_2, O_2, H_2O, CO and CO_2 will start rapidly, but after a very short period will virtually cease. The skin formed is then only a few monolayers thick, but this is not the case with hydrogen. Experiments show that powders of thorium, zirconium, Th_2Al and Ceto *) at room temperature take up pure hydrogen very rapidly until they are saturated. They then do not sorb any more even if the temperature is increased (on the contrary they desorb). Apparently no new phase is formed between the metal and the gas phase, or this new phase must at least be very permeable to hydrogen, either mechanically (cracks) or chemically. The hydrides have a larger molar volume than the metals. The rapid sorption of hydrogen at room temperature does not occur if the getter powders have not been previously "activated". The activation can consist of a short annealing period at temperatures between 750 and 1000 °C in a good vacuum. In the past other workers [3–6]) often

*) Ceto is the industrial name for a non-evaporating getter alloy of composition (in atoms) 10 Th 3Ce 6Al.

observed that metals like Zr or Ce, apparently in the non-activated state, only started to sorb hydrogen at higher temperatures ($\approx$ 400 °C). The starting temperatures varied from author to author, and so did the observed sorption rates.

In this paper I intend to show the influence of oxide or nitride layers on the hydrogen-sorption rate. This will be illustrated with experiments performed with getter powders of Th, Zr, Th_2Al and Ceto.

2. Specimen and apparatus

In an apparatus such as shown schematically in fig. 1, 200 mg of getter

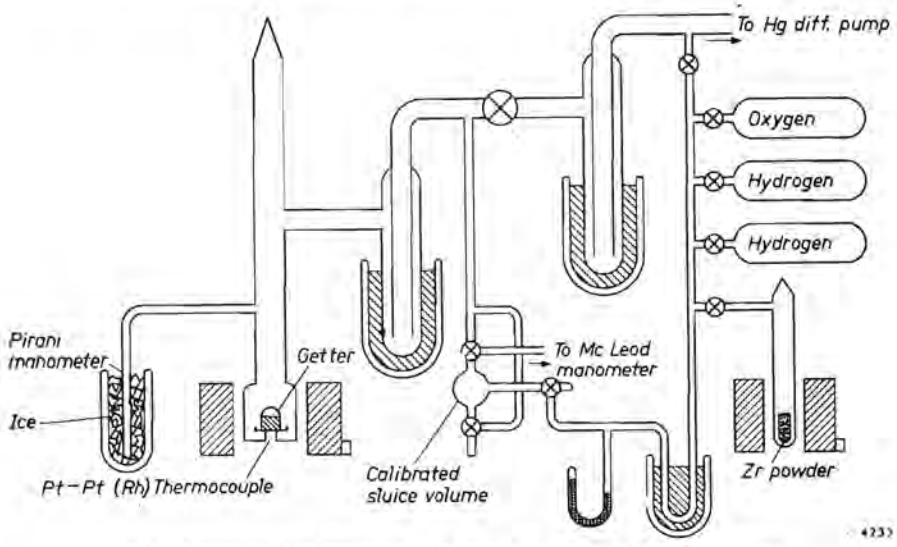

Fig. 1. Apparatus for measuring the sorption rates of getter powders.

powder was placed in a silica crucible. The apparatus was sealed and pumped out. Then, while pumping, the specimen was heated to about 900 °C and subsequently cooled rapidly by removing the furnace. By means of the "sluice" a measured amount of hydrogen, obtained by heating zirconium-hydride powder, was admitted by connecting rapidly the small sluice volume with the "getter" space. From this moment the hydrogen pressure above the getter was measured with a Pirani manometer and plotted against the time.

We always worked in pressure regions where the Pirani gauge, which had been calibrated previously for various gases with a McLeod gauge, indicated rapidly and precisely, i.e. from about 100 μ Hg initially down to the residual pressure obtained. In the important part of this region the gas-flow resistance of the tube connecting the Pirani gauge with the space housing the getter could be neglected, principally because of the small volume of the Pirani tube. The

volume of the "getter" space was always of the order of 1·5 litres and was calibrated beforehand with helium. The pressure in the sluice was measured with the McLeod gauge or sometimes with an oil manometer filled with a silicon oil.

The amount of getter powder was always 200 mg. The area of its reacting surface was unknown. With thorium or zirconium the available powders were used as such. If Th_2Al or Ceto or some other home-made materials were used they were crushed until all grains passed a sieve of 35 μ mesh. Later on, in a parallel-running investigation concerning the comparison of the gettering rates of Th_2Al and Ceto for nitrogen, the method of physical adsorption at low temperatures, commonly known as the B.E.T. method, was applied to determine the ratio of the surface areas of these powders. The areas found were of the order of 0·2 m^2 per gram, which means, for example, that 200 mg of Th_2Al must chemisorb about 0·01 torrlitre of oxygen, for a monatomic layer.

3. Experimental

While measuring the hydrogen sorption of thorium powder at room temperature it soon became apparent that the results were influenced by several factors. Vacuum and gas-purity conditions were obviously important. For example, fig. 2 gives the hydrogen-sorption rate of thorium powder (*a*) after the powder, activated by heating it up to 900 °C, was subsequently allowed to

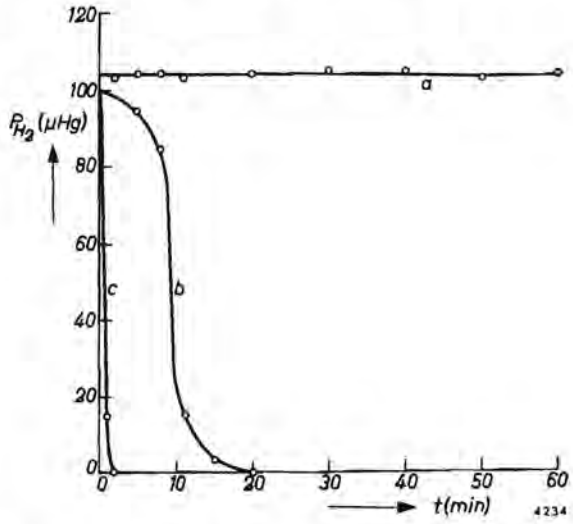

Fig. 2. Hydrogen sorption at room temperature of 200 mg thorium powder in a volume of 1·5 litres. Pressure versus time. Curve *a*: liquid-air traps not filled during cooling after activation. Curve *b*: trap was full originally but became nearly empty. Curve *c*: trap kept filled carefully.

cool overnight while the liquid-air trap was not filled; (*b*) same as (*a*), but with the liquid-air trap filled; this, however, was found nearly empty the next morning; and (*c*) after slowly cooling while the liquid-air trap was continuously kept filled. Other experiments showed that small quantities of oxygen admixed to the hydrogen decreased the sorption rate as well. Conditions during measuring the hydrogen-sorption rate in these experiments were always the same, i.e. the liquid-air trap kept filled. This always caused a cooling of the newly admitted gas, observed as a small fall of pressure in the first few minutes if a blank was run. Our curves were corrected for this effect.

In order to get reproducible results with the sorption experiments two alternatives were possible. Firstly a standard activation process could be used. Secondly it was possible to use a standard process of de-activation subsequent to an activation. The methods were essentially different, and showed different aspects about the getters.

Since, in comparing our getters, hydrogen sorption at normal temperature was in each case very rapid after activation, so that it was difficult to observe differences, we chose the second method. After activation, the getter was cooled down rapidly to room temperature under conditions of utmost purity. Then it was exposed to oxygen at 0·1 mm Hg for 10 minutes. At this temperature the quantity of oxygen adsorbed was too small to be detected because of the contraction of the gas in the liquid-air trap occurring simultaneously. After that the oxygen was pumped off and hydrogen was admitted; at this stage the sorption experiment began. For thorium powder the de-activation procedure yielded total inactivity with respect to hydrogen. For Th_2Al and Ceto, however, this was not the case. Figure 3 gives the hydrogen sorption for the

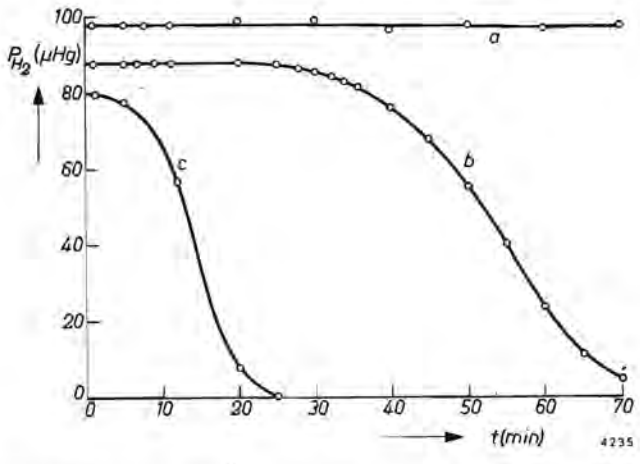

Fig. 3. Room-temperature hydrogen sorption after standard de-activation, for 200 mg of (*a*) thorium powder, (*b*) Th_2Al powder and (*c*) Ceto powder in a volume of 1·5 litres.

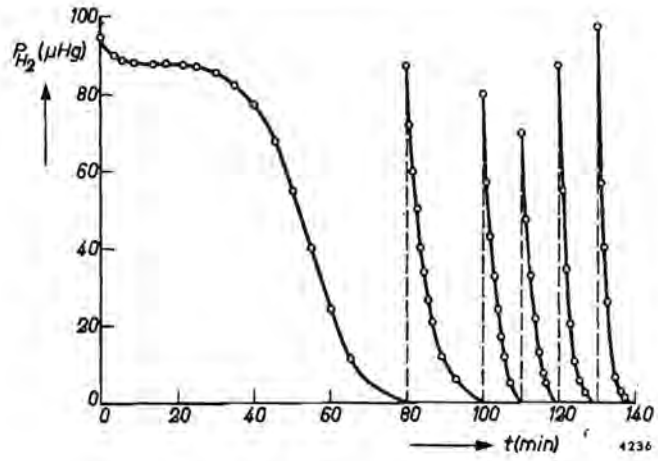

Fig. 4. Hydrogen sorption at room temperature by de-activated Th_2Al. After sorption of the first amount of hydrogen, new portions of gas were admitted successively, without changing the other conditions. The curves have not been corrected for contraction by cooling in the liquid-air trap.

three materials at room temperature after standard de-activation. Figure 4 shows an extended sorption experiment with Th_2Al. Here, after the total sorption of the first quantity of hydrogen, new amounts were admitted subsequently (without preliminary de-activation).

The rate of hydrogen sorption at room temperature by Th_2Al after de-activation lent itself particularly well for study. The reproducibility of the autocatalytic curve, provided that the greatest purity was observed, appeared to be fairly good. Table I contains some values found for the induction time t_i,

TABLE I

Induction times of autocatalytic hydrogen sorption by Th_2Al

exposure to oxygen		exposure to hydrogen	
p_{O_2} (μ Hg)	time (min)	p_{H_2} (μ Hg)	t_i (min)
63	15	109	27
83	15	91	30
70	15	92·5	30
71	5	91	27
71	30	78	28
76	5	88	21

after various oxygen-exposure times t_{O_2}, for various Th_2Al specimens all taken from a big stock. The induction time can be defined as the time difference between the moment of the exposure of the de-activated getter to hydrogen

and the moment at which the first pressure fall (in our case at least 0·2 μ Hg) can be observed. This induction time could also be seen when the experiment was carried out in the following way: The activation, as well as the de-activation with oxygen, was performed normally, except for the cooling of the trap by liquid air. Even after a previous baking out of the system for two or three days at 200 °C the autocatalytic gettering of hydrogen did not commence. However, if the liquid-air trap was then filled it was always possible to observe the beginning of sorption after about 30 minutes, measured from the time of

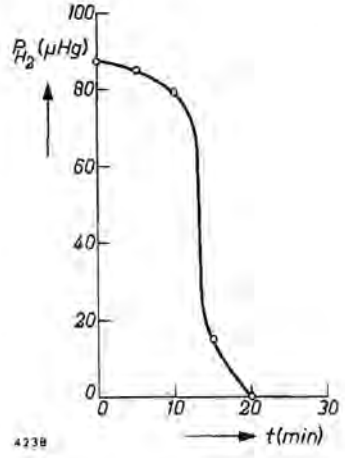

Fig. 5. Continuation of the experiment of fig. 4. In between the two experiments represented by the figures the getter (containing hydrogen) was subjected to exposure at room temperature with oxygen at 70 μ Hg during 10 minutes.

filling. If the liquid air was removed again, the sorption slowly came to a halt, but started again after some delay when the cooling of the trap was resumed.

The induction time was always much smaller — in fact the sorption already started with a measurable rate — if the described de-activation procedure was applied to Th_2Al which had already sorbed an amount of hydrogen previously (see fig. 5). The time of exposure to oxygen had then to be increased considerably in order to obtain comparable induction times.

4. Survey of the literature

The experimental results suggest that the hydrogen-sorption rate is strongly dependent on the presence or otherwise of an impeding non-metallic layer. This layer can be the cause both of irreproducibility of sorption-rate measurements, especially at lower temperatures (< 500 °C), and of the peculiar autocatalytic character of the sorption curves sometimes encountered. The properties of the impeding layer consisting mostly of oxides are therefore of

importance in a study of hydrogen sorption, but they also determine the general process of activation of the getter surface. In this section we shall give a survey of published facts and opinions about the above interconnected phenomena.

Sieverts and Müller-Goldegg [3]) in 1923 found that the temperature at which untreated cerium started to absorb hydrogen differed very much from that given by earlier workers (the values varied between 250 and 570 °C). An activation by vacuum melting often resulted in a quick hydrogen sorption at room temperature. They observed an autocatalytic sorption of hydrogen by cerium that had previously been vacuum melted and which, after cooling down, had been de-activated by nitrogen. About the steep part of the absorption curve (after the induction period) Sieverts and Müller-Goldegg stated that here the reaction rate increased because of "... die Reaktionswärme, die Veränderung der Oberfläche und vielleicht auch durch einen autokatalytischen Einfluß des schon aufgenommenen Wasserstoffs" *). Viallard (1945) in a paper [4]) on the reaction between H_2 or D_2 and cerium or gadolinium found that cerium turnings sorbed hydrogen at room temperature after an induction time which was dependent on the hydrogen pressure. During reaction the cerium warmed up. This was thought by Viallard to be the cause of the autocatalysis. His autocatalytic curves showed at the start a clearly discontinuous course. Gadolinium behaved in the same way, not at room temperature but only above 250 °C. Viallard gave (on page 48 of his article) an explanation of the autocatalytic behaviour, thereby associating himself with the views of Markowska and Valensi [5]). Two competing processes are distinguished, "penetration" and "fixation" of the hydrogen. The slow process at the start was the penetration or diffusion of the gas into the surface layer of the metal. This layer gradually became enriched with hydrogen, while the penetration proceeded. The enrichment resulted in an ever growing number of collisions between the atoms of the gas and those of the metal, which determined the "fixation". The reaction rate increased. In this stage, as Viallard stated, the reaction rate was not determined by diffusion but by the reaction between the atoms as such.

In a paper [6]) on the mechanism of the reaction of zirconium with hydrogen, Gulbranssen and Andrew (1954) clearly pointed out the role played by oxide films. The authors wanted to disprove the theory of Smith [7]), who explained the behaviour of metals with respect to hydrogen solely by means of rifts, i.e. cracks on a micro-micro scale. The absence of these rifts should be responsible for the inactivity, and their production should cause the autocatalysis. The experiments of Gulbranssen and Andrew, in which the sorption rates were measured by a vacuum microbalance, were for the rest quite similar to some of

*) "... the heat of reaction, the change of the surface, and perhaps also by an autocatalytic influence of the hydrogen already sorbed".

the experiments described in this paper. They found, after activation at increasing temperatures, an ever growing sorption rate (at 150 °C and 1·4 cm Hg pressure) of hydrogen. Above an activation temperature of 600 °C the rates at 150 °C became constant. The original inertness of the metal was, according to these authors, caused by a room-temperature oxide film 10 to 50 Å thick. This film was transparent and dissolved slowly in the metal while the zirconium was heated in a very good vacuum. Gulbranssen and Andrew observed that the sorption rates (in each case autocatalytic) increased with increasing film thickness, and also if the temperature at which the film formed was increased. They explained these facts by assuming that the greater part of the film dissolved in the metal at higher temperatures and that the high-temperature oxide crystals were larger and badly fitting. The autocatalytic character was attributed to "... the gradual breakdown of the oxide film physically by passage of hydrogen as well as to the gradual solution of the oxide into the metal".

5. Discussion

It seems worth while to compare the possibilities mentioned in the preceding section for thermal regeneration or for autocatalytic hydrogen sorption with our own experiments which were performed with powders of cerium, zirconium, thorium, Th_2Al and Ceto. All of these metals combine a very high stability of their oxides with a strong affinity for hydrogen. Therefore it is certain that they all have a "natural" oxide and/or nitride skin unless very great care has been taken during their previous history to prevent contamination of their surfaces. The original inactivity of cerium as found by Viallard must be due to such a skin, which seems much more plausible than that a hydride skin should be the cause.

Let us now discuss the activation mechanism of thorium when the powder is warmed up to 900 °C in a furnace at a pressure of less than 10^{-7} mm Hg (lower activation temperatures require longer annealing times). Before the treatment the powder is inactive at room temperature. It has a grey appearance, probably due to the oxide skin. X-ray diffraction yields ThO_2 lines (cubic CaF_2 type, $a = 5{\cdot}58$ Å) in addition to the Th lines. After activation the powder is black. The X-ray diagram, however, is only changed in so far as the diffraction peaks are more clearly defined. Now this powder is able to (ad)sorb in a very short time at room temperature an amount of oxygen that roughly corresponds to a few monatomic layers. Likewise it is able rapidly to (ab)sorb at room temperature very large amounts of hydrogen. What has happened to the original protecting oxide film? These are the possibilities:

(a) *dissolution of* ThO_2 in the thorium metal. Experiments show, however, that the solubility of oxygen in the metal is so small, even at 900 °C, that this cannot be the explanation. Gerds and Mallett [8]) in 1954 stated that the solubility was too small to be measured. Moreover the thorium used already contained an

amount of oxygen that was in equilibrium with ThO_2 at higher temperatures (the same holds for our Th_2Al and Ceto). ThO_2 was always found as a second phase in the thorium specimens.

(b) *reduction of* ThO_2 by the underlying metal to ThO. The compound ThO, which is mentioned by Zachariasen [9]) and which has the NaCl structure, with $a = 5{\cdot}20$ Å, has never been found in our experiments. The possibility remains that the compound is oxidizable to such an extent that it oxidizes despite the protection of the nitrocellulose coating that was always applied for the X-ray analysis. Another possibility is that ThO is formed at higher temperatures, but that at lower temperatures it is unstable and decomposes into Th and ThO_2. Various quenching methods were tried, but we were unable to obtain the ThO phase. Besides it is debatable whether a possible ThO layer still leaves the underlying thorium open to attack by hydrogen.

(c) One also can assume *a less far-going reduction of the oxide* layer i.e. to ThO_2 with a thorium excess (interstitial) or, what is more likely, with oxygen vacancies. This reduction would certainly imply a renewed activity with respect to oxygen. However, the permeability of the oxide with respect to H_2 will never increase to such an extent as to produce reaction rates as given in curve *c* of fig. 2.

(d) Another possibility might be that the *difference in thermal expansion* between thorium and the adherent oxide layer causes scaling of the skin at higher temperatures. The general opinion is, however, that oxide films produced at room temperature are very elastic. Furthermore experiments prove that activation of thorium can occur at temperatures lower than 900 °C, e.g. 400 °C, but in that case the annealing time has to be longer. This time effect is in contradiction to what was to be expected if mechanical strains were the cause.

(e) A *recrystallization* of the thin oxide film to localized oxide particles under the influence of temperature. This process creates a large new unprotected surface which is able both to adsorb oxygen or absorb hydrogen. The results, obtained by Bénard and co-workers while studying the first steps of the oxidation processes on copper and other metals, have added a new argument in favour of this process to those already mentioned in sec. 3.

According to Bénard [10]) the oxidation process at high temperatures begins with the forming of a thin film of oxide (invisible under the optical microscope) of about 50 Å thickness. Then "germs", little oxide crystals, are formed. During prolonged oxidation the crystals grow at a rate that is proportional to the impact of oxygen molecules on the *whole* surface. This means that there is, at these temperatures, a rapid surface diffusion. Now it is reasonable to assume that, after stopping the oxygen supply, the diffusion will continue. In this way the thin film, in kinetic equilibrium with the oxygen bombardment and the growing crystals, will be consumed until a clean surface with little crystals dispersed on it is obtained. In our case the thorium-oxide film, formed

at room temperature where surface diffusion is very slow, will tend to do the same if, in an inert atmosphere, surface diffusion is activated.

Which of the mechanisms discussed plays the most important role in the case of thorium cannot be definitely stated nor proved with simple experiments. Mechanism (e) appears to be the most probable one. In the case of other getter metals this will not be necessarily the same. It is known that a mechanism analogous to (a) is mainly responsible for the zirconium activation and that in the case of cerium the adherent CeO_2 is reduced to Ce_2O_3 if it is heated at 500 °C in a vacuum (mechanism (b)).

The autocatalytic H_2 sorption must also be connected, though Viallard does not mention this specifically, with a film of contaminating oxide having the above properties or with a film of nitride (see below, fig. 6). An explanation

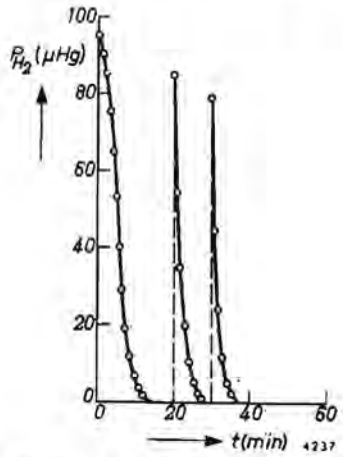

Fig. 6. Autocalatytic hydrogen sorption at room temperature by 200 mg of thorium powder, after de-activation with nitrogen in the same way as described for oxygen.

of the autocatalysis might be the following: The oxide (or nitride) film protects the active metal surface against a reaction with hydrogen, but not quite perfectly. Hydrogen seems to be able to penetrate the skin at a very slow rate. Whether this penetration occurs at definite sites, along imperfections (latent cracks) or whether an overall permeability is the cause (due to the atomic structure of the layer) is not of direct importance. The effect is that, very slowly, the underlying metal sorbs some hydrogen. The dilation of the metal lattice caused by this hydrogenation is to be held responsible for the participation of new unprotected surfaces in the sorption process. In the first case the latent cracks will become real ones and will extend as more hydride is formed underneath. In the second case the strain in the oxide layer will increase, particularly on the strongly convex curved surfaces, until the skin cracks ("mushroom effect"). In both cases the sorption rate may increase

discontinuously (provided the surface in question is geometrically favorable), as found by Viallard [4]). Gulbranssen and Andrew [11]), working with chemically polished sheets of Zircalloy (98·3% Zr, 1·45% Sn, 0·1% Fe, 0·05% Ni and 0·1% Cr) found after an induction period that hydride formed on the edges of their samples.

It is absurd to assume that in the induction period, where hydrogen sorption is immeasurably small, acceleration occurs as a result of warming up because of the heat of the reaction. This must certainly, however, be taken into account in the more rapid parts of the sorption process. Indeed, that this temperature effect should be the main cause conflicts with the permanent character of the change brought about by the self-activation as shown in fig. 4. The experiments described in sec. 2 make it clear that, if the hydrogen gas is contaminated, the newly created free surface is immediately de-activated by preferential sorption of the contaminant molecules. In the experiment described the contaminating gas could be condensed by liquid air, and therefore could consist of H_2O, CO_2 or grease vapour. The possibility that the length of the induction period might be independent of the contact with hydrogen (due to room-temperature re-crystallization or ageing) was investigated. Contact with hydrogen, however, was found to be a necessary condition for the increase in permeability of the protecting layer. Keeping the powder in a vacuum before the admission of hydrogen did not shorten the induction period. The protection by the oxide layer decreases when foreign elements like Al and Ce are added to the thorium metal (see fig. 3). These elements are likely to be incorporated in the oxide layer. Therefore this strengthens the assumption that an overall permeability as a result of the atomic structure causes the start of the reaction rather than the microcracks. The argument, however, is not conclusive.

In the preceding paragraph the swelling of the metal is supposed to be the accelerating factor as it strains the protecting adherent layer. It is clear that if this deformation is anisotropic, which is mostly the case, and if the metal is polycrystalline, the effect is increased even further. Let us refer to an experiment already mentioned in sec. 2 (and which will be worked out in sec. 5); there after de-activation of Th_2Al that had already sorbed an amount of hydrogen, a very rapid autocatalytic sorption was measured. One could here state that swelling was not the only factor but that the hydrogen present in the metal had some *chemical* influence causing the oxide to become more permeable. It is not certain, however, whether the observed effect was due to a more rapid activation, or to a slower de-activation during exposure to oxygen. It is known that zirconium after hydrogenation to saturation is far less readily oxidizable than before. The calculated equilibrium pressure of water vapour above thorium: $3\ Th + 2\ H_2O = ThO_2 + 2\ ThH_2$ at room temperature is about 10^{-92} atm. To think of a total reduction of ThO_2 by ThH_2 is therefore absurd.

Deal and Svec [12]) have studied the reaction of thorium and water vapour, albeit at the higher temperature of 200 °C. They found that ThO_2 and hydrogen were formed. The hydrogen was partly dissolved in the metal.

A last possibility remains that, in equilibrium with ThO_2, ThH_2 and Th, a certain amount of $Th(OH)_4$ might be dissolved in the oxide layer (OH^- ions in O^{2-} sites):

$$2\,ThO_2 + 2\,ThH_2 \rightleftarrows \{Th(OH)_4\}_{\text{in } ThO_2} + 3\,Th$$

This means a partial reduction of the oxide, but the concentration of $Th(OH)_4$ will only be of the order of 10^{-50} mol per cm^3 of oxide. It is impossible that such a concentration of OH^- ions could at all change the permeability of the oxide towards hydrogen. Besides, a similar autocatalytic hydrogen sorption can be observed with thorium covered with a nitride (ThN) layer (fig. 6), so that no specific hydrogen-oxide chemical reaction can be held responsible.

6. Theoretical

Though the process of autocatalytic sorption is not understood in detail, yet the attempt has been made to make a more or less quantitative analysis of it, using the simple model described in sec. 4.

In a constant volume at constant temperature the sorption rate of a getter will be linearly proportional to its active surface area ω, provided the gas can reach this surface directly. At the same time a certain pressure dependence will exist. In a constant volume then

$$-\frac{dp}{dt} = \omega f(p)\,. \tag{1}$$

The special features of the model we are now going to use are:
(1) the active metal surface is a function of the amount of hydrogen already sorbed after de-activation. As this is the hydrogen concentration in the metal (C_H) we can write:

$$-\frac{dp}{dt} = \omega\,(C_H) f(p)\,; \tag{2}$$

(2) since sorption must start there has to be a very small but distinct leakage of hydrogen through the protecting layer during the induction period.

In fig. 4 *) is shown a sequence of curves that makes it possible to eliminate the influence of pressure on the sorption rate. On a line of constant pressure the values for $-dp/dt$ increase in the successive curves. The only things that have changed in going from one curve to the other are time and the quantity

*) The curves of fig. 4 need a correction for the quick contraction of the gas admitted due to cooling in the cold trap. Therefore the first points of each curve are somewhat uncertain.

of hydrogen gettered in that time. Thus for each pressure the function $\omega(C_H)$ can be found. A set of those $-dp/dt$ versus C_H curves, corresponding to the curves of fig. 4, is given in fig. 7. They seem to originate from roughly one point. Furthermore for small hydrogen concentrations in the metal it seems permissible to consider the sorption rate at constant pressure to be a linear function of C_H. Consequently we can now write (2) as

$$-\frac{dp}{dt} = (a_1 C_H + b_1) f(p). \tag{3}$$

The constant term a_1 is related (in our model) to the swelling properties; the

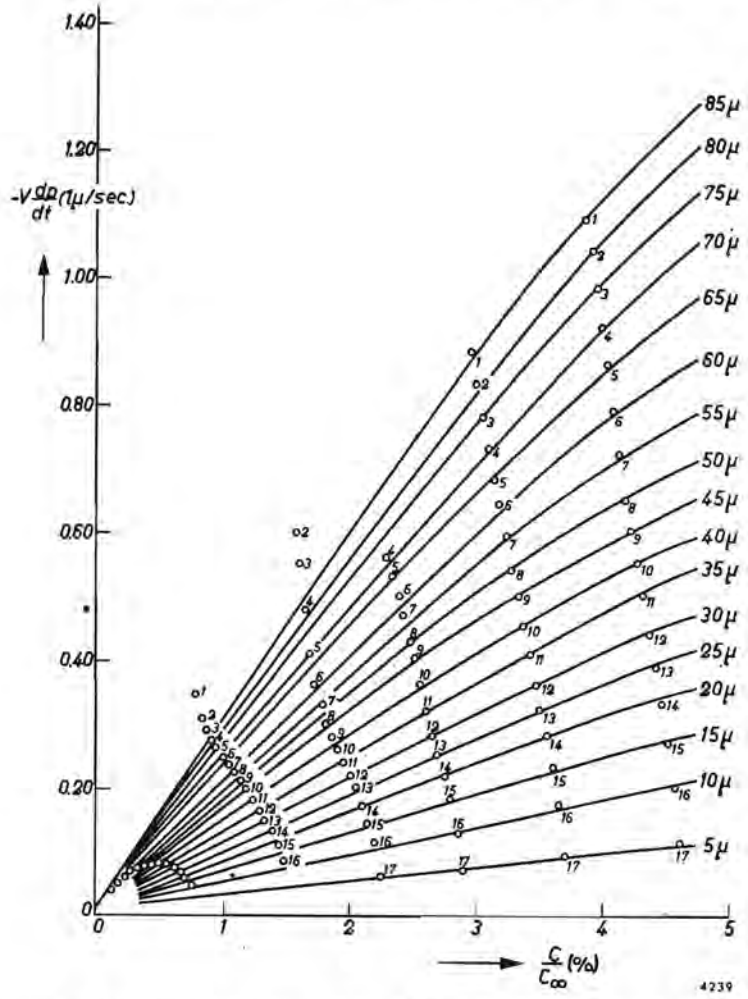

Fig. 7. Hydrogen-sorption rate ($-V dp/dt$) of fig. 4 plotted against the hydrogen concentration in the getter (C/C_∞) for various values of hydrogen pressure (p).

constant b_1 gives the "zero permeability", a property related to the protecting layer.

The linear shape of the isobaric sorption-rate curves of fig. 7 at low C_H values is not very surprising. It has been found [13]) that, by sorbing hydrogen at room temperature, Th_2Al immediately forms a new phase, isomorphous but expanded, containing some 6 H atoms per unit cell. Similar hydride phases are formed by Ceto, thorium and zirconium. The very first amounts of hydrogen presumably build up a surface layer of this second phase below the oxide coating. Up to this superficial "saturation" surface area, the increase is linear. This stage of the reaction, however, is already exceeded at a value of $C_H/C_\infty \approx 0{\cdot}01\,\%$ (C_∞ corresponds to the composition Th_2AlH_4 at total saturation). With hydrogen penetration proceeding into the deeper parts of the metal lattice, surface expansion will tend to increase somewhat slower. However, one can picture this surface increase as being disproportionately large because of the anisotropic, nearly uni-axial lattice expansion occurring in a polycrystalline material. (In the experiments it is always found that powders that originally are grey turn black on hydriding, which is generally believed to be due to a decreasing grain size.) In any case it is acceptable that the curves of fig. 7 approach linearity at somewhat larger values of C_H, certainly for the period of the first absorption curve of fig. 4.

On the one hand the graph of fig. 7 shows the dependence of the sorption rate at constant pressure — which, according to the model, means the active surface area — on the amount of hydrogen previously sorbed. On the other hand it is also possible to find from it the pressure dependence of the sorption rate at constant values of C_H. In fig. 8 the $-dp/dt$ values are plotted against the corresponding p values for a hydrogen concentration of $3{\cdot}6\,\%$ of total saturation on a log-log scale. This graph does not yield an exactly straight line. However, the accuracy is such that the conclusion seems justified that $-dp/dt$ at a constant surface activity is linearly dependent on p (for $p < 30$ μ Hg the linearity does not seem to hold). This result is in accordance with that found for the reactions of hydrogen with titanium or barium [14]).

Equation (3) can now be written as

$$-\frac{dp}{dt} = (a_1 C_H + b_1)\, p\,, \tag{4}$$

which strictly speaking is only valid for small C_H values.

If we restrict ourselves to the first sorption curve of the series of fig. 4, the equation becomes

$$-\frac{dp}{dt} = \Big\{ a\,(p_0 - p) + b \Big\} p\,, \tag{5}$$

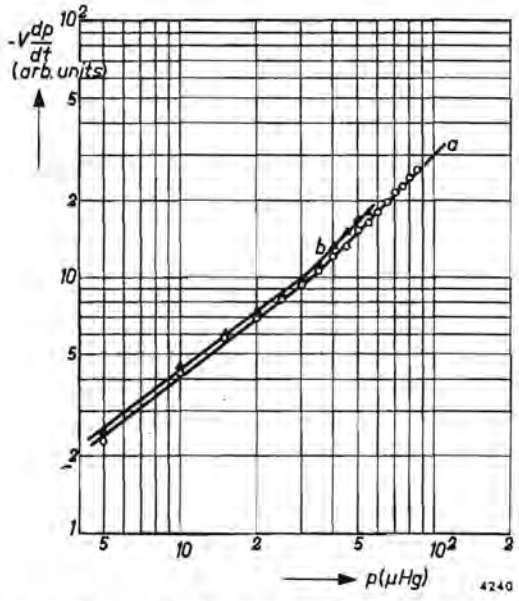

Fig. 8. Hydrogen-sorption rate ($-V\mathrm{d}p/\mathrm{d}t$) versus hydrogen pressure (p) at a constant hydrogen concentration in the getter.
Curve a: corresponding to figs 4 and 7; $C/C_\infty = 3{\cdot}6\,\%$.
Curve b: corresponding to figs 5 and 9; $C/C_\infty = 6{\cdot}4\,\%$.

where p_0 and p are the hydrogen pressures at time $t = 0$ and at t respectively. On integration this yields

$$t = \frac{1}{ap_0 + b} \ln\left(\frac{ap_0 + b}{b}\,\frac{p_0 - p}{p} + 1\right). \tag{6}$$

The point of inflection of this curve lies at

$$p = \frac{ap_0 + b}{2a}.$$

If $p_0 + \dfrac{b}{a}$ is expressed as p_0', then (6) becomes

$$ap_0'\,t = C + \ln\frac{p_0' - p}{p}, \tag{7}$$

where $C = \ln\left(\dfrac{ap_0' - b}{b}\right)$. The point of inflection is then given by $p = \frac{1}{2}p_0'$.

Here p_0' can be considered as the virtual starting pressure. Then $p_0' - p$ gives the amount of gas really absorbed, increased by an imaginary amount that might be ascribed to the zero-time surface area.

On the basis of eq. (7) one might in principle analyse such a first sorption curve as that in fig. 4 and determine the constants a and b: the point of inflection

gives p_0'. A plot of ln $[(p_0'-p)/p]$ versus t gives ap_0'. The accuracy with which this can be done is, however, very small, owing to experimental difficulties. Of course such an analysis is allowed only in those cases where a linear dependence of the sorption rate on p is certain.

The shape of the isobaric lines of fig. 7 must be determined, apart from the surface-area increase, by on the one hand the diffusion rates of hydrogen into the metal (or through metal hydride), or on the other by the diffusion rate of hydrogen in the gas phase towards the getter surface. With the large mobilities hydrogen atoms possess in the interstitial metal lattice[15]) (this is clearly demonstrated by the sorption rates of normal, active powder specimens) it is certainly possible that gas diffusion towards the surface becomes rate-determining, particularly in a heap of very finely powdered grains where the gas-flow resistance at low pressures can be very large. The influence of this take-over will be a slower than "normal" increase of $-\mathrm{d}p/\mathrm{d}t$. The following experiment shows some peculiar results which are believed to be mainly due to this diffusion resistance in the gas phase. Here the specimen of Th_2Al powder used in the experiment of fig. 4, having first sorbed hydrogen up to 4·6% of saturation, was exposed at room temperature to the action of oxygen for 5 minutes. After pumping away the oxygen a new series of hydrogen sorptions was made (fig. 5), in the same way as before the (second) de-activation. The application of the analysis described above yielded fig. 9. First of all we see that the zero-time active surface area, given by the point of intersection of the isobaric lines, is very large. Secondly we find that the linear character of the lines is totally lost. They cannot be looked upon as a logical continuation of those of fig. 7: the original slope is too large, and the final slope seems to be a little too small. Let us assume that the rapid start (just like the large zero activity) is due to special properties of the oxide coating (now formed on a hydride); then the unexpected large decrease remains to be explained. The log-log plot (curve *b*, fig. 8) this time shows a shape and slope almost identical with curve *a* in fig. 8, so again a satisfactory linear pressure dependence is encountered. With the aid of the following model the attempt will be made to show that gas-flow resistance may be the cause of the behaviour observed in fig. 9.

Let V be a volume, filled with hydrogen at a pressure p (see fig. 10). The getter powder is placed in a silica crucible C and is represented by a piece of metal M in which fine long pores extend from the upper metal surface to the bottom of the crucible. The pores are of the same width as the mean dimensions of the grains, viz. about 35 μ; they are very long compared to their width. For hydrogen in the pressure region of 0·1 mm Hg, where the mean free path is about 80 μ, and also at lower pressures, the pores are real Knudsen resistances. At $t = 0$ and during the first period — the induction period — of the autocatalysis, the pressure in the powder is everywhere $p = p_0$. As the metal surface becomes active (neglecting the dimensional changes of the pores due

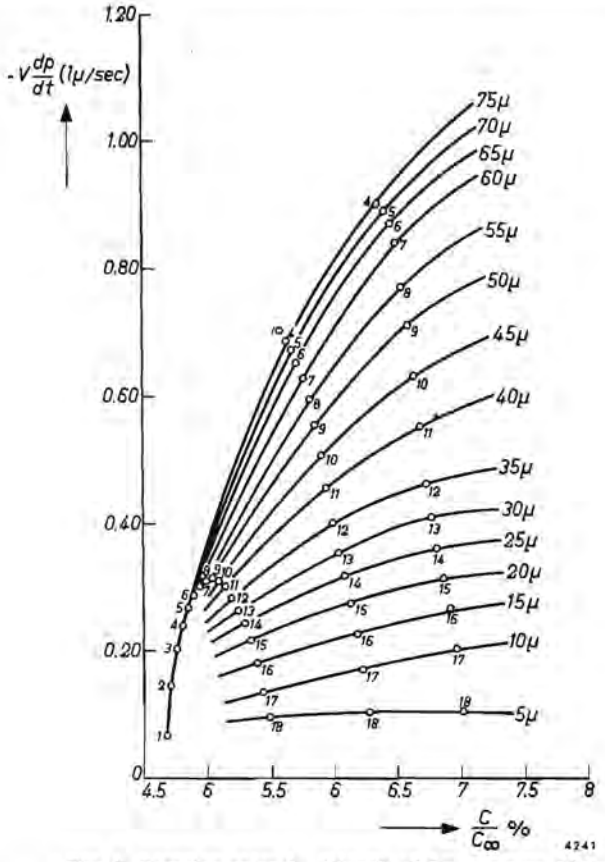

Fig. 9. Sorption rates ($-Vdp/dt$) of fig. 5 versus C/C_∞.

to expansion of the metal as being of minor importance) and begins to bind the gas present in the pores, new gas must enter from the volume V. Slowly a pressure gradient will be built up. This means that at the lower end of a pore the pressure will be smaller compared to that in the upper part. The metal wall of the lower part will therefore increase more slowly in activity than when hydrogen can reach it freely as in the upper part. Its sorbing ability will gradually fall further behind: it seems as if a part of the heap of powder took no part in the reaction. This deviation from normal behaviour will take place earlier if the zero-time activity is already appreciably large.

The constant a in eq. (5) may vary somewhat for diverse getter powders; in general the swelling properties are, however, of the same order. On the other hand the permeability of the oxide layers on the various getter powders, which is embodied in the constant b, will exhibit much divergence. Figure 3 gives a good example. Here the oxide on the pure element seems to be practically impenetrable at room temperature. For Th_2Al, where the oxide is likely

to contain Al_2O_3, or where Al^{3+} ions might be built into the ThO_2 lattice, an already more rapid activation is found. For Ceto, that is Th_2Al, in which some thorium atoms have been replaced by cerium atoms, a very rapid activation is observed. Consequently the oxide formed on its surface must be relatively very permeable to hydrogen. Another example is found in the reaction between

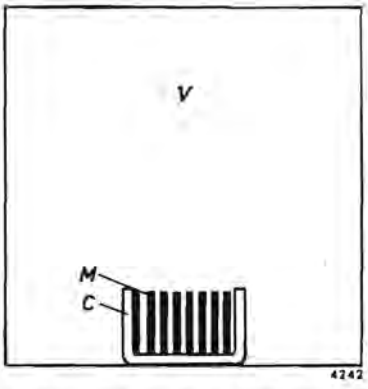

Fig. 10. Schematic model of a getter experiment.

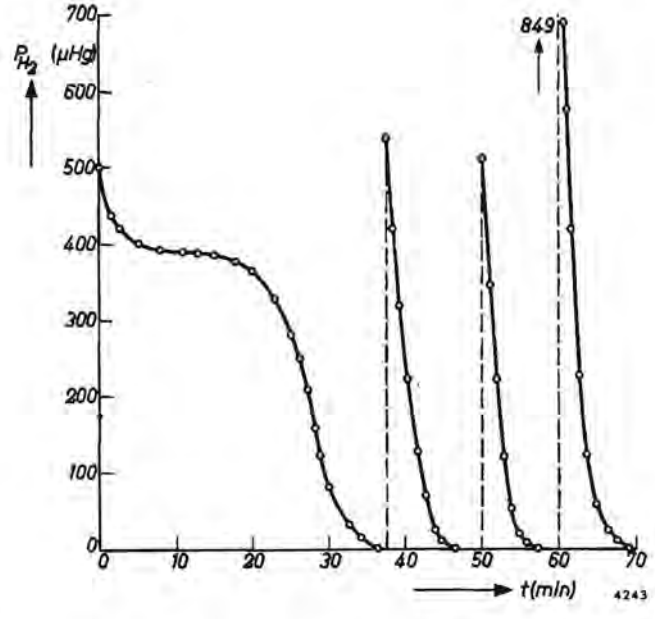

Fig. 11. Autocatalytic hydrogen-sorption curves for zirconium powder at 200 °C after oxygen de-activation at room temperature.

de-activated zirconium and hydrogen. The same autocatalysis *) can be observed there (see fig. 11) but only at somewhat higher temperatures (e.g., 200 °C).

As for Ceto, apart from the permeability of its oxide to hydrogen as mentioned above, it distinguishes itself by high reaction rates with oxygen at rather low temperatures (200 to 300 °C). The two properties may be linked, the common cause residing in the oxide. Since thorium and cerium have equa-affinities for oxygen it is very likely that a random mixture of thorium and cerium in the metal is reflected in the oxide composition. Both pure oxides are isomorphous with CaF_2 and their dimensions are such (ThO_2 : $a = 5{\cdot}58$ Å, CeO_2 : $a = 5{\cdot}41$ Å) that a large range of homogeneous mixtures may be expected. In fact this has been found [16]). At first sight, therefore, there is no reason why this mixture should be more permeable to oxygen and hydrogen than both the pure oxides. There is, however, one property of cerium that might be important here: the fact that it can form the sesquioxide Ce_2O_3. This Ce_2O_3 is isomorphous with La_2O_3 and of the latter oxide it is known [17]) that it also forms homogeneous mixtures with ThO_2, containing in this case a large amount of empty oxygen sites. These empty sites cause the oxide lattice to expand appreciably .The openness of the oxide skin on Ceto might now be explained in the following way, analogously to what is found with cerium [2]): Between the metal $(Th,Ce)_2Al$ and the normal oxide $(Th,Ce)O_2$ there might be a very thin layer of an expanded mixed oxide $ThO_2 - Ce_2O_3$. This thin layer would cause the outer layer of $(Th,Ce)O_2$ to crack (see fig. 12). The cracks would admit the free gases, oxygen in the case of oxidation, or hydrogen in the experiments described in this paper. In both cases we might imagine that the underlying metal is accessible more easily, because of the vacant oxygen sites.

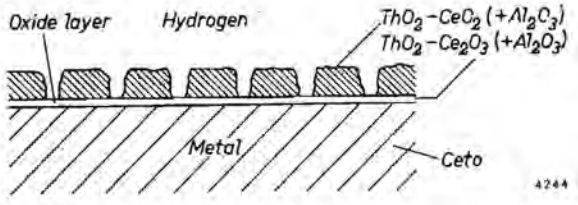

Fig. 12. Schematic illustration of oxide layer on Ceto metal.

7. Conclusions

Thermal regeneration, or activation, of surfaces of non-evaporating getters may be explained in several ways: firstly by dissolution of the adhering oxide

*) This incidental experiment with zirconium led (at a temperature of 200 °C and hydrogen pressures of 350 to 250 μ Hg) to a square-root pressure dependence of $-dp/dt$. When approaching lower pressures the index tended to increase to one. Gulbranssen stated that, at higher pressures, the hydrogen-sorption rate was independent of pressure.

(or nitride) — formed during exposure to air — such as is mainly the case in zirconium; secondly by some time-and-temperature-dependent change of the oxide which may be called ageing or recrystallization. This causes the oxide to become brittle and produces crystal boundaries that are easy pathways for new, active gas. A third possibility, as has just been shown, might be a recrystallization that goes much further, due to surface diffusion at higher temperature and resulting in a concentration of the oxide film into a few small out-crops of crystals, leaving the major part of the surface uncovered.

De-activation caused by reaction with hydrogen, which gives rise to autocatalytic hydrogen sorption, is thought to be due to a growing of the metal surface below the oxide skin causing the latter to crack. This view requires that the original oxide skin be more or less permeable to hydrogen. The experiments indicate that this permeability is strongly dependent on the chemical composition of the skin.

REFERENCES

1) N. B. Pilling and R. E. Bedworth, J. Inst. Metals **29**, 529-536, 1923.
2) J. Loriers, Rev. Métallurgie **49**, 801-810 and 883-905, 1952.
3) A. Sieverts and G. Müller-Goldegg, Z. anorg. Chem. **131**, 65-95, 1923.
4) R. Viallard, Ann. Chim. **20**, 5-72, 1945 (thèse).
5) D. Markowska and G. Valensi, Bull. Soc. Chim. France **6**, 1523-1529, 1939.
6) E. A. Gulbranssen and K. F. Andrew, J. electrochem. Soc. **101**, 348-353, 1954.
7) D. P. Smith, Hydrogen in Metals, University of Chicago Press, Chicago, 1948.
8) A. F. Gerds and M. W. Mallett, J. electrochem. Soc. **101**, 171-174, 1954.
9) W. H. Zachariasen, Acta cryst. **5**, 21, 1948.
10) J. Bénard, F. Grønlund, J. Oudar and M. Duret, Z. Electrochem. **63**, 799-804, 1959.
11) E. A. Gulbranssen and K. F. Andrew, J. electrochem. Soc. **104**, 709-714, 1957.
12) B. E. Deal and H. J. Svec, J. electrochem. Soc. **103**, 421-425, 1956.
13) J. H. N. van Vucht, this thesis, chapter 4.
14) J. J. B. Franssen and H. J. R. Perdijk, Philips tech. Rev. **19**, 290-301, 1957.
15) D. Kroon, C. van der Stolpe and J. H. N. van Vucht, Arch. Sciences **12**, 156-160, 1959.
16) L. Passerini, Gazz. Chim. Ital. **60**, 764-770, 1930.
17) F. Hund and W. Dürrwächter, Z. anorg. Chem. **265**, 67-72, 1951.

Samenvatting

Sinds enkele tientallen jaren kent men een niet verdampende getter (gasbinder), genaamd Ceto, bestaande uit Ce, Th en Al, welke naast een grote sorptiesnelheid en capaciteit voor zuurstof, stikstof en koolmonoxide ook zeer goede eigenschappen als waterstofbinder bezit. Dit proefschrift beschrijft een gedeelte van het onderzoek dat werd ingesteld naar de structuur van deze stof en het verband tussen deze structuur en zijn gettereigenschappen.

Met behulp van metallografische, thermoanalytische en vooral röntgenanalytische methoden wordt het ternaire systeem Ce-Th-Al onderzocht en o.a. bewezen dat Ceto in zuivere toestand de kristalbouw heeft van de intermetallische verbinding Th_2Al. In het rooster van deze verbinding is het mogelijk een gedeelte der thoriumatomen te vervangen door ceriumatomen tot ongeveer de samenstelling van Ceto wordt bereikt. Diepgaand bestudeerd is de absorptie van waterstof door de chemisch en physisch goed gedefinieerde verbinding Th_2Al. Echter wordt op enkele technisch belangrijke punten steeds de invloed nagegaan van een gedeeltelijke vervanging van thorium door cerium.

Enerzijds worden evenwichtstoestanden bestudeerd door het meten van de waterstofdruk boven het gettermetaal als functie van de temperatuur en van de reeds opgenomen hoeveelheid. Hieruit worden enkele thermodynamische gegevens verkregen. Het blijkt dat de waterstof in atomaire vorm in het metaalrooster aanwezig is. Anderzijds wordt in het laatste hoofdstuk ook aandacht gewijd aan de kinetiek der waterstofabsorptie, vooral in verband met de storende invloed van bijgemengde gassen. Volgens het daar beschreven onderzoek is de snelheid van de reactie tussen Th_2Al en H_2 evenredig met de druk en onafhankelijk van de tijd. Autokatalyse treedt echter op als het getteroppervlak aanvankelijk bedekt is met een afsluitende oxide- of nitridehuid.

De andere hoofdstukken bevatten experimenten die het gedrag van waterstof in het metaalrooster betreffen. In een model van het Th_2Al-rooster zijn interstities aan te wijzen waar het H-atoom zich zou kunnen bevinden. De meeste van deze interstities, 16 in getal, zijn paarsgewijs gerangschikt. Met behulp van röntgendiffractie kan de plaats van de H-atomen niet direct worden bepaald. Wel kan worden vastgesteld dat het Th_2Al-rooster als zodanig niet verandert wanneer het waterstof absorbeert. Slechts zeer kleine verschuivingen der thorium- en aluminium-atomen ten opzichte van elkaar treden op en wel zodanig dat de afmetingen der eenheidscel op een bepaalde wijze veranderen. Uit de aard dezer verandering en uit enkele gegevens verkregen uit het meten der evenwichtsdrukken, wordt het vermoeden verkregen dat het opvullen van het Th_2Al-rooster met waterstof niet geheel ongeordend geschiedt. De opvulling is gedacht te bestaan uit twee etappes waarbij de toestand halfweg als een speciale ordening, of zo men wil, een tussenverbinding kan worden opgevat. Deze orde zou hieruit kunnen bestaan dat de holteparen in het tussenrooster ieder slechts

één H-atoom bevatten. Het vinden van de juiste plaatsen der H-atomen en het zoeken naar een eventuele ordening op deze plaatsen zijn het onderwerp van de rest van het proefschrift. Twee elkaar aanvullende technieken zijn daarbij gebruikt: neutronendiffractie en kernspinresonantie.

Om de incoherente straling te vermijden, die optreedt als neutronen worden verstrooid door protonen, is de neutronendiffractie uitgevoerd aan preparaten die het waterstofisotoop deuterium bevatten. De gemeten diffractogrammen bevestigen de reeds vermoede plaatsing der waterstofatomen in de gepaarde interstities. Zij sluiten, bij kamertemperatuur zowel als bij het kookpunt van vloeibare stikstof, duidelijk elke conventionele vorm van orde uit. Zij kunnen echter geen onderscheid maken tussen de volkomen ongeordendheid der verdeling van 8 waterstofkernen over de 16 (tot 8 paren verenigde) interstities en de mogelijke toestand waarbij precies ieder paar dezer interstities een kern bevat doch waar deze kern zich in willekeurig welke partnerholte van het paar bevindt. De kernspinresonantie is toegepast op oplossingen van normale waterstof in Th_2Al en wel bij kamertemperatuur en lagere temperaturen (tot het kookpunt van stikstof). De vorm van de resonantielijn verraadt de grote beweeglijkheid bij kamertemperatuur der protonen in het tussenrooster van Th_2Al zolang dit nog niet verzadigd is. Als praktisch alle 16 tussenroosterplaatsen gevuld zijn, of ook, als zij niet gevuld zijn, bij temperaturen onder 210 °K, zijn de protonen nauwelijks beweeglijker dan normale metaalatomen. In tegenstelling tot de neutronendiffractie blijkt de kernspinresonantie wel in staat te zijn te onderscheiden tussen een volkomen willekeurige verdeling der 8 protonen over de 16 holten bij de halve verzadiging, en de bovenbeschreven ordening van één proton per dubbele holte. Berekeningen, waarbij mede gebruik gemaakt werd van gegevens verkregen door de neutronendiffractie, wekken de indruk dat geen enkele vorm van orde aanwezig is, zelfs niet de bovengenoemde partiële orde. Theoretisch wordt echter bewezen dat de vorm der boven besproken drukisothermen van waterstof in evenwicht met zijn vaste oplossingen in Th_2Al, nadrukkelijk wijst op een tendentie der waterstofatomen de dubbele holten enkelvoudig te bezetten, zolang plaatsgebrek dit niet onmogelijk maakt. Een kleine inhomogeniteit der waterstofconcentratie in de preparaten wordt gedacht oorzaak te zijn van het negatieve kernspinresonantieresultaat.

Levensbericht

Het diploma H.B.S.-B werd behaald aan de R.K.H.B.S. te Arnhem in juli 1941. Na een jaar als leerling-analist bij de N.V. AKU te Arnhem werd in november 1942 ingeschreven aan de R.U. te Utrecht. In februari 1943 moest de studie der chemie daar worden onderbroken wegens een weigering de door de toenmalige bezetter geëiste loyaliteitsverklaring te tekenen, en werd de loopbaan bij de N.V. AKU vervolgd. Na de oorlog werd in november 1945 de universitaire studie opnieuw begonnen. In juni 1952 werd het doctoraal examen in de fysische chemie, hoofdvak colloidchemie met succes afgelegd. In september 1952 werd een betrekking als researchchemicus bij de N.V. Philips' Gloeilampenfabrieken aanvaard.

STELLINGEN

I

De bewering van Rodewald dat de stabiliteiten van diamant en grafiet thermodynamisch niet met elkaar vergeleken mogen worden, is onjuist.

H. J. Rodewald, Helv. chim. Acta **43,** 1657-1666, 1960.

II

De waterstofbroosheid, optredende in koolstofhoudende staalsoorten bij temperaturen onder 400 °C, moet worden toegeschreven aan de vorming van methaan, in plaats van aan de adsorptie van waterstof aan inwendige oppervlakken.

M. L. Hill en E. W. Johnson, Trans. met. Soc. AIME **215,** 717, 1959.
I. Class, Stahl und Eisen **80,** 1117, 1960.
L. C. Weiner, Corrosion **17,** 109, 1961.

III

De conclusie van Grimes dat plastische deformatie de diffusie van waterstof in nikkel niet beïnvloedt, wordt niet gerechtvaardigd door zijn experimenten.

H. H. Grimes, Acta met. **7,** 782-786, 1959.
F. Bell en O. Krisement, Z. Metallk. **53,** 115, 1962.

IV

De door Novy, Vickery en Kleber opgegeven eenheidscelafmetingen van de intermetallische verbindingen $GdFe_3$, $GdNi_3$ en $GdCo_3$ kunnen niet de juiste zijn.

V. F. Novy, R. C. Vickery en E. V. Kleber, Trans. met. Soc. AIME **221,** 580, 1961.
221, 585, 1961.
221, 588, 1961.

V

Het verschil in uitkomst bij de smeltpuntsbepalingen van CdTe door Kobayashi en door De Nobel is kwantitatief te verklaren uit de gevolgde methoden.

M. Kobayashi, Z. anorg. Chem. **69,** 1-11, 1911.
D. de Nobel, Thesis, Leiden, 1958.

VI

De door Zijlstra gevonden geringe grensvlakspanning tussen de magnetische en de niet magnetische fase in Ticonal wijst op een gering verschil in chemische samenstelling der beide fasen. Dit valt moeilijk te rijmen met het grote verschil in magnetische verzadiging der beiden fasen, dat moet worden aangenomen om de grote magnetische hardheid te verklaren.

Zijlstra, Thesis, Amsterdam, 1960.

VII

De wijze van vervorming van het wolfraamrooster tijdens het trekken van draad, zoals door Opinsky et al. voorgesteld, leidt niet tot de door hen waargenomen texturen.

A. J. Opinsky, J. L. Orehotsky and L. L. Seigle, Trans. met Soc. AIME **221**, 1083, 1961.

VIII

De bewering van Hauser, dat dislocaties moeten worden gezien als de filamenten die verantwoordelijk worden gesteld voor de harde suprageleiding van sommige metalen, is aanvechtbaar.

J. J. Hauser and E. Buehler, Phys. Rev. **127**, 142, 1962.
J. J. Hauser, J. appl. Phys. **33**, 3074, 1962.
W. F. Druyvesteyn and D. J. van Ooijen. Physics Letters **2**, 328, 1962.

IX

Het is gewenst dat op verantwoorde wijze een ernstige poging wordt gedaan tot het bevorderen van een natuurlijke samensmelting der West-Europese vaktalen, in plaats van met alle middelen deze te conserveren en ieder afzonderlijk te voorzien van kunstmatig geschapen nieuwe termen.

X

Meer nog dan op het probleem der spoorstudenten dient onze aandacht gericht te zijn op het analoge probleem der spoorprofessoren.

26 maart 1963

J. H. N. van Vucht